

AD-A237 945

ITIC

(2)

GL-TR-90-0321 (I)



1991



Hydrogen Fluoride and Fluorine Dispersion  
Models Integration Into the Air Force  
Dispersion Assessment Model (ADAM)

Phani K. Raj

Technology & Management Systems Inc  
99 South Bedford Street, Suite 211  
Burlington, MA 01803-5128

7 December 1990

Final Report, Vol. I  
1 March 1989-30 November 1990

Approved For	
Original	<input checked="" type="checkbox"/>
Dist. To	<input type="checkbox"/>
Dist. To	<input type="checkbox"/>
Justification	
Distribution Code	
Availability Codes	
Dist	Avail And/or Special
A-1	

APPROVED FOR PUBLIC RELEASE; DISTRIBUTION UNLIMITED


GEOPHYSICS LABORATORY  
AIR FORCE SYSTEMS COMMAND  
UNITED STATES AIR FORCE  
HANSCom AIR FORCE BASE, MASSACHUSETTS 01731-5000

91-04380



"This technical report has been reviewed and is approved for publication"

  
BRUCE A. KUNKEL  
Contract Manager

  
DONALD D. GRANTHAM, Chief  
Atmospheric Structure Branch  
Atmospheric Sciences Division

FOR THE COMMANDER

  
ROBERT A. McCLATCHEY, Director  
Atmospheric Sciences Division

Qualified requestors may obtain additional copies from the Defense Technical Information Center. All others should apply to the National Technical Information Center (NTIS)

If your address has changed, or if you wish to be removed from the mailing list, or if the addressee is no longer employed by your organization, please notify GL/IMA, Hanscom AFB, MA 01731. This will assist us in maintaining a current mailing list.

Do not return copies of this report unless contractual obligations or notices on a specific document requires that it be returned.

UNCLASSIFIED

SECURITY CLASSIFICATION OF THIS PAGE

## REPORT DOCUMENTATION PAGE

1a. REPORT SECURITY CLASSIFICATION			1b. RESTRICTIVE MARKINGS			
2a. SECURITY CLASSIFICATION AUTHORITY Unclassified			3. DISTRIBUTION/AVAILABILITY OF REPORT Approved for Public Release Distribution Unlimited			
2b. DECLASSIFICATION/DOWNGRADING SCHEDULE						
4. PERFORMING ORGANIZATION REPORT NUMBER(S)			5. MONITORING ORGANIZATION REPORT NUMBER(S) GL-T2-90-0321 (1)			
6a. NAME OF PERFORMING ORGANIZATION Technology & Management Systems, Inc.		6b. OFFICE SYMBOL (if applicable)	7a. NAME OF MONITORING ORGANIZATION Geophysics Laboratory			
6c. ADDRESS (City, State, and ZIP Code) 99 S. Bedford Street, Suite 211 Burlington, Massachusetts 01803-5128			7b. ADDRESS (City, State, and ZIP Code) Hanscom AFB, Massachusetts 01731-5000			
8a. NAME OF FUNDING/SPONSORING ORGANIZATION		8b. OFFICE SYMBOL (if applicable)	9. PROCUREMENT INSTRUMENT IDENTIFICATION NUMBER F1962B-89-C-0056			
8c. ADDRESS (City, State, and ZIP Code)			10. SOURCE OF FUNDING NUMBERS			
			PROGRAM ELEMENT NO. 63723F	PROJECT NO. 6670	TASK NO. 14	WORK UNIT ACCESSION NO. AF
11. TITLE (Include Security Classification) Hydrogen Fluoride and Fluorine Dispersion Models; Integration into the Air Force Dispersion Assessment Model (ADAM)						
12. PERSONAL AUTHOR(S) Phani K. Raj						
13a. TYPE OF REPORT Final Report Vol I		13b. TIME COVERED FROM Mar 90 to Nov 90		14. DATE OF REPORT (Year, Month, Day) 90/12/07		
15. PAGE COUNT 152						
16. SUPPLEMENTARY NOTATION						
17. COSATI CODES			18. SUBJECT TERMS (Continue on reverse if necessary and identify by block number)			
FIELD	GROUP	SUB-GROUP	Dispersion, Hydrogen, Fluoride, Aerosol, Monomer, Oligomers, Reaction, Heavy Gas, Fluorine			
19. ABSTRACT (Continue on reverse if necessary and identify by block number)..... Hydrogen fluoride and fluorine are two of the chemicals that are handled, transported, and used by the U.S. Air Force. Because of the need to develop contingency planning to manage potential accidents involving the release of either of these two toxic chemicals, dispersion models have been developed and integrated into the Air Force Dispersion Assessment Model ("ADAM") system. The thermodynamic aspects of HF polymerization reaction and dissociation when mixed with air have been modeled and considered in dispersion calculations. The dispersion results have been compared with test results from the Goldfish Series of field tests. The agreement is good between predicted and measured parameters such as cloud temperature, cloud width, and downwind concentration. Two different types of fluorine releases from a road trailer have been considered. The mixing of fluorine with ambient air has been modeled. Dispersion results for Fluorine are presented; however, due to the absence of any field data, no verification of predicted results are possible.						
20. DISTRIBUTION/AVAILABILITY OF ABSTRACT <input checked="" type="checkbox"/> UNCLASSIFIED/UNLIMITED <input type="checkbox"/> SAME AS RPT <input type="checkbox"/> OTIC USERS			21. ABSTRACT SECURITY CLASSIFICATION Unclassified			
22a. NAME OF RESPONSIBLE INDIVIDUAL Bruce Kunkel			22b. TELEPHONE (Include Area Code) 617-377-2972		22c. OFFICE SYMBOL GL/LYA	

DD FORM 1473, 84 MAR

DD FORM edition may be used until exhausted  
All other editions are obsolete.

(11)

SECURITY CLASSIFICATION OF THIS PAGE  
UNCLASSIFIED

# TABLE OF CONTENTS

	Page
LIST OF FIGURES . . . . .	vi
LIST OF TABLES . . . . .	viii
ACKNOWLEDGEMENTS . . . . .	ix
EXECUTIVE SUMMARY . . . . .	xi
Scope of Work . . . . .	xi
Project Accomplishments . . . . .	xi
Hydrogen Fluoride (HF) . . . . .	xii
Fluorine (F <sub>2</sub> ) . . . . .	xiii
Conclusions . . . . .	xv
CHAPTER 1 - INTRODUCTION. . . . .	1-1
1.1 Background. . . . .	1-1
1.2 Hydrogen Fluoride and Fluorine. . . . .	1-2
1.2.1 Hydrogen Fluoride. . . . .	1-2
1.2.2 Fluorine . . . . .	1-2
1.3 Objectives of the Work. . . . .	1-3
1.4 Scope of Work . . . . .	1-3
1.5 Organization of the Report. . . . .	1-4
CHAPTER 2 - HYDROGEN FLUORIDE - MOIST AIR MIXING THERMODYNAMIC MODEL . . . . .	2-1
2.1 Anhydrous Hydrogen Fluoride Physical Properties . . . . .	2-1
2.2 Physical Processes in HF-Humid Air Mixing . . . . .	2-5
2.2.1 Description of the Problem. . . . .	2-5
2.2.2 Hydrogen Fluoride Polymerization. . . . .	2-5
2.2.3 Aqueous HF Aerosols . . . . .	2-6
2.2.4 Adiabatic vs. Non-adiabatic Mixing. . . . .	2-7
2.2.5 Summary of the Principal Assumptions. . . . .	2-7

## TABLE OF CONTENTS (contd)

	Page
2.3 Review of Existing Thermodynamic Models . . . . .	2-8
2.3.1 TMS Modification to the Schotte Model.	2-12
2.3.2 Schotte (1988) Correlations. . . . .	2-12
2.3.3 Solution to the Equations of the Model	2-15
2.3.4 Cloud Density. . . . .	2-17
2.3.5 Computer Program . . . . .	2-17
2.4 Results and Discussions. . . . .	2-17
 <b>CHAPTER 3 - REVISIONS, MODIFICATIONS, ENHANCEMENTS AND CORRECTIONS TO ADAM CODE . . . . .</b>	 <b>3-1</b>
3.1 Correction of Large Aerodynamic Roughness in the Dispersion Path. . . . .	3-1
3.1.1 Assumptions. . . . .	3-2
3.2 Calculation of Atmospheric Turbulence Friction Velocity . . . . .	3-8
3.2.1 Assumptions. . . . .	3-8
3.2.2 Analysis . . . . .	3-8
3.3 Correlation for Molecular Diffusion Coefficient.	3-10
3.4 Other Corrections To and Enhancements in ADAM. .	3-10
3.4.1 Corrections. . . . .	3-10
3.4.2 Enhancements . . . . .	3-11
3.4.3 Panel/Menu Driven Inputs . . . . .	3-14
 <b>CHAPTER 4 - COMPARISON OF EXPERIMENTAL DATA AND MODEL RESULTS FOR HYDROGEN FLUORIDE. . . . .</b>	 <b>4-1</b>
4.1 Brief Description of Field Tests . . . . .	4-1
4.2 Release Rate and Flash . . . . .	4-1
4.3 Dispersion Results . . . . .	4-6
4.3.1 Jet Dispersion Regime. . . . .	4-6
4.3.2 Plume Temperature. . . . .	4-13
4.3.3 Heavy Gas Dispersion Regime. . . . .	4-20

## TABLE OF CONTENTS (Contd)

	Page
<b>CHAPTER 5 - FLUORINE MODELS FOR AIR MIXING AND DISPERSION . . . . .</b>	5-1
5.1 Introduction . . . . .	5-1
5.1.1 Details of $LF_2$ Transport. . . . .	5-1
5.2 Properties of Fluorine . . . . .	5-3
5.2.1 Physical Properties . . . . .	5-3
5.2.2 Chemical Properties . . . . .	5-3
5.3 Release Scenarios. . . . .	5-7
5.3.1 Explosive Release of Fluorine and Flash Vaporization (Scenario A) . . . . .	5-7
5.3.2 Liquid Release and Boiling Pool Source of Vapor (Scenario B) . . . . .	5-8
5.3.3 Flashing of the Liquid Released . . . . .	5-8
5.4 Thermodynamic Model for Fluorine Liquid Aerosol, Vapor, and Humid Air Mixing. . . . .	5-13
5.4.1 Description of the Mixing Phenomenon. . . . .	5-13
5.4.2 Calculation Procedure . . . . .	5-15
5.4.3 Results from the Fluorine - Humid Air Mixing Model. . . . .	5-17
5.5 $LN_2$ and $LF_2$ Pool Boiling Model (Scenario B). . . . .	5-20
5.5.1 Source Rate Calculations. . . . .	5-20
5.5.2 Consideration of Source Rate in Dispersion Model . . . . .	5-22
5.6 Discussion of Results from the Fluorine Dispersion Calculations . . . . .	5-25
<b>CHAPTER 6 - CONCLUSIONS. . . . .</b>	6-1
Hydrogen Fluoride . . . . .	6-1
Fluorine. . . . .	6-2
<b>APPENDIX A . . . . .</b>	A-1,4
<b>APPENDIX B . . . . .</b>	B-1,12
<b>APPENDIX C . . . . .</b>	C-1,12
<b>REFERENCES . . . . .</b>	R-1,3

# LIST OF FIGURES

NO.	DESCRIPTION	Page
2.1	Vapor Pressure/Temperature - Anhydrous Hydrogen Fluoride . . . . .	2-3
2.2	Apparent Molecular Weight of the Vapor Versus Temperature. . . . .	2-4
2.3	Saturated HF Vapor Density vs. Temperature . . . . .	2-4
2.4	Variation of HF-Humid Air Mixture Temperature with Dilution Ratio . . . . .	2-21
2.5	Variation of Fractional Mass of Initial HF Condensed into Aerosol with Dilution Ratio . . . . .	2-22
2.6	Mass Fraction HF Concentration in the Condensed Aqueous (Aerosol) Solution vs. Dilution Ratio. . . .	2-23
2.7	Variation of Mixture Density with Dilution Ratio . .	2-24
2.8	Variation of HF-Humid Air Mixture Temperature with Dilution Ratio . . . . .	2-25
2.9	Variation of Fractional Mass of Initial HF Condensed into Aerosol with Dilution Ratio . . . . .	2-26
2.10	Mass Fraction HF Concentration in the Condensed Aqueous (Aerosol) Solution vs. Dilution Ratio. . . .	2-27
2.11	Variation of Mixture Density with Dilution Ratio . .	2-28
2.12	Variation of Mixture Temperature with Air Dilution for High Temperature HF Release. . . . .	2-30
2.13	Variation of Mixture Density with Air Dilution for High Temperature HF Release. . . . .	2-31
3.1	Wind Velocity Profile. . . . .	3-3
4.1a	Variation of Jet Parameters vs. Dist, Test #1. . . .	4-7
4.1b	Variation of Jet Parameters vs. Dist, Test #2. . . .	4-8
4.1c	Variation of Jet Parameters vs. Dist, Test #3. . . .	4-9
4.2a	Temperature of HF-Air Mixture. . . . .	4-14
4.2b	Temperature of HF- Air Mixture . . . . .	4-15
4.3a	Measured & Predicted Temperature vs. X, Test #1. . .	4-16

# LIST OF FIGURES (contd)

NO.	DESCRIPTION	Page
4.3b	Measured & Predicted Temperature vs. X, Test #2. . .	4-17
4.3c	Measured & Predicted Temperature vs. X, Test #3. . .	4-18
4.4a	Ground Level Concentration vs. Distance, Test #1 . .	4-23
4.4b	Ground Level Concentration vs. Distance, Test #2 . .	4-24
4.4c	Ground Level Concentration vs. Distance, Test #3 . .	4-25
5.1	Cross-Sectional View of Fluorine (Road) Transport Trailer. . . . .	5-2
5.2	Liquid Fluorine (Road) Trailer - Tank System . . . .	5-2
5.3	Schematic Representation of Scenario "A" Type Release of Fluorine. . . . .	5-9
5.4	Schematic Representation of Scenario "B" Type Release of Fluorine. . . . .	5-9
5.5	Fraction Flash vs. Fluorine Temperature in Tank. . .	5-12
5.6	Post Flash Vap-Aerosol Mix Density vs. Tank Temp . .	5-14
5.7	F <sub>2</sub> Air Mixture Thermodynamic Conditions. . . . .	5-18
5.8	F <sub>2</sub> -Air Mixture Thermodynamic Conditions. . . . .	5-19
5.9	Mole Fractions in Vapor vs. Time . . . . .	5-23
5.10	Mass Evaporation Rate vs. Time . . . . .	5-24
5.11	Dispersion under Neutral Stability Fluorine Cloud Released by a Transport Tank Burst . . . . .	5-26
5.12	Dispersion under Stable Weather Conditions of a Fluorine Vapor Cloud Released by a Transport Tank Burst. . . . .	5-26
5.13	Dispersion under Neutral Stability Fluorine Cloud Released by a Transport Tank Breach. . . . .	5-28
5.14	Dispersion under Stable Weather Conditions of a Fluorine Vapor Cloud Released by a Transport Tank Breach . . . . .	5-28



## LIST OF FIGURES (Contd)

B.1	Liquid Mole Fraction with Time . . . . .	B-10
B.2	Vapor Mole Fraction with Time . . . . .	B-11
B.3	Liquid Molar Content of Pool vs Time . . . . .	B-12

## LIST OF TABLES

NO.	DESCRIPTION	Page
2.1	Some Thermodynamic Properties of Anhydrous Hydrogen Fluoride (HF) . . . . .	2-2
2.2	FORTTRAN Subroutine for HF-Humid Air Mixing Thermodynamic Model. . . . .	2-18
2.3	Index to HF and Air Parameters Varied in Different Figures. . . . .	2-19
3.1	Atomic Diffusion Volumes . . . . .	3-11
4.1	Summary of Test Conditions - Goldfish Series of HF Releases . . . . .	4-2
4.2	Test Data and Calculated Flow and Post Flash Conditions of Jet . . . . .	4-3
4.3	Selected Results from Jet Regime Calculations. . . . .	4-11
4.4	Goldfish Test Data for Plume Temperature . . . . .	4-19
4.5	Measured Data on HF Concentrations . . . . .	4-22
5.1	Liquid Fluorine Transport Specifications . . . . .	5-4
5.2	Thermodynamic Properties of Fluorine and Nitrogen. . . . .	5-5
5.3	Fluorine Flash Calculations. . . . .	5-11
5.4	Results of Calculations. . . . .	5-21

#### ACKNOWLEDGEMENTS

This study was undertaken by Technology & Management Systems, Inc. (TMS) under contract # F19628-86-C-0056 from the U.S. Air Force, Electronic Systems Division, PKR, Air Force Systems Command, Hanscom AFB, MA 01731-5260. The Contracting Officer's Technical Representative on this project was Mr. Bruce Kunkel. The project manager and principal analyst at TMS was Dr. Phani K. Raj. He was assisted by other TMS staff including Mr. John Morris, Ms. Cynthia Mullet, and Mrs. Susan Webster. Dr. Robert C. Reid, Professor (Emeritus) of Chemical Engineering, MIT, provided very valuable analyses of the reaction kinetics and thermodynamics.

The TMS team acknowledges with thanks the valuable technical input and guidance provided throughout the project by the Technical Project Monitor, Mr. Bruce Kunkel, of the USAF Geophysics Laboratory, Hanscom AFB. We also thank Captain Mike Moss of the USAF Engineering and Services Center, Tyndall AFB, for providing numerous reports on field tests, and other related information.

**This page is left blank intentionally**

(x)

## EXECUTIVE SUMMARY

The Air Force Dispersion Assessment Model ("ADAM") was developed in 1987 to assess the potential hazard areas arising from the accidental release of several chemicals of interest to the U.S. Air Force ("USAF"). The models developed primarily focused on simulating the dispersion in the atmosphere of vapors and any entrained liquid aerosols. Dispersion regimes in both the heavy gas region and the neutral density region were modeled. Reactions of the chemical with ambient moisture were also modeled and considered in the ADAM programs. The list of chemicals whose dispersion behavior was modeled included i) nitrogen tetroxide, ii) chlorine, iii) anhydrous ammonia, iv) phosgene, v) hydrogen sulphide, and vi) sulfur dioxide. Because of potential hazards associated with USAF and industry handling, storage, and transport of hydrogen fluoride and liquid fluorine, it was decided to add these two chemicals to the list of chemicals in the ADAM code. This report deals with the details of modeling hydrogen fluoride and fluorine dispersion in the atmosphere.

### SCOPE OF WORK

The scope of work described in this report included:

- development/modification of thermodynamic models for the mixing of hydrogen fluoride (HF)-humid air as well as fluorine ( $F_2$ ) - humid air.
- integration of the dispersion models for HF and  $F_2$  into ADAM.
- evaluation of the model results with available field test data.

### PROJECT ACCOMPLISHMENTS

In this project, the relevant thermodynamic properties of hydrogen fluoride and fluorine were gathered, reviewed carefully, and included in the ADAM database. In addition, thermodynamic models were developed to determine the final state of the released chemical (either HF or  $F_2$ ) after mixing adiabatically with humid air of specified mass. These models were incorporated into ADAM. Source models describing the release and formation of the vapor clouds were developed and integrated into ADAM. Finally, the dispersion of HF and  $F_2$  were modeled and included in the ADAM routines. Discussed below are more details of the special behavior properties of the two chemicals considered and analyses performed.

## **HYDROGEN FLUORIDE (HF)**

### **HF Properties**

Anhydrous HF boils at 20 °C at atmospheric pressure. Release of this liquid from tanks at higher than 20 °C results in the formation of vapor by flash vaporization and entrainment of liquid droplets into the vapor. In this project, the detailed physical and chemical properties of HF were gathered, tested, and incorporated into the ADAM database. Also, the flashing of HF has been modeled.

### **HF Thermodynamic Model**

The vapor in equilibrium with liquid at 20 °C comprises a mixture of HF vapors of different molecular weights. This is due to the polymerization (or association) property of HF. A thermodynamic model was developed to determine the vapor mass fractions of the various oligomers in the saturated vapor at 20 °C and from it the density of vapor.

Hydrogen fluoride vapor not only polymerizes and dissociates when mixed with air, but also reacts with the atmospheric moisture. The reaction with moisture is exothermic while dissociation reaction is endothermic. Also, the chemical properties are such that at low vapor pressures and high temperatures the oligomer-to-monomer reaction is favored. Because of this reactivity and associative properties, the final thermodynamic state of a mixture of HF and humid air varies considerably depending on the initial conditions and the amount of air mixed. The final conditions of interest to dispersion are the cloud density, cloud quality, and temperature.

In this project, an elementary thermodynamic model developed by Schotte of DuPont Inc. was modified to extend its range of applicability both in HF initial temperature and HF concentration. Some of the HF property correlations were modified to enhance both the accuracy of prediction and the use in a computer program for quick convergence. The modified thermodynamic model for the mixing of anhydrous HF (which may or may not contain aerosols) with humid air is discussed in Chapter 2. The temperature range of applicability of the model has been extended to an initial HF temperature of 1000 K.

The thermodynamic model calculates the final mixture conditions given HF initial conditions, temperatures and relative humidity of atmospheric air and the mass of air mixed with a unit mass of HF. These final conditions include the mixture density and temperature, mass fractions in vapor and liquid phases, and mass and mole fractions of individual species of HF (various oligomers) in vapor and liquid phases. The model results have been compared with results from a model developed by Clough, et al. The agreement is good. No experimental data are available to check the predictions of the thermodynamic model over the full range of HF concentrations and temperatures.

## HF Dispersion Model

The HF-Air thermodynamic model has been integrated into the ADAM code. The dispersion results from ADAM have been tested against the data from a single series of field tests. These tests, called the Goldfish Series, were conducted by an industry consortium headed by Amoco, Inc. Three dispersion tests with anhydrous HF releases were conducted in a desert environment.

The ADAM results for the conditions of the test and experimental data are compared in Chapter 4. The data and results compared include the i) source rate, ii) plume temperature, and iii) variation of centerline ground level concentration with downwind distance.

It is seen that the measured and predicted source rates agree very closely. The measured minimum temperatures at various downwind locations and those predicted at the same locations agree reasonably close. Some of the temperature data from the test may not be accurate because their values are below what are predicted by the thermodynamic model.

The overall trend in the predicted concentration variation with distance agrees closely with the test data. The numerical agreement in the predicted vs. measured concentration data are close within a factor of 2 in Tests #1 and #3 and within a maximum deviation of a factor of 5 in Test #2. A number of reasons as to why there are discrepancies in the predicted vs. measured data values are discussed in Chapter 4. Some of the errors may be due to significant scatter in the concentration data reported from the tests. Overall, however, ADAM predictions are reasonable representation of the test results within the accuracy needed for hazard area estimation.

## FLUORINE ( $F_2$ )

### $F_2$ Properties

Fluorine is a highly reactive chemical which is in the gaseous state at ambient pressure and temperature. It boils at 84.5 K at ambient pressure and is highly reactive with most substances. Fluorine at normal temperatures reacts with water (vapor or liquid) forming the fluorides of hydrogen and oxygen. However, there is no evidence of occurrence of this reaction when the fluorine temperature is at or near its boiling point (84.5 K).

Fluorine is normally shipped as a liquid in double-tanked road or rail tankers. The outer tank contains liquid nitrogen (at 77.4 K) which maintains the  $F_2$  as a liquid in the inner tank. Nitrogen temperature is maintained at its boiling point by allowing a small amount of evaporation to be vented to the atmosphere.

## **F<sub>2</sub> Release Scenarios**

Two release scenarios have been considered in this report, namely, the tank burst scenario ("Scenario A") and the tank breach scenario ("Scenario B"). The former is assumed to occur when, due to an accident, the outer tank is breached and all of the liquid nitrogen is lost. The inner tank heats up and when the internal fluorine pressure reaches the tank failure pressure all of the fluorine is released instantaneously. The fluorine released flashes forming a cloud of vapor and liquid aerosols at a temperature of 84.5 K. Also, the violence of release will entrain air from the ambient. It is assumed that the amount of air entrained is about 10 times the volume of the vapor volume produced.

In Scenario B, the breach occurs simultaneously in both the outer and inner tanks leading to the release of both liquid nitrogen and liquid fluorine. These liquids form a pool on the ground and evaporate, rather quickly, because of the very cold temperature of each liquid. It is estimated that the liquid pool formed by the release of the entire contents of a road tanker of fluorine will evaporate within 13 seconds. The initial vapor cloud formed will consist of only vapors of fluorine and nitrogen (at 77.4 K).

## **F<sub>2</sub> Thermodynamic Model**

The mixing of humid air and cold fluorine vapor containing liquid aerosols has been modeled. It is assumed that there are no chemical reactions between the water and fluorine because of the very cold temperature. The condensation and freezing of water vapor has been accounted for. Also, the evaporation of the fluorine liquid aerosols has been modeled. In the case of mixing of pure vapor, initially diluted with nitrogen vapor a similar thermodynamic modeling approach as that above is used. The final thermodynamic state of the mixture is determined and used in the subsequent dispersion calculations.

It is seen that the density of fluorine vapor at saturated condition at ambient pressure is about 5.5 kg/m<sup>3</sup> which is about 5 times the density of air. The presence of liquid aerosols and condensed or frozen water makes the cloud even heavier. The mixture density decreases monotonically with increased air dilution in both the aerosol case and in the initial vapor case.

## **F<sub>2</sub> Dispersion Model Results**

We have calculated the dispersion behavior of fluorine released under scenario A and scenario B. In each case, the release is assumed to be from the road tanker. It is further assumed that both releases could be classified as "instantaneous" releases because in scenario B the duration of evaporation of the pool formed on the ground is extremely short.

The short term exposure (concentration) limit for fluorine is very low, and is 1 ppm. It is seen that the dispersion distances to achieve this level of concentration are very large, in tens of kilometers! This is because not only is the entrainment reduced due to the very heavy (and therefore stratified) cloud, but also the degree of dilution required is of the order of magnitude  $10^6$ . In the case of neutral atmospheric condition at release, the hazard distance is calculated to be greater than 20 km, and in the case of stable condition, the same distance increases to 60+ km! These results imply that during a significant portion of the dispersion the cloud can be considered to be neutrally buoyant. As a matter of fact, the downwind hazard distance can be calculated with the simple point source Gaussian model without losing much accuracy.

## CONCLUSIONS

Based on the work indicated in this report, it is concluded that:

1. The thermodynamic model developed for HF is robust and is applicable over a wide range of HF temperatures (290 K to 1000 K) and initial conditions (pure vapor, vapor mixed with liquid aerosols) and atmospheric humidity conditions (0% to 100% relative humidity).
2. While the reactivity of  $F_2$  is very high at ordinary temperatures, it is unlikely to have any reactions with water vapor in the atmosphere when released from a saturated liquid condition.
3. The integration of the source models and atmospheric dispersion models for both HF and  $F_2$  into ADAM has been accomplished successfully.
4. The ADAM predicted concentration variation with downwind distance agrees reasonably well with data from HF field tests.
5. Disagreements between HF test data and predictions have been discussed and explained to the extent possible (with publicly available information).
6. There are no experimental dispersion data for  $F_2$  with which to compare the ADAM results. Hence, no comparisons have been made.



**This page is left blank intentionally**

## CHAPTER 1

### INTRODUCTION

#### 1.1 Background

The hazards of toxic vapors arising from the accidental releases of chemicals have received considerable public attention because of the potential for affecting large areas and large numbers of people. A number of experimental studies and mathematical modeling analyses have been undertaken both in the U.S. and abroad. Research is continuing to understand various aspects of the dispersion of chemicals including modeling different types of chemical sources, effect of properties of chemicals on the dispersion phenomenon, effects of terrain and obstructions in the path of dispersing clouds/plumes, etc. The study documented here forms part of the continuing research efforts sponsored by the U.S. Air Force (USAF) to understand and model chemical vapor dispersion so that both contingency planning and emergency response can be effectively implemented.

Until a decade ago, most of the mathematical models used for gas concentration predictions were based on Gauss's theory of diffusion of ensemble of particles (the "Gaussian Model"). It has become obvious, from the several field experiments involving the release of heavy gases, that the conventional approach of using the Gaussian model to describe the dispersion behavior of gases and vapors that are heavier than air ("heavy gases") leads to significantly distorted results for the hazard area, downwind distance extent of hazard and the duration of the hazard. The vapors of many chemicals that are handled by the USAF are heavier than air. Some of the chemicals, when released from containment, form liquid aerosols which adds to the negative buoyancy of the vapor clouds. Some may even react with the ambient moisture or polymerize upon release into air forming new species.

A heavy gas dispersion model was recently developed under the sponsorship of the USAF (Raj and Morris, 1987). This model, called the Air Force Dispersion Assessment Model (ADAM), models the release of liquid or gaseous chemicals into the environment, and the dispersion of the vapor clouds formed taking into consideration the negative buoyancy caused by gas density and the density of liquid aerosols, if any. The model also takes into account the effects of any chemical reaction with the ambient moisture. The model has been tested against several field test results and found to give reasonable estimates of the cloud behavior and concentration contours. ADAM is expected to be used in conjunction with the Air Force Toxic Chemical Dispersion Model ("AFTOX"). The original version of ADAM contains the behavior models for six (6)

chemicals, nitrogen tetroxide, phosgene, ammonia, chlorine, hydrogen sulphide and sulphur dioxide.

The ADAM code is versatile in that the dispersion of vapors of chemicals that are not a part of the original six chemicals can be incorporated into the model provided the physical and chemical properties of the chemicals are provided in the ADAM database. In addition, if the chemical is reactive or exhibits other types of behavior, then it is necessary to develop thermodynamic/reaction models for incorporation into ADAM. Two chemicals of interest to the USAF, namely, hydrogen Fluoride (HF) and fluorine ( $F_2$ ) were added to the list of chemicals in ADAM. HF is used in lasers and in alkylation units in the petroleum industry.  $F_2$  is transported in bulk quantities as a liquid in highway and rail tankers.

This report documents the mathematical models developed to simulate the dispersion of HF and  $F_2$  in the atmosphere. The thermodynamic and reactive properties of the two chemicals are indicated in the report and these have been considered in the dispersion models.

## **1.2 Hydrogen Fluoride and Fluorine**

### **1.2.1 Hydrogen Fluoride**

The dispersion behavior of hydrogen fluoride in the atmosphere is very complex. HF has the property of molecular association and dissociation. Depending on the temperature and HF partial pressure, the HF forms a mixture of monomers and high molecular weight polymers. In addition, HF can react with moisture in the atmosphere forming aqueous HF. These properties have profound effects on the density of the dispersing cloud and hence on the process of dispersion.

Large quantities of HF are transported in bulk tanks as an anhydrous liquid. The normal boiling point of HF is 20° C. Shipments of HF are made both by rail and highway. Rail tank car sizes are 20 ton, 40 ton and 80 ton, whereas highway shipments are generally in 20 ton quantities. Occasionally, HF is transported in a variety of cylinder sizes (200 lb., 850 lb., 1300 lb., etc.). Tanks are of single skin construction with no insulation. Liquid valves (generally two for each tank) dip into the liquid space and the vapor vent valves are at the top of the tank. In general, the valves are all 1-inch size (nominal).

Any leak from a tank at a temperature greater than 20° C will lead to flash vaporization of a part of the liquid. Also, some liquid aerosol may be entrained into the dispersing vapor cloud resulting in the formation of a stratified, negatively buoyant intrusion layer in the atmosphere.

### 1.2.2 Fluorine

Fluorine is a very reactive element; it combines with most organic and inorganic materials at or below normal temperature. Reactions with organic materials is highly exothermic; hydrogen containing compounds react with fluorine explosively. While this element reacts with water or water vapor at ambient temperature to form oxygen fluoride and hydrogen fluoride, it is uncertain whether such reactions are possible at very low temperatures.

Fluorine is transported in bulk as a liquid at very low temperatures (at liquid nitrogen temperature) and ambient pressure.  $F_2$  boils at about 85 K at normal atmospheric pressure. Normally, about 2260 kg (5,000 lbs) of fluorine is carried in each road tanker. The chemical is maintained in a cryogenic liquid state by surrounding the fluorine tank with a liquid nitrogen jacket. About 1.3 m<sup>3</sup> of liquid nitrogen ( $LN_2$ ) surrounds the liquid fluorine ( $LF_2$ ) and is maintained at 77 K temperature by venting the nitrogen boil-off.

Because of the double tank construction of the road transport, accidental releases of  $F_2$  can occur only due to puncture of both  $LN_2$  and  $LF_2$  tanks. A loss of  $LN_2$  cooling can result in the heating up of  $LF_2$  ultimately resulting in a tank burst and the release of the entire  $F_2$  content explosively. In this latter release scenario, fluorine vapor and liquid aerosols are formed and a two-phase vapor cloud will disperse in the atmosphere. This vapor cloud is very cold at release (85 K) and will condense the water vapor from the ambient into ice. It is uncertain whether there will be any reaction between the  $F_2$  and condensed water.

The original version of ADAM did not treat the dispersion of HF or  $F_2$ . The development of the appropriate thermodynamic and dispersion models for both chemicals and their integration into ADAM is described in this report. In addition, several improvements to the ADAM program and the correction of certain features was undertaken in this study and these changes are also documented.

### 1.3 Objectives of the Work

The objective of the work was to:

- o develop appropriate thermodynamic and dispersion models to describe the dispersion behavior of (each of) hydrogen fluoride and fluorine chemicals released accidentally.
- o integrate the models into the ADAM system.

#### 1.4 Scope of Work

The following tasks were performed in order to achieve these objectives:

1. HF-humid air thermodynamic models available in the literature were reviewed. The model selected was improved by expanding its applicability to a wider range of conditions.
2. The HF-thermodynamic program was integrated into ADAM.
3. Fluorine release/source models were developed.
4. Thermodynamic model describing the mixing of cold fluorine two-phase mixture with ambient air was formulated and solved.
5. The  $F_2$  release model, thermodynamic model, and dispersion model were integrated into ADAM.
6. Routines in ADAM related to the determination of atmospheric stability were improved.
7. ADAM was modified to take into consideration large aerodynamic roughness effects.
8. The input and output features of ADAM were substantially improved to make them very user friendly.

#### 1.5 Organization of the Report

The general physical and chemical properties of hydrogen fluoride (HF), as they relate to the dispersion, are discussed in Chapter 2. Included in Chapter 2 are the details of the thermodynamic model for the hydrogen fluoride - moist air system and results from the thermodynamic model. The modifications made to the ADAM code are discussed in Chapter 3 including the improvements to the ADAM input panels. The results from ADAM using the Goldfish (HF) field tests release data are compared with sparse data available from the tests in Chapter 4.

The fluorine ( $F_2$ ) models are discussed in Chapter 5. In this chapter are given the details of fluorine transport, fluorine properties, release scenarios, the thermodynamic model for fluorine mixing with humid air, etc.

Also discussed are the results from the dispersion model.

Discussions, conclusions, and recommendations are indicated in Chapter 6.

Several appendices are also included. These provide additional details of the model derivations, chemical property database listings and FORTRAN source codes for the thermodynamic model. In Appendix A is illustrated the calculations of HF flashing. The distillation and evaporation of the two liquid ( $LF_2$  and  $LN_2$ ) pool is described in Appendix B. The printout of the thermodynamic properties of hydrogen Fluoride and fluorine are given in Appendix C.

**This page is left blank intentionally**

## CHAPTER 2

### HYDROGEN FLUORIDE - MOIST AIR MIXING

#### THERMODYNAMIC MODEL

In this chapter, we present a thermodynamic analysis to predict the physical state, temperature and density of a mixture of anhydrous hydrogen fluoride (HF) and humid air. First, we discuss the physical and chemical properties of HF followed by the presentation of the details of the thermodynamic model.

#### 2.1 Anhydrous Hydrogen Fluoride Physical Properties

Hydrogen fluoride (HF) is an extremely reactive chemical which is gaseous at ordinary temperatures (above 20° C) and atmospheric pressure. HF, also known as hydrofluoric acid, is a very strong acid which can severely burn skin and eyes and may be fatal if swallowed. Liquid anhydrous HF and water solutions above 70% HF fume copiously and these fumes can be dangerous to skin, eyes, and the respiratory system (Allied, 1978). Liquid and gaseous forms of HF, both anhydrous and aqueous, are colorless.

Anhydrous HF is rather unique among hydrogen halides, especially with respect to one property: its tendency toward association or polymerization. In both the liquid and gaseous states, anhydrous HF is believed to exist mostly as a polymer, though at high temperatures and low pressures, the average molecular weight of anhydrous HF gas may approach that of the monomer. At this time, there is conflicting evidence as to the nature of associated HF molecules. Some information suggests open chains while other information suggests cyclic forms or combinations of the two. Nevertheless, it is generally agreed that the degree of association is increased in the gaseous state as HF goes from high temperature or low pressure toward low temperature or high pressure or into a liquid state. The association property of anhydrous HF gas and other factors cause it to behave in a manner quite different from that of an ideal gas. Therefore, even the property measurements and characterizations are difficult.

The physical and chemical properties available in the literature are summarized in Table 2.1. Figure 2.1 shows the vapor pressure-saturation temperature relationship. The normal boiling point is 19.54° C which means the chemical is in a liquid for most transportation conditions. Figure 2.2 shows the variation of apparent molecular weight of HF vapor as a function of temperature and pressure. From the figure, it can be seen that saturated HF vapor at the normal boiling point has an apparent molecular weight of 68 kg/kmol which is about 3.5 times the molecular weight of the



TABLE 2.1

SOME THERMODYNAMIC PROPERTIES OF  
ANHYDROUS HYDROGEN FLUORIDE (HF)

PROPERTY	PROPERTY VALUES IN		
	SI UNITS	FPS UNITS	OTHER UNITS
Molecular Weight	20.0064 kg/kmol	20.0064 lb/lb mol	
Boiling Point at Pressure	292.69 K	62.4 °F	19.54 °C
Critical Density	290 ± 30 kg/m <sup>3</sup>	18.1 ± 1.9 lb/ft <sup>3</sup>	0.29 ± 0.03 g/cc
Critical Pressure	(64.862 ± 3.378) × 10 <sup>5</sup> N/m <sup>2</sup>	941 ± 1.9 lb/ft <sup>2</sup>	
Critical Temperature	461.15 ± 3 K	370 ± 5 °F	188 ± 3 °C
Density of Liquid at 20°C	973.5 kg/m <sup>3</sup>	8.124 lb/gal	0.9735 g/cc
Freezing Point	189.78 K	-118.07 °F	-83.37 °C
Heat of Formation of Ideal Gas at 25°C	-13.584 MJ/kg	-5840 Btu/lb	-3.245 kcal/g
Heat of dilution to 80% aqueous	381 kJ/kg	----	----
Heat of dilution to 50% aqueous	731 kJ/kg	----	----
Heat of Fusion at Melting Point	196.48 kJ/kg	84.47 Btu/lb	46.93 cal/g
Heat of Vaporization at NBT	208.06 kJ/kg	161.01 Btu/lb	89.45 cal/g
Specific Heat of Liquid at NBT	2524.16 J/kg K	0.603 Btu/lb °F	0.603 cal/g °C
Surface Tension at NBT	8.6 × 10 <sup>-3</sup> n/m	----	8.6 dyne/cm
Surface Tension at 0°C	10.2 × 10 <sup>-3</sup> n/m	----	10.2 dyne/cm
Refractive Index at 25° (and 5892.6 Å)	1.1574	----	----
Toxic Concentrations of Vapor			
Threshold Limit Value	3 ppm (2 mg/m <sup>3</sup> )		
Detectable by Smell	2 to 3 ppm		
Throat Irritation Threshold	5 ppm		
Dangerous for Short Term Exposure	50-250 ppm		

## Sources of Data:

- 1) Allied (1978)
- 2) Chem Ind Assn (1978)

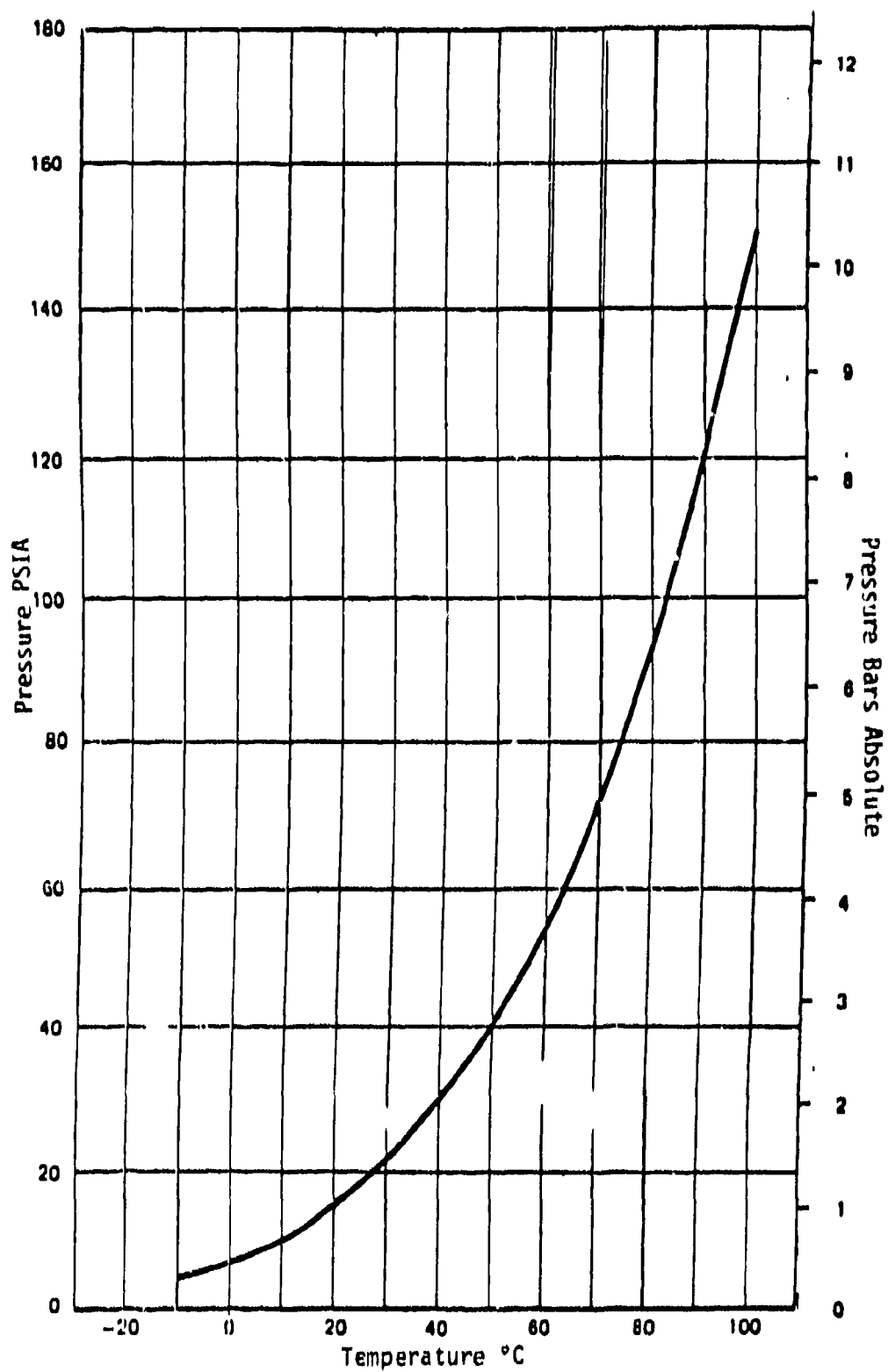


FIGURE 2.1: VAPOR PRESSURE/TEMPERATURE - ANHYDROUS HYDROGEN FLUORIDE

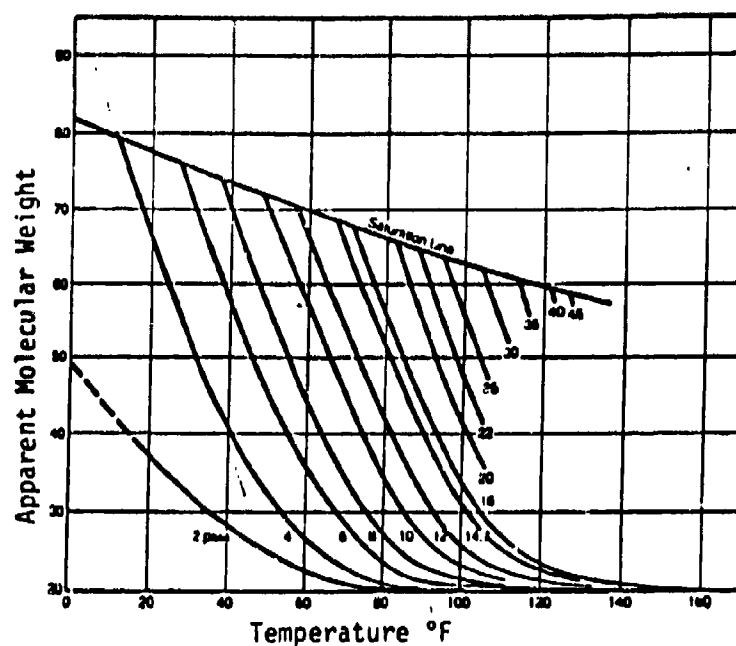


FIGURE 2.2: APPARENT MOLECULAR WEIGHT OF THE VAPOR  
VERSUS TEMPERATURE

Source: Allied (1976)

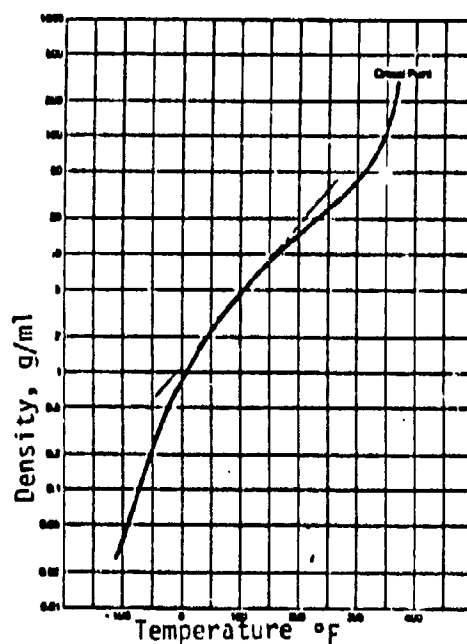


FIGURE 2.3: SATURATED HF VAPOR DENSITY  
VS. TEMPERATURE

Source: Allied (1978) 2-4

monomer! Figure 2.3 shows the variation of saturated vapor density with temperature. Saturated vapor at the normal boiling point has a density of  $3 \text{ kg/m}^3$  (about 2.5 times the density of air at  $20^\circ \text{C}$ ).

## 2.2 Physical Processes in HF-Humid Air Mixing

In this section, we discuss the physical processes occurring during the mixing of anhydrous HF at specified conditions with humid air of a given mass at specified temperature and relative humidity. The mixing is assumed to occur at constant pressure.

### 2.2.1 Description of the Problem

For an accidental release of HF, the source of the escaping chemical is a storage vessel containing gaseous and liquid HF. There may be an inert gas such as nitrogen in the HF source tank, but this inert is neglected in the calculations as it would only appear as a transient component in any large HF loss. The released HF may be either a vapor or a mixture of vapor and liquid. We assume any liquid lost from the tank is carried as aerosol droplets and is well distributed in the HF vapor phase. Since, at one bar, HF boils at about  $19.5^\circ \text{C}$  ( $292.7 \text{ K}$ ), if any liquid were present in the leaking HF and the ambient temperature is greater than  $19.5^\circ \text{F}$ , the temperature is set at  $19.5^\circ \text{C}$  due to flash expansion cooling. For releases containing only HF vapor, the temperature must be  $19.5^\circ \text{C}$  or greater.

Thus the initial input to the problem provides the specification of:

- o total mass flow of HF
- o fraction of the flow that is liquid
- o temperature of the HF. If liquid is present and the ambient temperature is  $19.5^\circ \text{C}$  or greater, the temperature is set to  $19.5^\circ \text{C}$

The HF accident is assumed to occur into a one bar environment.

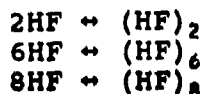
Upon release of the HF, ambient air is entrained. The conditions of the air that must be specified are:

- o mass ratio (total air/total HF)
- o air temperature
- o relative humidity of the air

The thermodynamic analysis assumes that the only independent variable is the mass ratio, i.e., for all possible end states, each increment of the air mixed in has the same temperature and relative humidity.

### 2.2.2 Hydrogen Fluoride Polymerization

One of the complications when dealing with hydrogen fluoride (with or without air dilution) is that the actual "chemical" state of the HF is not that of a simple species but, due to the interactions between HF molecules, the true state is a mixture of oligomers. The predominant components of this mixture, besides the monomer, are the dimer  $(\text{HF})_2$ , the hexamer  $(\text{HF})_6$ , and the octamer  $(\text{HF})_8$ , i.e.,



where the double arrows indicate that a chemical equilibrium is attained.

The presence of such oligomers in the HF affects the volumetric properties of the vapor, i.e., as more of the higher oligomers are formed, the volume occupied by a given mass of HF decreases. The oligomer concentration varies with pressure (and dilution) as well as with temperature. As the pressure is lowered - or as the fraction of air increases so as to decrease the partial pressure of HF - the distribution of oligomers shifts toward the lighter entities. As a limit, at very low HF pressures, only HF monomer remains.

Similarly, as the temperature increases, the distribution changes to more of the smaller oligomers. Thus one can infer that the breaking of oligomers is an endothermic process whereas the formation is exothermic.

Knowing this, one can begin to visualize the interplay between air dilution and oligomer distribution. For example, if dry air were mixed with HF vapor (no liquid) as a simple case, the dilution process would decrease the fraction of higher oligomers and, in so doing, endothermic reactions would cause a drop in the mixture temperature until a new equilibrium state was achieved.

Therefore, any thermodynamic model must have the ability to track the HF oligomer distribution to maintain chemical equilibrium at the system temperature and HF partial pressure.

### 2.2.3 Aqueous HF Aerosols

Water and HF are miscible in all proportions and form aqueous non-ideal solutions that show negative deviations from Raoult's law. What results physically are solutions in which the partial pressures of both water and HF are depressed below what might be expected from Raoult's law. (Raoult's law states that the component partial pressures are equal to the liquid mole fraction multiplied by the pure component vapor pressure.) The consequences of such behavior are that aqueous HF aerosols are readily formed when humid air encounters HF vapor. This process removes water and HF from the vapor phase, liberates energy due to the phase change of condensation, and increases the density of the resulting

vapor-aerosol mixture. The concentration of water and of HF in the aerosol as well as the extent of condensation can vary over a wide range. As in any thermodynamic analysis, one must allow for such events in energy, mass, and volume balances to be certain that the mixture is in vapor-liquid equilibrium.

#### 2.2.4 Adiabatic vs. Non-adiabatic Mixing

Most models of the mixing of air with a released chemical assume there is a negligible loss or gain of energy from the environment. Assuming this is true since the pressure is constant during the entrainment of air, one would base the thermodynamic analysis on the conservation of enthalpy of the species involved, i.e.:

$$H \text{ (HF)} + H \text{ (wet air)} = H \text{ (mixture)} = \text{constant} \quad (2-1)$$

where  $H \text{ (HF)}$  and  $H \text{ (wet air)}$  represent the total enthalpies of the HF and wet air streams before mixing whereas  $H \text{ (mixture)}$  would be the total enthalpy of the final mixture. Equation (2-1) will form the basis of the thermodynamic analysis to follow.

However, if one desired to include energy losses or gains from the environment during mixing, Equation (2-1) would be modified to

$$H \text{ (HF)} + H \text{ (wet air)} + Q = H \text{ (mixture)} = \text{constant} \quad (2-2)$$

where  $Q$  is positive if energy is added to the cloud and negative if energy is lost. The value of  $Q$  is associated in some manner with the mixing ratio.

We note that while enthalpies are state functions and are independent of the path between the initial and final states, the parameter  $Q$  is clearly related to the history of the cloud from the initial states of anhydrous HF and wet air to the final mixed state. The "path" of the cloud with mixing ratios from 0 to some final value affects the magnitude of  $Q$ . Normally, however, this path specific property is ignored and the value of  $Q$  employed is based on "average" cloud properties.

#### 2.2.5 Summary of the Principal Assumptions

Several assumptions have been noted or inferred in the discussion to this point. We summarize these below.

- o the hydrogen fluoride source is chemically pure, anhydrous HF; vapor or vapor plus liquid may be present.
- o the HF is mixed with constant temperature, constant relative humidity air to form a well-mixed cloud that is in chemical equilibrium with respect to the HF oligomers and in phase equilibrium with respect to the HF-H<sub>2</sub>O aerosols. All kinetic steps are instantaneous in nature and no supersaturation states are allowed.

- o the entire mixing process is isobaric. If adiabatic, the total enthalpy of the system is conserved [Equation (2-1)]. If energy is allowed to enter from the environment, the enthalpy conservation relation is modified [Equation (2-2)].

### 2.3 Review of Existing Thermodynamic Models

Two thermodynamic models have been developed to treat the mixing of hydrogen fluoride and wet air. These will be compared and contrasted below. However, as they differ primarily in the nature of the property correlations employed and in the computer logic, it is convenient to introduce the general program outline separately so as to be able to emphasize the logic of the approaches. Later, when examining specific treatments, the differences can be more readily appreciated.

Recall that in Section 2.1 we indicated the general problem was to calculate the physical composition of a mixture of HF and humid air based on utilizing as input

- HF (flow, fraction liquid, temperature)

and

- Air (flow, temperature, relative humidity)

To achieve a solution, we employ Equation (2-1) or Equation (2-2).

Step 1: We first must decide if the final state is all vapor or whether there are aqueous HF aerosols present. To accomplish this, we assume that initially there are no aerosols present. If this assumption is proved false, then we begin again but with the knowledge that aerosols are present.

Beginning with the assumption of no aerosols, a final temperature is assumed. From the mixing ratio and input air relative humidity, the final partial pressures of HF and  $H_2O$  are computed. Note that at this stage all components are assumed to be in gaseous phase. Using the assumed temperature and effective HF partial pressure after dilution, the oligomeric distribution in the HF is calculated. Comparing the component distribution with that in the initial HF, the degree of the oligomer reactions is found. An enthalpy balance is carried out between the initial and final states employing heats of reaction and heat capacities of the various components. Closure of the enthalpy balance indicates that the correct final temperature was assumed. Non-closure requires a new choice of final temperature and the computations are repeated until there is closure.

Having a solution for the single phase (vapor) case, one now tests to ascertain if a liquid phase could exist. In all cases, vapor-liquid equilibrium correlations for HF and water may be expressed, in general, as

$$p_{HF} = f_1(T, x_{HF}) \quad (2-3)$$

$$p_w = f_2(T, x_{HF}) \quad (2-4)$$

where  $p_{HF}$  is the effective partial pressure of hydrogen fluoride in the vapor phase based on the monomer molecular weight,  $p_w$  is the partial pressure of water vapor in the gaseous phase,  $T$  is the temperature, and  $x_{HF}$  is the mole fraction hydrogen fluoride in the liquid phase (again with the monomer molecular weight). The form of the functions  $f_1$  and  $f_2$  in equations (2-3) and (2-4) have been developed empirically from experimental data. In the present situation, values of  $T$ ,  $p_{HF}$  and  $p_w$  are available (with the assumption of no liquid present).

Testing for a liquid phase can be accomplished in various ways. As an illustration, suppose one employed Equation (2-3) to compute  $x_{HF}$ , knowing  $T$  and  $p_{HF}$ . Then, using this value and the known value of  $T$ , with Equation (2-4), one determines an expected value of the water vapor partial pressure. Let this calculated water vapor pressure be  $p_w^*$ . The liquid test is then

if  $p_w^* > p_w$ , a liquid phase exists

if  $p_w^* < p_w$ , no liquid phase exists

If no liquid phase exists, the problem is solved and the computed temperature and vapor phase compositions are employed to estimate the cloud density. However, if a liquid phase exists, the calculations in Step 1 are invalid and one proceeds to Step 2.

**Step 2:** We now know that HF-water aerosols are present in the HF-air cloud, but we do not know their extent or composition. Nor do we know the mixture temperature. The computational procedure becomes more complex, but, in essence, a double trial and error technique is initiated wherein both the final temperature and final HF composition in the aerosol are assumed. Then, employing the enthalpy balance (Equation 2-1 or 2-2), the phase equilibrium relations (Equations 2-3 and 2-4), the chemical equilibrium relationships for the various HF oligomers in the vapor, along with mass balances, one can arrive at a solution.

This computational procedure has been used by Clough and his colleagues at the Health and Safety Executive in Great Britain (Clough et al., 1987a,b) and by Schotte (1987, 1988) at duPont in the United States.

Models developed by both Clough et al. and by Schotte are acceptable. The original Schotte model (1987) was limited to HF concentrations below 20 mole percent HF, but the range was later expanded to cover 0 to 100% HF. Also, the Schotte model lacks a satisfactory single phase methodology, but the model was originally developed to treat cases where HF aerosols would be present. As noted later, the TMS version of the Schotte model does have single phase capabilities. Both the Clough et al. and Schotte models have temperature limitations in that the vapor-liquid equilibrium data



upon which the correlations were based did not exceed about 60°C.

In treating the vapor-equilibrium of HF and water, as noted earlier, the system is highly non-ideal and exhibits negative deviations from ideal-solution behavior. A number of investigators have studied this system (Munter et al., 1947, 1949; Vieweg, 1963; Tyner, 1949; Brosheer et al., 1947; and Johnson et al., 1973). Schotte (1987) correlated the experimental data in equation form to relate the partial pressures of both water and HF to temperature and mole (or weight) fraction HF in the liquid. The partial pressures of HF were based on an effective mole fraction HF as shown later in Eq. (2-14). Clough et al. (1987a,b) have treated aqueous HF solutions by standard phase equilibrium relationships and employed a three parameter correlation for the activity coefficients as a function of temperature (Wheatly, 1985). The parameters were assumed composition dependent. Values of the coefficients are tabulated in their paper. Comparing calculated vs. experimental partial pressures of HF and water over a wide temperature range, the relations given by Schotte were shown to be significantly more accurate.

In the enthalpy balances, Schotte (1987, 1988) computed the specific enthalpy of an aqueous HF solution relative to the enthalpies of pure vapor HF and H<sub>2</sub>O at a reference temperature of 25°C. The appropriate quantities of HF and H<sub>2</sub>O were first condensed and then mixed. The enthalpy of mixing was obtained from data by Johnson et al. (1973). Then the solution temperature was raised (lowered) from 25°C to the desired value using solution heat capacities reported by Thorvaldson and Bailey (1946), Kozhevnikov et al. (1982), and Franck and Spalthoff (1957).

In contrast, Clough et al. (1987a,b) employed their activity coefficient correlation and, by differentiation with respect to reciprocal temperature, were able to obtain partial molar enthalpies and, also, solution enthalpies as a function of composition and temperature.

When comparing calculated enthalpies of mixing (Schotte, 1988) vs. the experimental results of Johnson et al. (1973), Schotte's method was shown to be more accurate. An illustrated comparison is shown in the table below.

# Enthalpy of Mixing, J/mole HF

$x_{HF}$	Experimental	Calculated	
	Johnson et al. (1973)	Clough et al. (1987a,b)	Schotte (1988)
0.0909	-18,500	-24,700	-18,690
0.2000	-17,900	-24,300	-18,100
0.3333	-16,670	-22,900	-16,750
0.4000	-15,840	-21,760	-15,800
0.5000	-14,210	-19,600	-14,100

As noted earlier, HF in the vapor phase is comprised of oligomers. Clough et al. (1987a,b) only considered the monomer, dimer, and hexamer forms whereas Schotte (1987, 1988) expanded the list to include octamers and an  $(HF \cdot H_2O)$  complex suggested by Thomas (1975). Chemical equilibrium constants for these reactions are given by Schotte (1987) and by Clough et al. (1987). In essence, these values were derived from vapor density data for HF assuming it to be composed of an ideal-gas mixture of HF,  $(HF)_2$ ,  $(HF)_6$ , and, possibly,  $(HF)_8$  and  $(HF \cdot H_2O)$ . Other studies include those of Rushmere (1954), Maclean et al. (1962), Vanderzee and Rodenburg (1970), Jarry and Davis (1953), and Armitage et al. (1963). There is good agreement between the two models for the chemical equilibrium constants and for the enthalpies associated with the reactions.

In the two models, other physical properties are necessary. Vapor heat capacities (or enthalpies) are required for all components as a function of temperature. The vapor phase is normally considered an ideal-gas mixture so vapor enthalpies of mixing or compressibility factor deviations are not required. The HF is normally treated as the monomer and polymerization effects are considered separately. For both HF and water, vapor pressures, liquid densities, and phase change enthalpies are also needed. There are many sources of reliable data for the required properties in this group, e.g., Reid et al., (1987), Sheft et al., (1973), Allied Chem. Corp. (1978), Jarry and Davis (1953), Yabroff et al., (1964), and Vanderzee and Rodenburg, (1970, 1971). In comparing the two models, there is reasonable agreement between the physical properties employed although the heat capacity of water vapor (at constant volume) as used by Clough appears to be far too small (3.04 J/mole K). In running any comparisons, this heat capacity was increased to 25.9 J/mole K.

Schotte (1988) has made a few comparisons between the results of his model and that of Clough et al. (1987a,b). In Figure 2.4, calculated cloud temperatures are shown for both models for a case wherein HF vapor (no liquid) at 19.5°C was mixed with air at 20°C and 50% relative humidity. The agreement between the two models is excellent. In Figures 2.5 to 2.7, for the same case, comparisons are made for the fraction of HF which condensed into the aerosols, the computed aerosol compositions and for the cloud densities. In all cases, the results from both models are in good agreement.

Figures 2.8 through 2.11 show similar results for a case in which HF containing 50% liquid is mixed with air at 20°C and 95% relative humidity. As before, there is surprisingly good agreement between the two models.

In conclusion, it would appear that either model could have been selected to serve as the basis to develop the TMS version of the HF-wet air mixing model. However, because the Schotte case seems to provide more accurate physical property correlations, we chose this model for further development.

### 2.3.1 TMS Modification to the Schotte Model

The Schotte model is discussed below. The TMS version of this model differs in four areas.

- o addition of a separate subroutine to test whether only the vapor phase exists and to calculate the final temperature, vapor composition, and cloud density of the vapor only mixture.
- o addition of a subroutine to model the mixing of high temperature HF gas (1000 K).
- o providing an option to have an energy gain or loss during the mixing of the HF with humid air.
- o changes were made to incorporate the model into ADAM.

### 2.3.2 Schotte (1988) Correlations

The modifications to the Schotte model are presented after the basic model structure and correlations are described. It should be noted that the Schotte model as presented is significantly different from the one originally published (Schotte, 1987) and is contained in an internal duPont document that was made available to TMS (Schotte, 1988).

### Partial Pressures of HF and Water over Aqueous Solutions

The following equations are correlations used to calculate partial pressures:

$$\ln p_{HF} = A_{HF} + B_{HF}/T \quad (2-5)$$

$$\ln [p_w/(1-x_{HF})] = A_w + B_w/T \quad (2-6)$$

where  $p_{HF}$  and  $p_w$  are partial pressures in mm Hg,  $T$  is in Kelvin, and  $x_{HF}$  is the mole fraction of HF in the liquid.  $x_{HF}$  is based on the monomer molecular weight (20.01). The valid temperature range of the correlations is 0 to 60°C.

The coefficients in Equations 2-5 and 2-6 are determined using the following correlations:

$$A_{HF} = 16.9181 + 21.7958x_{HF} - 52.3860x_{HF}^2 + 82.4252x_{HF}^3 - 106.184x_{HF}^4 + 54.4291x_{HF}^5 \quad (2-7)$$

$$B_{HF} = -5902.78 - 586.903x_{HF} + 1340.82x_{HF}^2 + 6822.09x_{HF}^3 + 2113.93x_{HF}^4 - 6818.84x_{HF}^5 \quad (2-8)$$

For  $x_{HF} < 0.4738$

$$A_w = 21.1017 - 3.22961x_{HF} + 7.90730x_{HF}^2 \quad (2-9)$$

$$B_w = -5387.02 + 1483.60x_{HF} - 4818.83x_{HF}^2 \quad (2-10)$$

For  $x_{HF} > 0.4738$

$$A_w = -0.0628905 + 43.2439x_{HF} + 4.26882x_{HF}^2 \quad (2-11)$$

$$B_w = 2639.16 - 17849.4x_{HF} + 192.177x_{HF}^2 \quad (2-12)$$

#### Vapor Phase Hydrogen Fluoride Composition

The hydrogen fluoride in the vapor phase is assumed to be composed of the HF monomer and several oligomers as well as in a complex with water. We summarize the species below with the designation used in the equations to follow.

Species	Mole Fraction	Molecular Weight	Partial Pressure
HF	$Y_1$	$m_1 = 20.01$	$p_1 = Y_1 P$
$(HF)_2$	$Y_2$	$m_2 = 2m_1$	$p_2 = Y_2 P$
$(HF)_6$	$Y_6$	$m_6 = 6m_1$	$p_6 = Y_6 P$
$(HF)_8$	$Y_8$	$m_8 = 8m_1$	$p_8 = Y_8 P$
$HF \cdot H_2O$	$Y_c$	$m_c = 38.03$	$p_c = Y_c P$

The effective mole fraction hydrogen fluoride in the vapor,  $y_{HF}$ , is

$$y_{HF} = Y_1 + Y_2 + Y_6 + Y_8 + Y_c \quad (2-13)$$

and the effective partial pressure of the hydrogen fluoride (as in Equation 2-5) is

$$p_{HF} = y_{HF} P = p_1 + p_2 + p_6 + p_8 + p_c \quad (2-14)$$

When chemical equilibrium effects are considered, as an example,



then

$$K_2 = f_2/f_1^2 \quad (2-15)$$

where  $f_2$  and  $f_1$  represent the fugacities of the dimer and monomer HF. While Schotte employed fugacities in his treatment, he assumed, for all HF species,

$$f_j = y_j \phi_j P \quad (2-16)$$

$\phi_1$  is the fugacity coefficient of the monomer. The numerical values of  $\phi_1$  ranged only from about 0.98 to 1.00 at the low pressures found in atmospheric mixing. Thus, while  $\phi_1$  is retained in the computer program for purposes of clarity, we have set  $\phi_1 = 1$ .

Then, Equation 2-15 becomes

$$K_2 = y_2/y_1^2 P \quad (2-17)$$

or

$$y_2 = y_1^2 P K_2 \quad (2-18)$$

Similarly,

$$y_6 = y_1^6 P^6 K_6 \quad (2-19)$$

$$y_8 = y_1^8 P^8 K_8 \quad (2-20)$$

For the complex,



$$K_c = f_c/(f_1 f_w) = (y_c P)/[(y_1 P)(p_w - y_c P)] = y_c/(y_1 p_w) \quad (2-21)$$

$$y_c = y_1 p_w K_c \quad (2-22)$$

Substituting Equations 2-18 through 2-22 into Equations 2-13 and 2-14,

$$p_{\text{HF}} = y_1 P + y_1^2 P^2 K_2 + y_1^6 P^6 K_6 + y_1^8 P^8 K_8 + y_1 P p_w K_c \quad (2-23)$$

Thus, knowing  $p_{\text{HF}}$  and  $p_w$ , one can obtain a value of  $y_1$  and, therefore,  $y_2$ ,  $y_6$ ,  $y_8$ , and  $y_c$ .

The equations for the chemical equilibrium constants are:

$$\ln K_2 = 6,429.729/T - 24.14682 \quad (2-24a)$$

$$\ln K_6 = 21,101.965/T - 69.73267 \quad (2-24b)$$

$$\ln K_8 = 25,225.720/T - 83.47307 \quad (2-25a)$$

$$\ln K_c = 3,154/T - 11.425 \quad (2-25b)$$

T is in Kelvin and  $K_2$  has the unit  $\text{atm}^{-1}$ ;  $K_6$ ,  $K_8$ , and  $K_c$  have the units  $\text{atm}^{-3}$ ,  $\text{atm}^{-7}$ , and  $\text{atm}^{-1}$ .

### Material Balances

Let  $M_a$  be the moles of air added. With this air there are  $M_w$  moles of water where

$$M_w = p_w^0 M_a / (P - p_w^0) \quad (2-26)$$

and  $p_w^0$  is the partial pressure of the water in the air that is entrained.

With

$$\begin{aligned} M_{HF} &= \text{moles of HF added based on the monomer,} \\ M_{HF} &= M_{HFV} + M_{HFV} \end{aligned} \quad (2-27)$$

with  $M_{HFV}$  and  $M_{HFV}$  as the moles of HF (as the monomer) in the escaping hydrogen fluoride vapor and liquid fractions.

After mixing and attaining an equilibrium state, the hydrogen fluoride mass balance is ( $x_{HF}$  the mole fraction HF in the aerosol (as the monomer) and L as the moles of liquid aerosol):

$$M_{HFV} + M_{HFV} = x_{HF} L + (Y_1 + 2Y_2 + 6Y_6 + 8Y_8 + Y_c) M_a / Y_A \quad (2-28)$$

where  $M_a / Y_A$  are the moles of vapor since  $y_A$  is the mole fraction air. For water,

$$M_w = (1 - x_{HF}) L + (Y_w + Y_c) M_a / Y_A \quad (2-29)$$

If no aerosol is formed,  $L = 0$ .

### 2.3.3 Solution to the Equations of the Model

It was noted earlier that one must first determine if an aerosol is present. Depending upon the outcome of that test, different enthalpy balances are employed to obtain closure of the enthalpy conservation equation (Equation 2-1 or 2-2). If no aerosol is formed, a single trial and error procedure is used with the final temperature as the search variable. If aerosol is formed, the procedure is more complex as a double iteration is required with

temperature and aerosol composition as the search variables. In both cases, enthalpies of reactions related to variations in the oligomer population must be employed. These enthalpies may be obtained from the leading term in Eqs. (2-22) through (2-25) by multiplying by  $(-RT)$ . With  $R = 8.314 \times 10^{-3}$  kJ/mole K,

$$\Delta H_2 = -53.46 \text{ kJ/mole HF}$$

$$\Delta H_6 = -175.44 \text{ kJ/mole HF}$$

$$\Delta H_8 = -209.73 \text{ kJ/mole HF}$$

$$\Delta H_c = -26.22 \text{ kJ/mole HF}$$

In tracking the enthalpies of the various HF species for use in Equation 2-1 or 2-2, one employs the monomer as the basis since all polymerization equilibrium constants and reaction enthalpies are relative to the monomer. For example, suppose the initial HF stream were all vapor at some  $T_i$  and  $P_i$ . One first computes the moles of monomer ( $N_1$ ), dimer ( $N_2$ ), ... in the initial stream. Then, this stream is assigned a "chemical" enthalpy as

$$N_2 \Delta H_2 + N_6 \Delta H_6 + N_8 \Delta H_8 + N_c \Delta H_c$$

which would be the true enthalpy of the monomer if all the oligomers were broken down to the monomer to form  $N_1 + 2N_2 + 6N_6 + 8N_8 + N_c$  moles of monomer. Note that this stream would then have a negative initial enthalpy if the heat of formation of HF monomer is given a value of zero at  $T_i$  since the breaking of oligomers to form monomer is an endothermic process.

For the hydrogen fluoride enthalpy in the final state at  $T_f$ , assume that no aerosol has formed. There is then a different distribution of HF oligomers ( $N_1'$ ,  $N_2'$ ,  $N_6'$ ,  $N_8'$ ,  $N_c'$ ). To determine the enthalpy of this stream, the oligomers are decomposed to the monomer as before and the total moles of monomer then cooled to  $T_f$ . (Since no aerosol was assumed, the total moles of HF monomer would equal those initially). The enthalpy of this final HF is:

$$N_2' \Delta H_2 + N_6' \Delta H_6 + N_8' \Delta H_8 + N_c' \Delta H_c + (N_1' + 2N_2' + 6N_6' + 8N_8' + N_c') \int_{T_i}^{T_f} C_p(\text{HF}) dT$$

where  $C_p(\text{HF})$  is the isobaric heat capacity of the monomer HF.

If aerosols are formed, the final vapor HF enthalpy is computed as above, but some HF then exists in the aerosol and this HF would have an enthalpy equal to vapor HF (monomer) at  $T_f$  less the molar enthalpy of condensation and the enthalpy of mixing the HF with water.

### 2.3.4 Cloud Density

Computations in the computer program are made using moles since this is more convenient to employ in the chemical and phase equilibrium balances. For the final state, one has a vector of mole fractions as well as the moles of aerosol (L) and the mole fraction HF in the aerosol ( $x_{HF}$ ). Thus, the mass of the cloud per mole of vapor phase is

$$W = 20.01(y_1 + 2y_2 + 6y_6 + 8y_8) + 18.02y_w + 38.03y_e + 28.97y_A + (LM'y_A/M_A) \quad (2-30)$$

where the mean molecular weight of the aerosol is

$$M' = 20.01x_{HF} + 18.02(1 - x_{HF}) \quad (2-31)$$

The cloud volume per mole of vapor is

$$V = (ZRT/P) + LM'y_A/M_A\rho_L \quad (2-32)$$

Normally, the compressibility factor Z is set equal to 1.0. The second term in Equation 2-32 is small compared to the first so only an approximation to  $\rho_L$  is necessary. Schotte set it equal to 1200 kg/m<sup>3</sup>, independent of composition and temperature. Finally, the cloud density is

$$\rho_c = W/V \quad (2-33)$$

### 2.3.5 Computer Program

A subroutine called HFTHRM was written, incorporating the procedure outlined in the above sections, to calculate the final thermodynamic conditions of a mixture of anhydrous HF and humid air. The FORTRAN subroutine call statement and the definition of the parameters are shown in Table 2.2. The routine was written to be compatible with the overall structure and calling conventions used in ADAM.

## 2.4 Results and Discussions

The HF-humid air thermodynamic model, HFTHRM, was exercised for several test cases. The results are presented in a series of figures, with variation in the values of selected parameters. The principal parameter varied is the dilution ratio (i.e., the ratio of mass of air mixed with a unit mass of hydrogen fluoride). The initial conditions of HF used include the following:

- i) saturated HF vapor at ambient pressure;
- ii) saturated HF vapor + liquid aerosols at ambient pressure;
- iii) high temperature HF vapor at ambient pressure.

Table 2.3 shows the parameters varied and the abscissa and ordinates of the various figures.



TABLE 2.2

**FORTRAN SUBROUTINE FOR HF-HUMID AIR MIXING  
THERMODYNAMIC MODEL**

```

C
C SUBROUTINE HFTHRM(MHF, FL, THF, MAIR, TAIR, RH, Q,
C & TMIX, RHOMIX, VOLMIX, NSPECS, SPLIST, CSOL, CLIQ, CVAP)
C
C This is the TMS subroutine for calculating thermodynamic
C properties of the mixture resulting from the isobaric mixing of
C hydrogen fluoride and humid air. The initial condition of HF can
C be a saturated vapor or a saturated vapor containing liquid aerosols.
C
C The program is modeled after the work of William Schotte,
C Ind. & Eng. Chem. Res., 26, p. 300 (1987).
C
C ***INPUT PARAMETERS***
C
C MHF      = Total mass of HF stream, vapor + liquid      kg (or kg/s)
C FL       = Mass fraction liquid
C THF      = Temperature of HF stream                      K
C MAIR     = Mass of moist air stream                      kg (or kg/s)
C TAIR     = Dry bulb temperature of the air stream        K
C RH       = Relative Humidity of the air stream           %
C Q        = Excess heat (+ added, - extracted) from system J (or J/s)
C
C ***OUTPUT PARAMETERS***
C
C TMIX     = Final temperature of the mixture              K
C RHOMIX   = Density of the mixture                        kg/m^3 (or /s)
C VOLMIX   = Final volume of the mixture                   m^3 (or /s)
C NSPECS   = Number of chemical species in the mixture = 7
C SPLIST   = List of specie names in 3 letter codes
C CLIQ(n)  = A vector of liquid mass fractions for n ≤ nspecs
C CSOL(n)  = A vector of solid mass fractions for n ≤ nspecs
C CVAP(n)  = A vector of vapor mass fractions for n ≤ nspecs
C CVAP(nspec+1) = Total mass of all species in vapor phase (kg)
C CVAP(nspec+2) = Total moles of all species in vapor phase (Kmol)
C CSOL(nspec+1) = Total mass of all species in solid phase (kg)
C CSOL(nspec+2) = Total moles of all species in solid phase (Kmol)
C CLIQ(nspec+1) = Total mass of all species in liquid phase (kg)
C CLIQ(nspec+2) = Total moles of all species in liquid phase (Kmol)
C
C *** DEFINITIONS OF OTHER PARAMETERS ***
C
C SPLIST(1) = 'H2O'; SPLIST(2) = 'AIR'; SPLIST(3) = 'HF1'
C SPLIST(4) = 'HF2'; SPLIST(5) = 'HF6'; SPLIST(6) = 'HF8'
C SPLIST(7) = 'WHF'
C
C CLIQ(1) through CLIQ(7) = mass fraction of species in the liquid phase
C                          corresponding to the specie number.
C
C CLIQ(8) = Total mass of Liquid phase (kg)
C
C CVAP(1) through CVAP(7) = mass fraction of species in the vapor phase
C                          corresponding to the specie number.
C
C CVAP(8) = Total mass of vapor phase (kg)

```

TABLE 2.3

INDEX TO HF AND AIR PARAMETERS VARIED IN DIFFERENT FIGURES

Figure #	Abscissa (x)	Ordinate (Mixture condition) (y)	Initial Conditions of HF and Air				
			HF			Air	
			Temp	fL	Condition	Temp	% RH
2.4	Dilution Ratio	Cloud Temperature	19.54°C	0	Sat. Vapor	20°C	50
2.5	Dilution Ratio	Mass Fraction of HF Condensed into Aerosol Phase	19.54°C	0	Sat. Vapor	20°C	50
2.6	Dilution Ratio	Mass Concentration of HF in the Aqueous Solution (Aerosol)	19.54°C	0	Sat. Vapor	20°C	50
2.7	Dilution Ratio	Density	19.54°C	0	Sat. Vapor	20°C	50 & 95
2.8	Dilution Ratio	Temperature	19.54°C	0.5	Sat. Vapor & Liquid	20°C	95
2.9	Dilution Ratio	Mass Fraction of HF Condensed into Aerosol Phase	19.54°C	0.5	Sat. Vapor & Liquid	20°C	95
2.10	Dilution Ratio	Mass Concentration of HF in the Aqueous Solution (Aerosol)	19.54°C	0.5	Sat. Vapor & Liquid	20°C	95
2.11	Dilution Ratio	Cloud Density	19.54°C	0.5	Sat. Vapor & Liquid	20°C	95
2.12	Dilution Ratio	Temperature	1000 K	0	Vapor at Amb. Pr.	20°C	50
2.13	Dilution Ratio	Density	1000 K	0	Vapor at Amb. Pr.	20°C	50

Figure 2.4 shows the variation of HF-air mixture temperature as a function of dilution ratio for the case of initial HF being a saturated vapor at ambient pressure. The predictions by the HFTHRM program (modified Schotte model) and by the model of Clough, et al., are shown. It is seen that the predictions by both models are very close.

Note that for dilution ratios less than about 10 the temperature of the mixture decreases (substantially) even though the initial temperature of both air and vapor are 20° C. This is because the saturated HF vapor at ambient pressure is a mixture of several associated molecules ("oligomers") and as dilution takes place, the molecules dissociate towards a monomer. The dissociation reaction is endothermic resulting in the lowering of temperature. Above a dilution ratio of 10, almost all of the oligomers have dissociated and additional dilution increases the temperature of the mixture, ultimately approaching the air temperature at large dilutions.

Figure 2.5 shows the variation of the mass fraction of HF that is condensed (into the liquid aerosol) with variation in the dilution ratio. Condensation occurs because of lowering of temperature as well as due to the lowering of HF partial pressure in the mixture. However, at large dilution ratios the condensed HF evaporates and the final mixture consists essentially of HF monomer vapor and air.

The strength of the HF acid (aqueous in the form of aerosol) with dilution is shown in Figure 2.6. An increase in the dilution results in condensation of water vapor (due to lowering of mixture temperature) and dilutes the aqueous solution. Hence, the mass concentration of HF in the liquid aerosol decreases. At very high dilution ratios ( $> 10$ ), the partial pressure of HF in the vapor phase is low and because of equilibrium the concentration of HF in the liquid phase also is low, even though a part of the water in the aqueous phase may start to re-evaporate.

The variation of cloud density with dilution ratio is shown in Figure 2.7. It is seen that for dilution ratio below 50 for air at normal ambient temperature, the cloud density decreases continuously as dilution increases for all relative humidities. For air at or below 50% relative humidity, the density of the mixture is always greater than that of ambient air at 20° C. However, for relative humidities greater than 50%, there is a region beyond dilution ratio  $> 50$  in which the cloud is lighter than air. This is because of the residual heat of reaction between HF and high humidity in the air at higher relative humidities.

The variations of cloud parameters with dilution when the initial HF contains anhydrous liquid aerosol particles are indicated in Figures 2.8 through 2.11. It is seen that the behavior of all of the mixture parameters are similar to that described earlier except that the liquid fractions are higher. The density of the cloud is higher at low dilutions ( $< 10$ ) compared to the case where the initial HF was all in vapor form. However, the differences in cloud density for dilutions  $> 10$  are negligible.

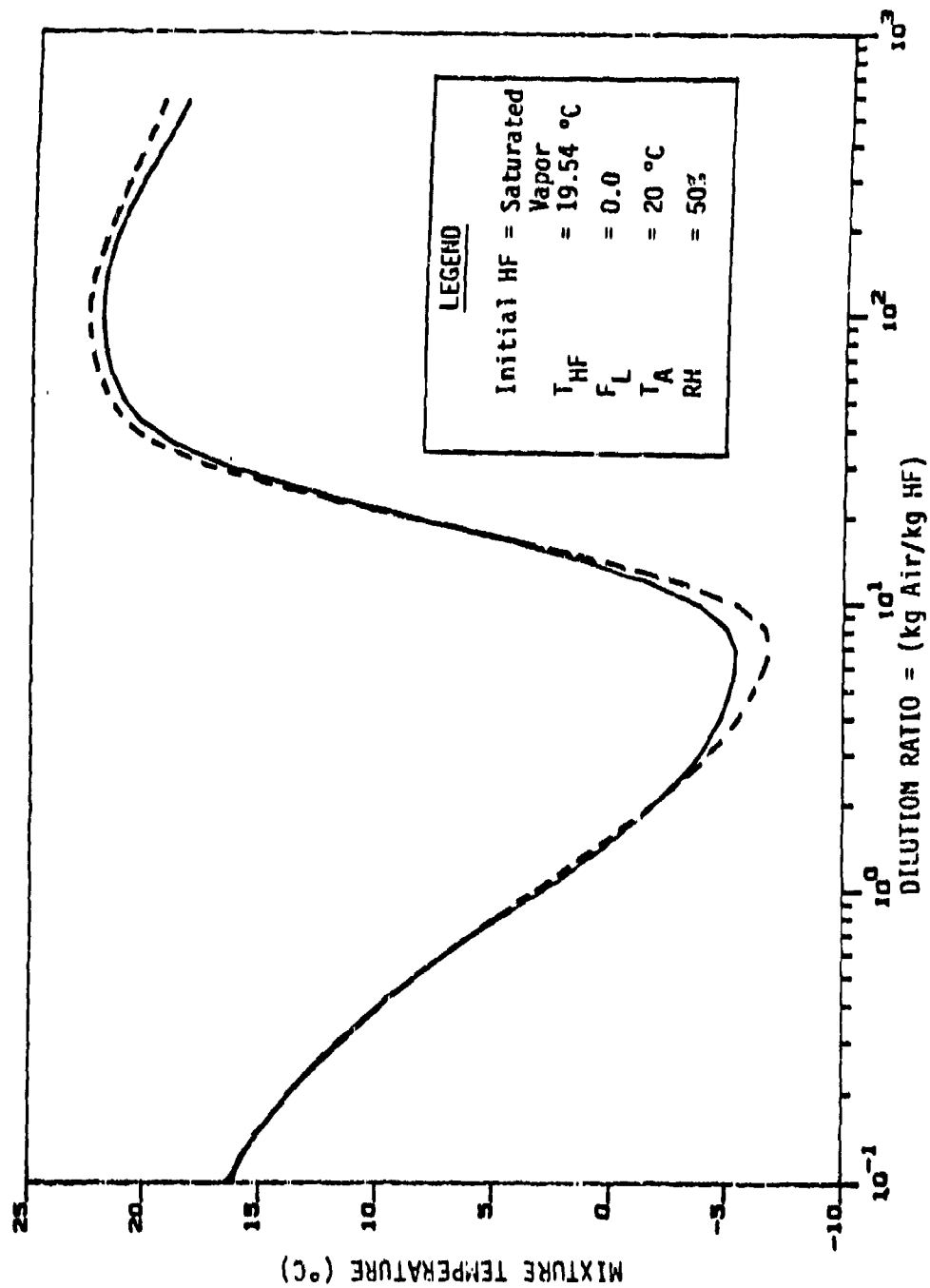
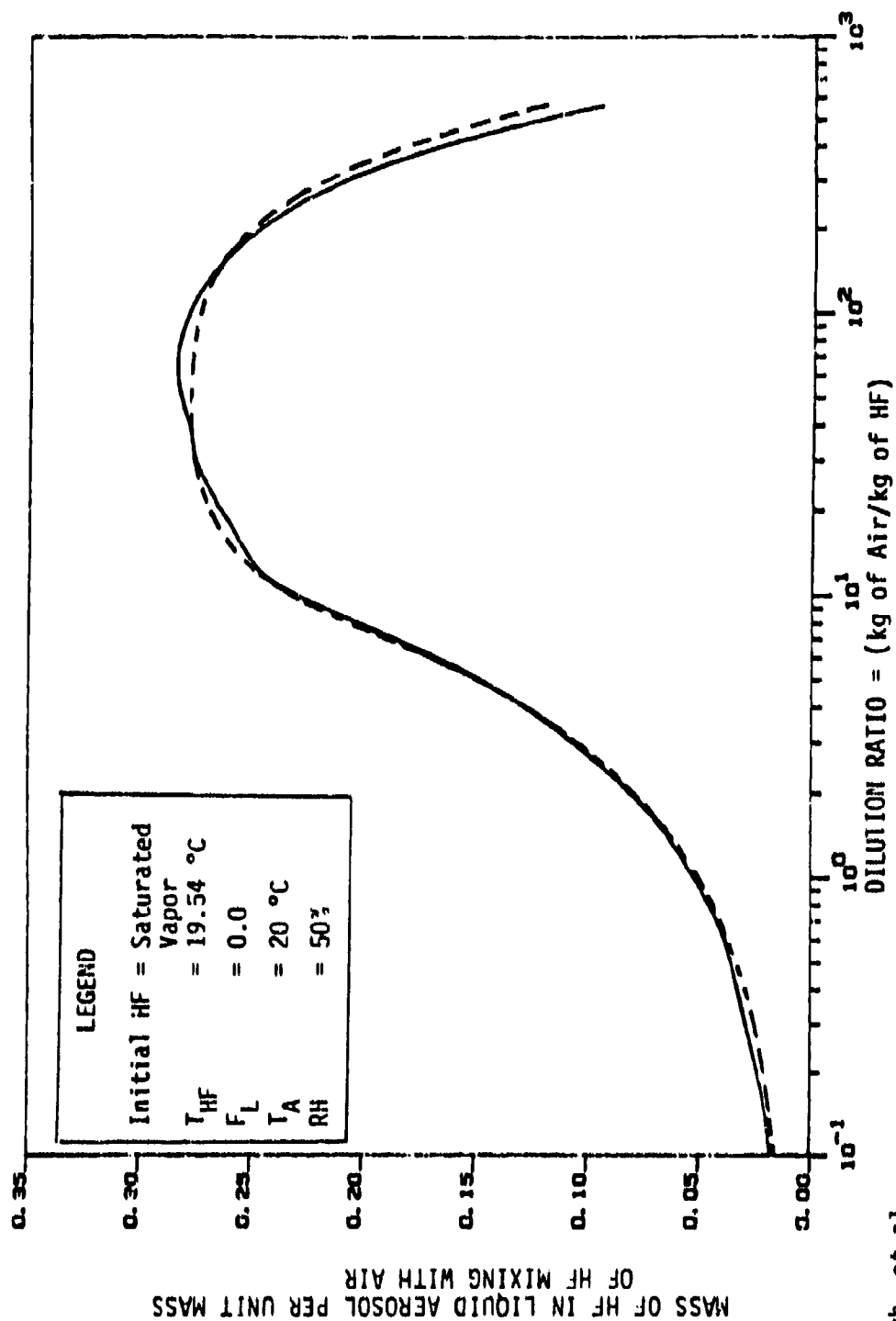


FIGURE 2.4: Variation of HF-Humid Air Mixture Temperature with Dilution Ratio

— Clough, et al.  
 ---- Schotbe/TMS



— Clough, et al.  
 ----- Schotte/TMS

FIGURE 2.5: Variation of Fractional Mass of Initial HF Condensed into Aerosol with Dilution Ratio

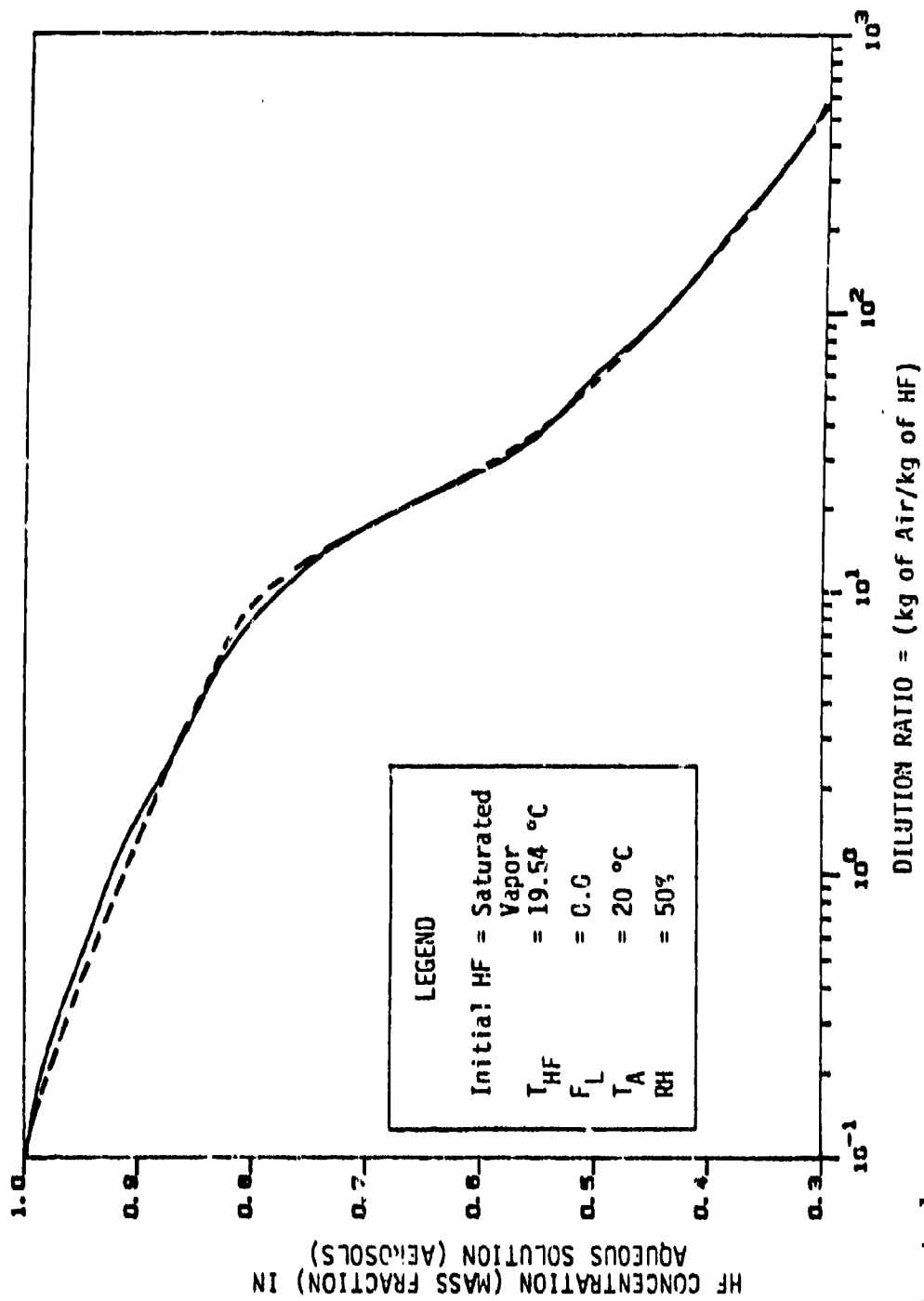


FIGURE 2.6: Mass Fraction HF Concentration in the Condensed Aqueous (Aerosol) Solution vs. Dilution Ratio

— Clough, et al.  
 ---- Schotte/TMS

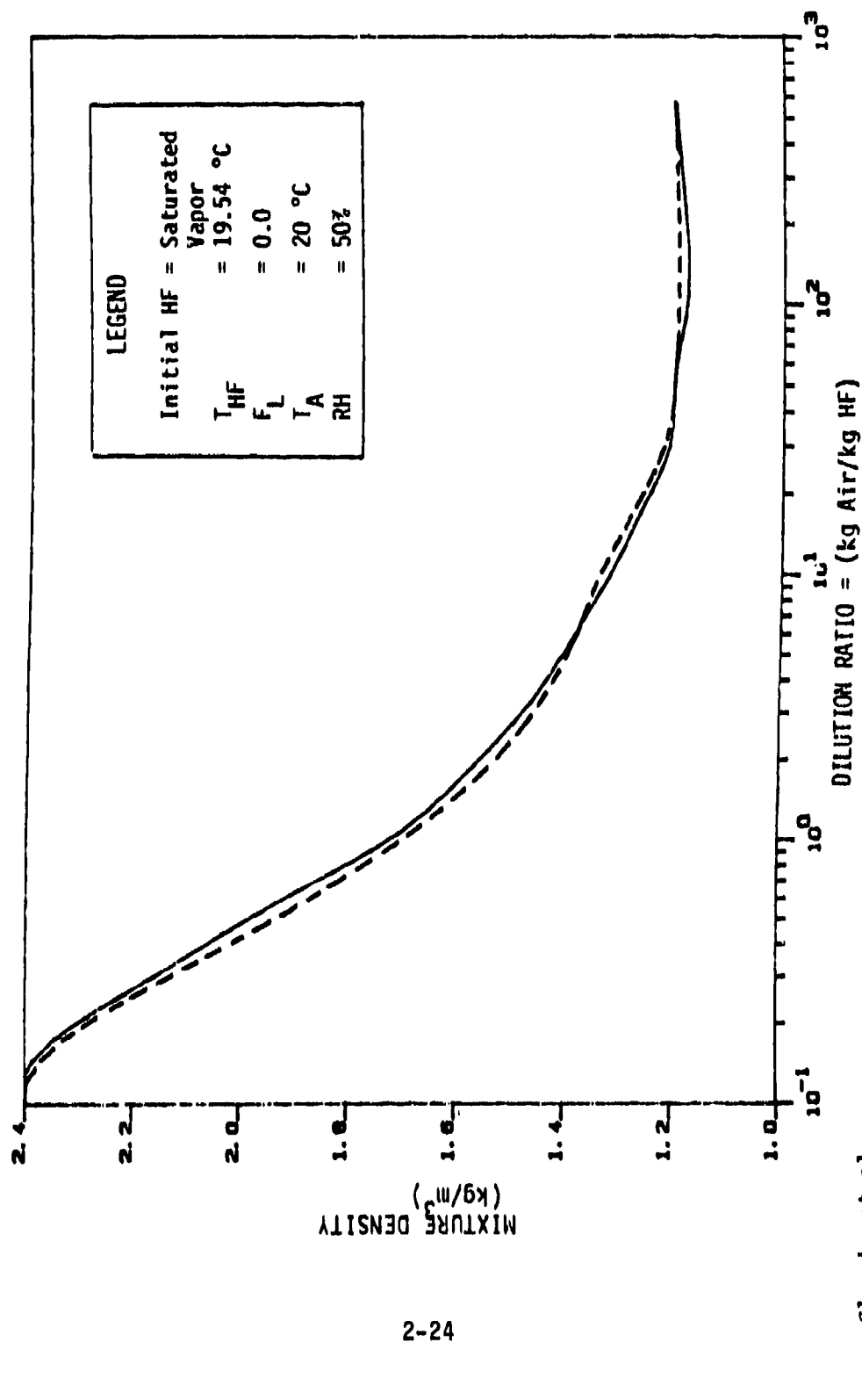
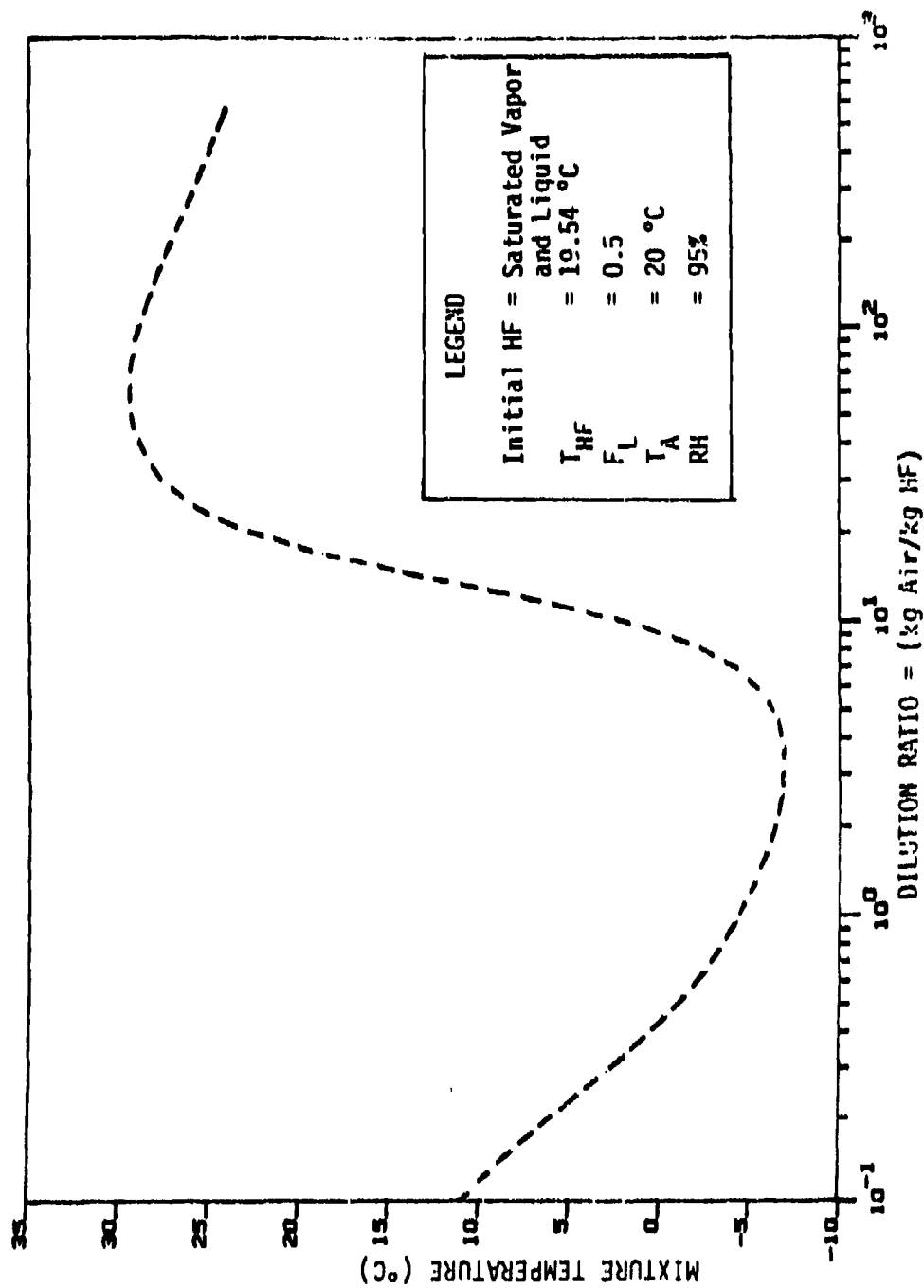


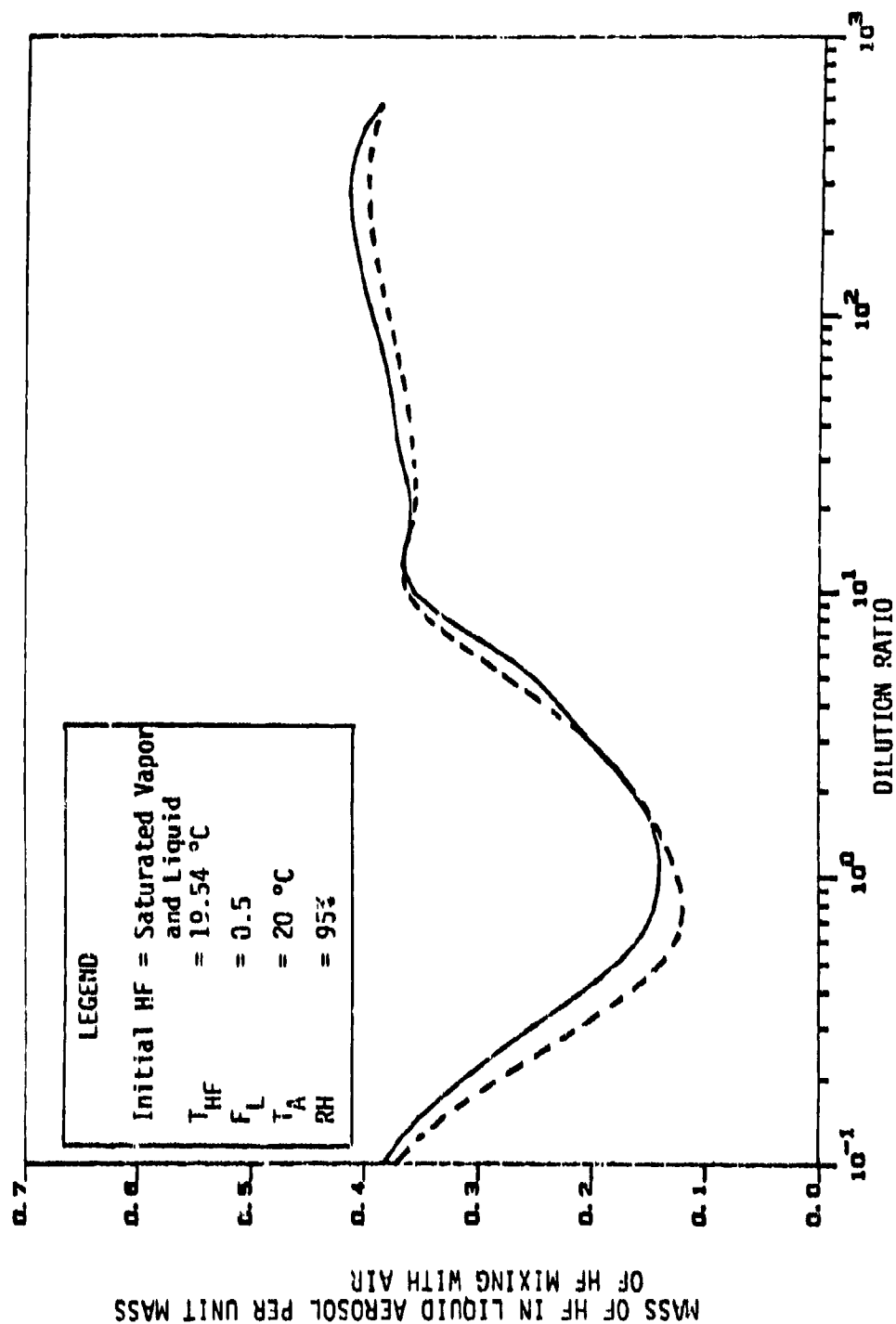
FIGURE 2.7: Variation of Mixture Density with Dilution Ratio



— Clough, et al.  
 ---- Schotte/TMS

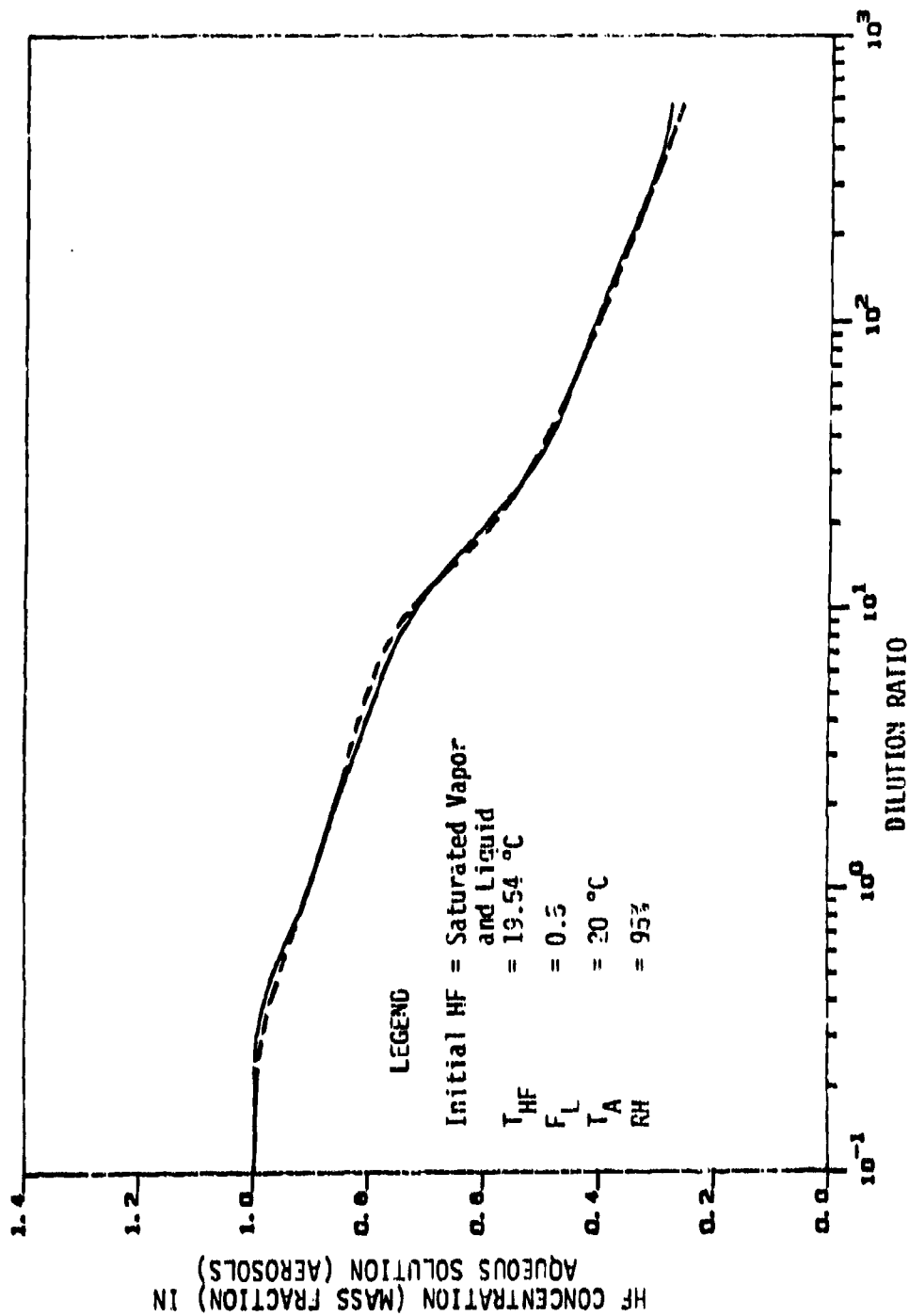
FIGURE 2.9: Variation of HF-Humid Air Mixture Temperature with Dilution Ratio





— Clough, et al.  
----- Schotte/TMS

FIGURE 2.9: Variation of Fractional Mass of Initial HF Condensed into Aerosol with Dilution Ratio



— Clough, et al.  
 ---- Schotte/TIS

FIGURE 2.13: Mass Fraction HF Concentration in the Condensed Aqueous (Aerosol) Solution vs. Dilution Ratio

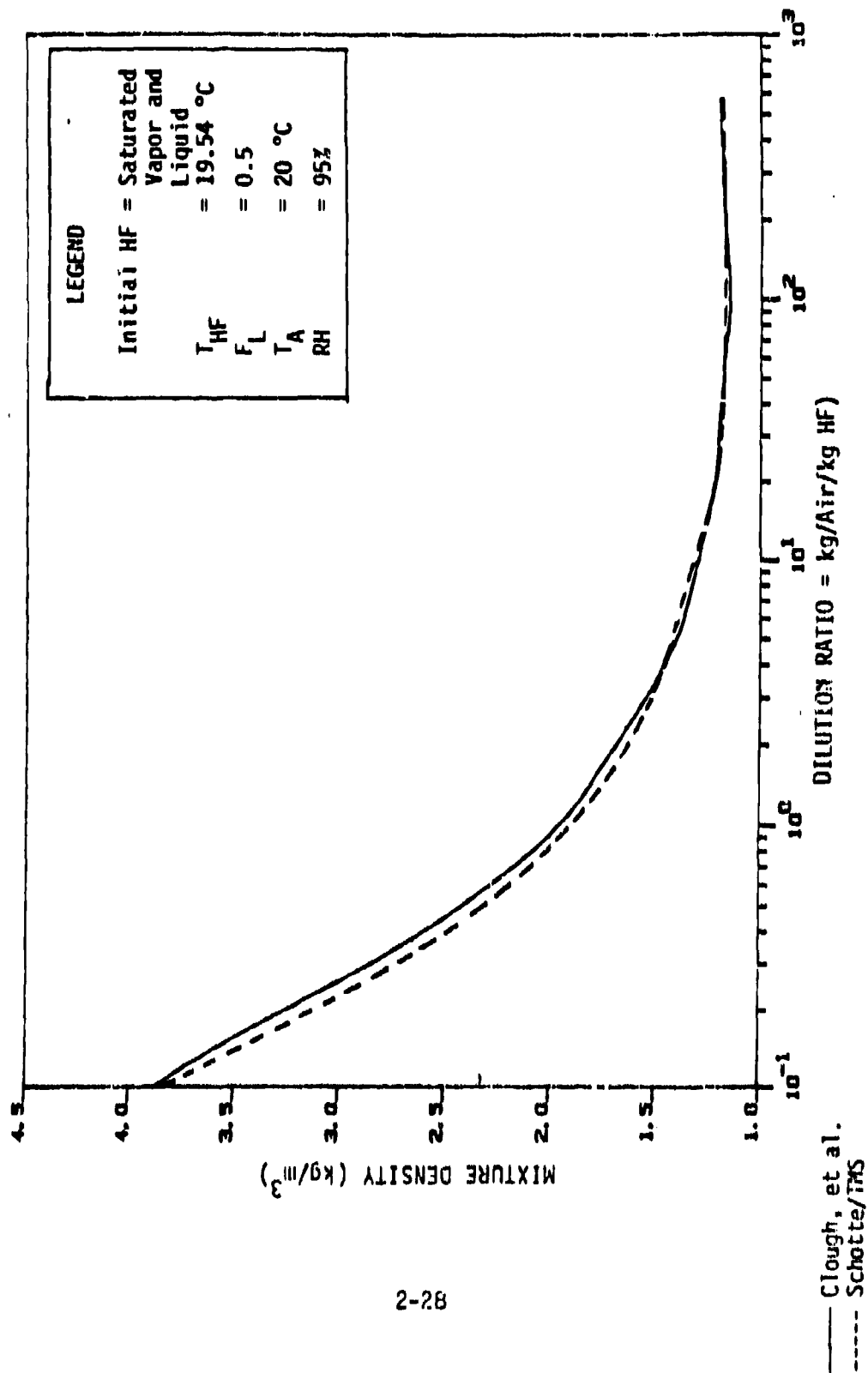
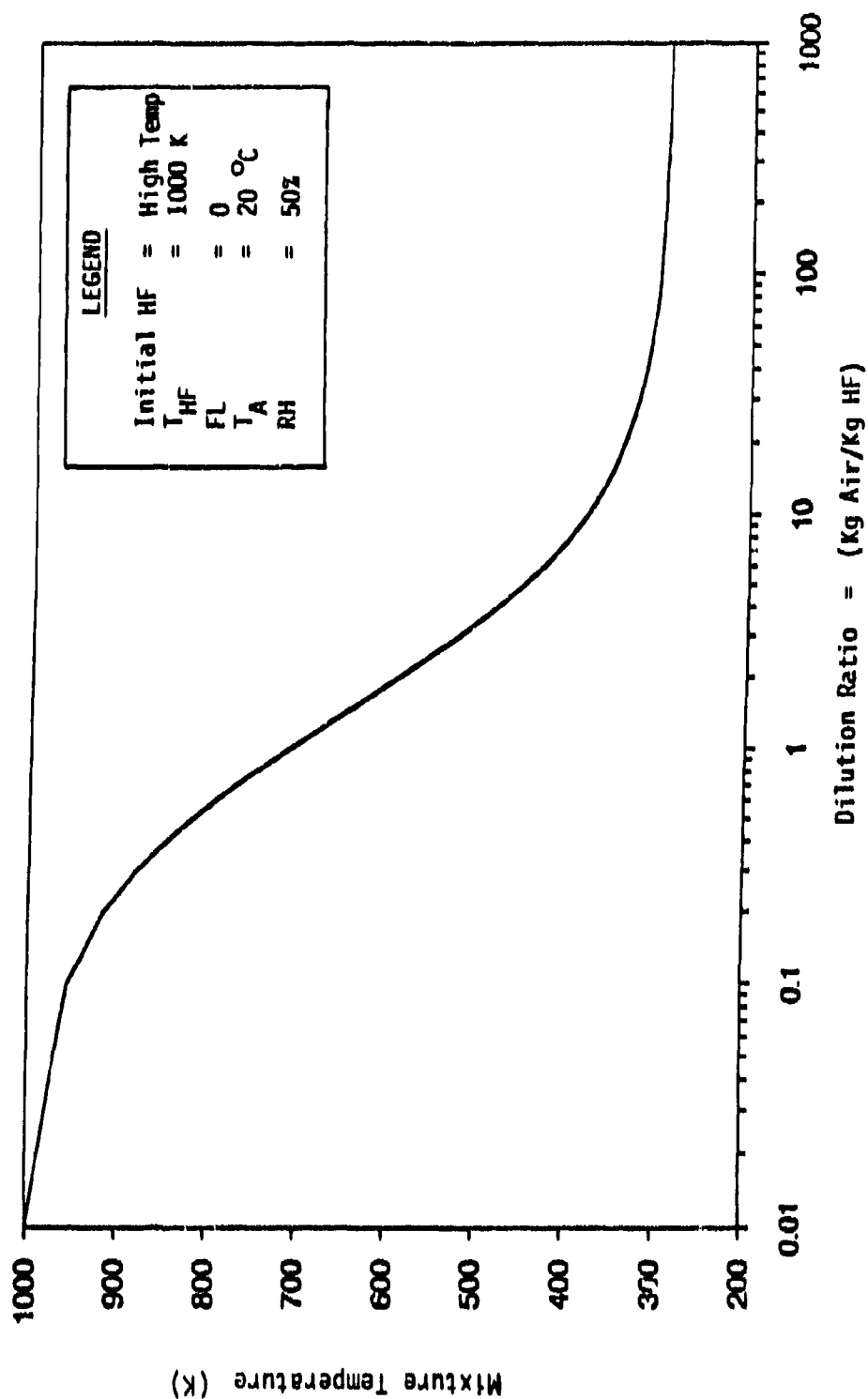


FIGURE 2.11: Variation of Mixture Density with Dilution Ratio

The effect of high temperature HF release are indicated in Figures 2.12 and 2.13. Figure 2.12 shows the variation of mixture temperature with dilution for a 1000 K HF release at ambient pressure. At this high temperature, almost all of the HF released is in the form of monomer and the dilution further promotes the monomer phase. The mixture temperature decreases continuously. However, it is noticed that the temperature decrease is not the same as would be the case when two ideal gases at different temperatures are mixed. This is because higher molecular weight oligomers are formed during dilution of high temperature HF. The association reaction is exothermic, thus the rate of temperature drop is lessened compared to that in the case of ideal gases. However, at large dilution ratios the partial pressure of HF decreases rapidly resulting in the promotion of dissociation reactions to monomer. Hence, the curvature of the temperature vs. dilution flattens.

The density variation is shown in Figure 2.13. The initial density of the high temperature HF monomer is quite low (compared to ambient air density). In fact, at 1000 K, HF acts very much like an ideal gas. Dilution of this with ambient temperature air results in a monotonic increase in mixture density. Note, however, the changes in the curvature of the density vs. dilution curve. This is due to the association and dissociation reactions as explained in the previous paragraph.



**FIGURE 2.12:** VARIATION OF MIXTURE TEMPERATURE WITH AIR DILUTION FOR HIGH TEMPERATURE HF RELEASE

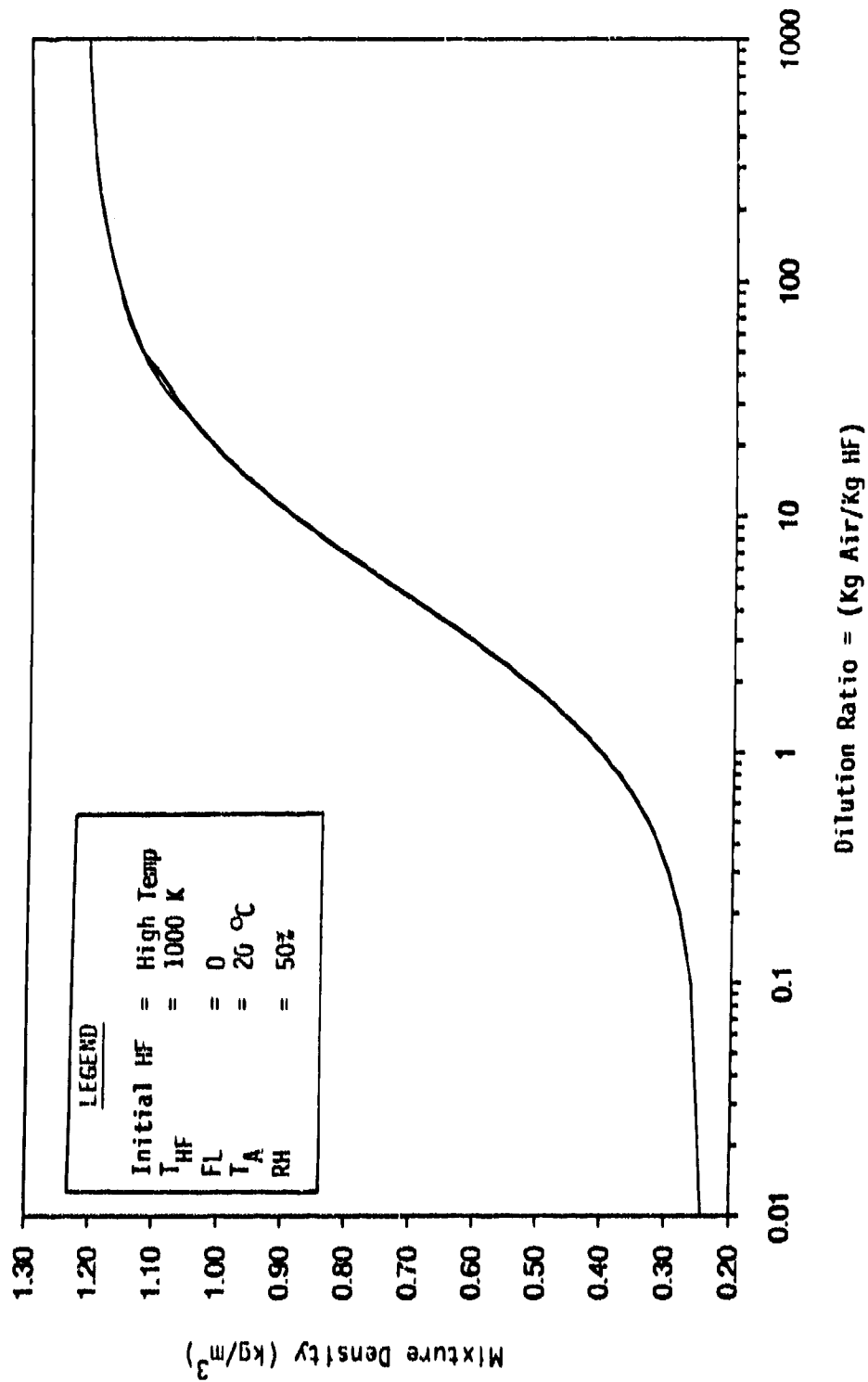


**FIGURE 2.13: VARIATION OF MIXTURE DENSITY WITH AIR DILUTION FOR HIGH TEMPERATURE HF RELEASE**

**This page is left blank intentionally**

## CHAPTER 3

### REVISIONS, MODIFICATIONS, ENHANCEMENTS

#### AND CORRECTIONS TO ADAM CODE

Several modifications were made to routines in ADAM to make the program more robust and applicable over a greater range of parameters. In this chapter, we discuss the theoretical and physical bases of these modifications, and the changes in detail.

The principal changes made include:

1. Calculation of atmospheric wind velocity profile for flow over very large aerodynamic roughnesses and the impact on dispersion of a heavy gas cloud whose vertical depth is smaller than the mean height of the roughness elements.
2. Determination of atmospheric wind friction velocity under specified atmospheric conditions.
3. Modification of algorithms to calculate certain diffusion property values.
4. Enhancement of the calculation procedure to determine the atmospheric stability value.
5. Corrections of the code to remove certain incorrect equations or parameter value estimations.

Each of these is discussed below.

#### 3.1 Correction of Large Aerodynamic Roughness In The Dispersion Path

The roughness of the ground over which wind blows influences the distribution of time averaged wind profile variation with height. In the report by Raj and Morris (1987), equations were presented for average wind velocity distribution with height under different types of atmospheric stabilities. These equations contain a length scale  $z_0$  representing the "aerodynamic roughness" of the path over which the wind is flowing. The correlations presented in the referenced report are accurate only for the case where the magnitude of the aerodynamic roughness ( $z_0$ ) is small compared to the vertical depth of the dispersing vapor cloud.

Occasionally, the aerodynamic roughness of the path may be large compared to the depth of the cloud (example: a large forest of tall trees or tall buildings). The dispersion of a cloud under these conditions is very complex and will depend on not only the height of the roughness elements, but also the fractional horizontal area occupied by the solid elements, the mean distance between the solid elements as a fraction of the height of solid



elements, etc. The cloud may be split up, caught up in the wake cavities of the tall elements, be mixed with air more due to higher-than-ambient turbulence, etc. However, the mean velocity of the cloud within the tall elements will be lower because the wind speed within the interstices of the elements will be lower than in the upstream of the high aerodynamic roughness region. These phenomena are extremely difficult to model. Only an approximation is included in the modified version of ADAM.

In the previous version of ADAM, the occurrence of a large aerodynamic roughness region (simulation in the code) would have resulted in the calculation of negative wind speeds (for  $z < z_0$ ) - a physically unacceptable solution. We have modified the wind velocity profile (described below) to take into account large aerodynamic roughness heights and atmospheric stabilities.

### 3.1.1 Assumptions

We assume that

1. The mean wind speed varies linearly with height above ground in the region of large aerodynamic roughness, up to a "critical height" ( $z_c$ ).
2. The magnitude of the critical height is dependent on the magnitude of the aerodynamic roughness  $z_0$  and not on the atmospheric stability.
3. The wind velocity distribution above the critical height is the same as in undisturbed flow.

The value of this critical height ( $z_c$ ) is determined by forcing the continuity of both the wind velocity value as well as its slope at  $z = z_c$  from the velocity profiles above  $z = z_c$  and below  $z = z_c$ . This is illustrated schematically in Figure 3.1 and discussed below in more detail. All three types of atmospheric stabilities are discussed.

#### a) Neutral Stability Atmosphere (Monin-Obukhov Length, $L = 0$ )

The wind speed distribution with height is assumed to be given by:

$$U_w(z) = \begin{cases} (u_* / k) \ln(z/z_0) & \text{for } z \geq z_c & (3.1a) \\ (u_* / k) (z/z_c) & \text{for } z \leq z_c & (3.1b) \end{cases}$$

where  $z_c$  is a yet-to-be determined height whose value depends on the value of the aerodynamic roughness height  $z_0$ . It is noted that the form of Equation 3.1a is identical to the distribution under neutral stability when  $z_0$  is small. Equation 3.1b represents the linear distribution assumption that we have made.

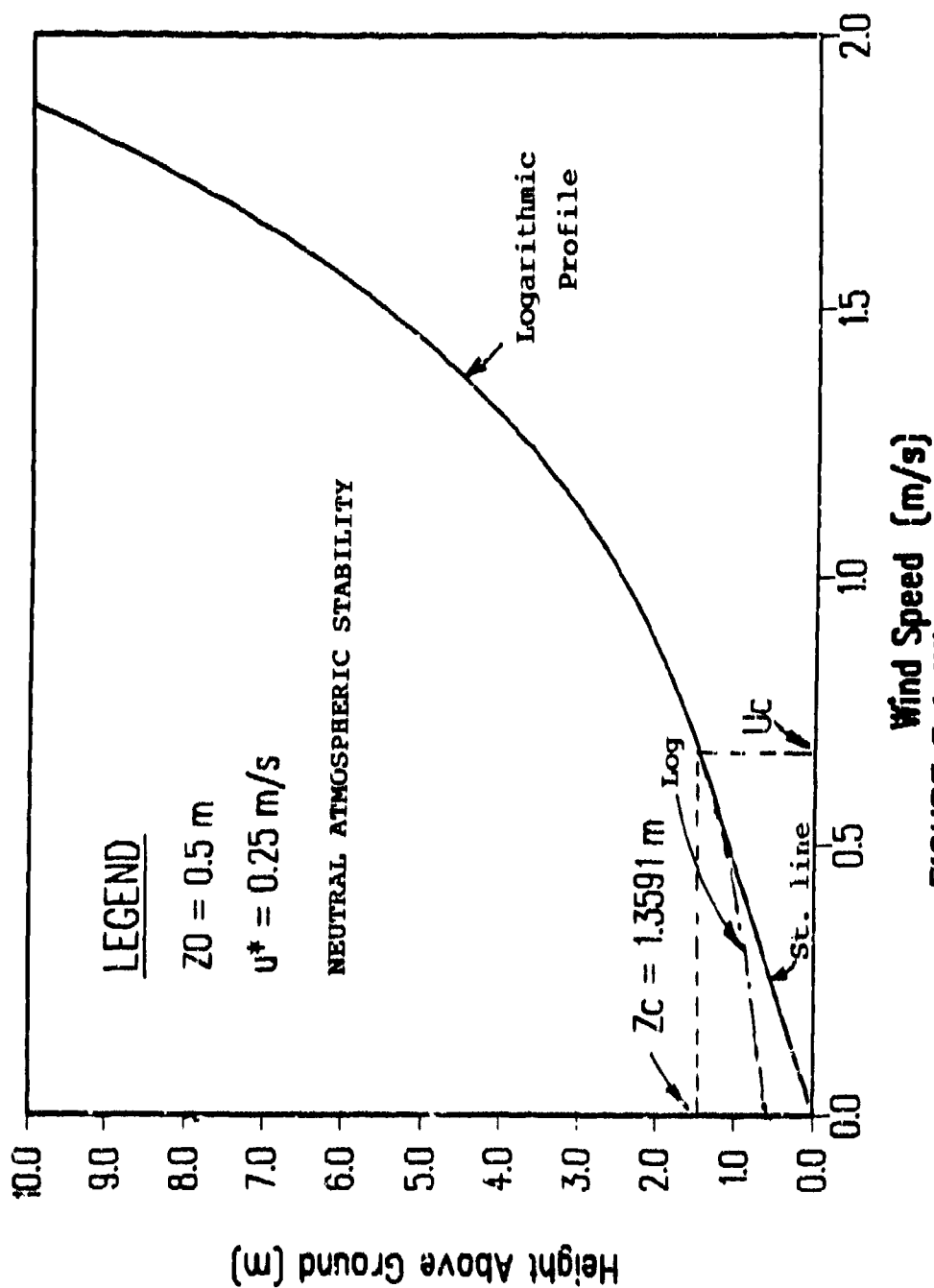


FIGURE 3.1: Wind Velocity Profile

To calculate the value of  $z_c$ , we impose the following conditions:

1.  $U_w(z)$  is continuous at  $z = z_c$ .
2.  $\frac{d}{dz} U_w(z)$  is also continuous at  $z = z_c$ .

It can be shown that with the above conditions and Equations 3.1a and 3.1b, we get

$$z_c = e z_0 \quad (3.2)$$

where  $e$  is the base of the natural logarithm.

The average wind speed over a specified height  $z$  is given by

$$\overline{U_w(z)} = (1/z) \int_{z=0}^z U_w(z) dz \quad (3.3)$$

Substituting Equations 3.1a and 3.1b in Equation 3.3 and noting Equation 3.2, we get

$$\overline{U_w(z)} = (u_*/k) [0.5 (z/z_c)] = 0.5 U_w(z) \quad \text{for } z \leq z_c \quad (3.4a)$$

$$(u_*/k) [0.5*(z/z_c) + \ln(z/z_0) - 1] \quad \text{for } z > z_c \quad (3.4b)$$

(b) Stable Atmosphere ( $L > 0$ )

The wind speed distribution in a stable atmosphere again is assumed to be given by:

$$U_w(z) = \begin{cases} (u_*/k) [\ln(z/z_0) + 5.2 \alpha] & \text{for } z > z_c \\ U_w(z_c) (z/z_c) & \text{for } z \leq z_c \end{cases} \quad (3.5a)$$

$$\text{where,} \quad \alpha = \begin{cases} (z/L) & \text{for } z < L \\ 1 & \text{for } z \geq L \end{cases} \quad (3.6a)$$

where,  $L$  = Monin-Obukhov turbulence length scale in the atmosphere where  $U_w(z_c)$  is the wind speed at a height  $z_c$ . The values of  $z_c$  and  $U_w(z_c)$  are found by imposing the continuity conditions for both velocity function and its derivative with height at  $z = z_c$ . There are two cases to consider; namely,  $z_c < L$  and  $z_c \geq L$ . Applying the continuity conditions and using the velocity distribution Equations 3.5a and 3.5b, it can be shown that in both cases  $z_c = e z_0$  (as indicated in Equation 3.2).

Also, the wind speed  $U_c$  at  $z = z_c$  is given by:

$$\frac{k U_c}{u_*} = 1 + 5.2 \alpha_c \quad (3.7a)$$

where,

$$\alpha_c = \begin{cases} (z_c/L) & \text{for } z_c < L \\ 1 & \text{for } z_c \geq L \end{cases} \quad (3.7b)$$

$$(3.7c)$$

The average wind speed is calculated using Equations 3.3, 3.5a and 3.5b with conditions of Equations 3.2 and 3.6.

i.e.,

$$\frac{k \bar{U}_w}{u_*} = \frac{1}{z} \int_{z=0}^z \frac{k U_w(z)}{u_*} dz \quad (3.8)$$

The above equation reduces to

Case 1 ( $z < z_c$ )

$$\bar{U}_w(z) = 0.5 (z/z_c) U_c = 0.5 U_w(z) \quad (3.9)$$

Case 2 ( $z > z_c$ )

Equation (3.8) can be written as

$$\frac{k \bar{U}_w}{u_*} = \frac{k}{zu_*} \int_{z=0}^{z_c} U dz + \int_{z=z_c}^z U dz \quad (3.10)$$

With  $z_c = ez_0$  and substituting Equations 3.5b and 3.5a respectively in the integrals on the RHS of the above equation and simplifying, we get

$$\frac{k \bar{U}}{u_*} = 0.5 (z_c/z) \frac{k U_c}{u_*} + [\ln(z/z_0) - 1] + \frac{5.2}{z} \int_{z=z_c}^z \alpha dz \quad (3.11)$$

Again depending on the relative values of  $\alpha$ ,  $L$  and  $z_0$ , there are three cases to consider. The results are summarized below.

$$\frac{k \bar{U}_w(z)}{u_*} = 0.5 (z_c/z) \frac{k U_c}{u_*} + [\ln(z/z_0) - 1] + 5.2x$$

$$\text{where } x = [1 - z_c/z] \quad \text{for } z > z_c > L \quad (3.12a)$$

$$x = \frac{[(z/L)^2 - (z_c/L)^2]}{2(z/L)} \quad \text{for } L > z > z_c \quad (3.12b)$$

$$x = \frac{[2(z/L) - (z_c/L)^2 - 1]}{2(z/L)} \quad \text{for } z > L > z_c \quad (3.12c)$$

(c) Unstable Atmosphere ( $L < 0$ )

The velocity distribution in an unstable atmosphere for small values of  $z_0$  is given by

$$\frac{k \bar{U}_w(z)}{u_*} = 2 \left[ \tan^{-1}(x) - \tan^{-1}(x_0) \right] + \ln \frac{(x-1)(x_0+1)}{(x+1)(x_0-1)} \quad (3.13a)$$

where,

$$x = [1 - 15 z/L]^{0.25} \quad \text{and} \quad x_0 = [1 - 15 z_0/L]^{0.25} \quad (3.13b)$$

We assume that within reasonable limits for  $z_0$ , the Equations in 3.13 will apply to the region above a value of  $z = z_c$ , when a surface with large values of aerodynamic roughness is encountered. We assume that in the case of unstable weather, also we have the following relationship:

$$z_c = e z_0 \quad (3.14)$$

$$x_c = [1 - 15 z_c/L]^{0.25} \quad (3.15)$$

$$U_c = \frac{u_*}{k} 2 [\tan^{-1} x_c - \tan^{-1} x_0] + \ln \frac{(x_c - 1)(x_0 + 1)}{(x_0 - 1)(x_c + 1)} \quad (3.16)$$

and the velocity distribution is

$$U_w(z) = \begin{cases} U_c (z/z_c) & \text{for } z \leq z_c \\ \frac{u_*}{k} 2 [\tan^{-1} x - \tan^{-1} x_0] + \ln \frac{(x - 1)(x_0 + 1)}{(x_0 - 1)(x + 1)} & \text{for } z > z_c \end{cases} \quad (3.17a)$$

$$(3.17b)$$

The average velocity over a height  $z$  can be determined by the equation:

$$\overline{U}_w(z) = (1/z) \int_{z=0}^z U_w(z) dz \quad (3.18)$$

Since it is assumed that the velocity distribution is linear for  $z < z_c$ , we can show that

$$\overline{U}_w(z) = 0.5 (z/z_c) U_c \quad \text{for } z \leq z_c \quad (3.19a)$$

However, for  $z > z_c$ , the integration in Equation 3.18 has to be performed in two regions. In the region  $z > z_c$ , the velocity distribution is given by Equation 3.17b - a very complicated expression for integration. We, therefore, make a simplifying assumption that for obtaining mean velocity above  $z = z_c$ , the following approximate form of the velocity distribution is assumed

$$U_w(z) = U_c (z/z_c)^{1/7} \quad \text{for } z \geq z_c \quad (3.20)$$

Using Equations 3.20 and 3.17a in Equation 3.18, we get

$$\overline{U}_w(z) = U_c (z_c/z) \frac{[7 (z/z_c)^{8/7} - 3]}{8} \quad \text{for } z > z_c \quad (3.19b)$$

or

$$\overline{U}_w(z) = (7/8) U_w(z) - (3/8) (z_c/z) U_c \quad \text{for } z > z_c \quad (3.19c)$$

It should be noted that the value of  $L$ , the Monin-Obukhov turbulence length scale in the atmosphere and the friction velocity  $u_*$  are calculated using the  $z_0$  value. Therefore, the use of the above equations may not be appropriate if the meteorological information is taken at one place and the cloud dispersion is at a different place where the aerodynamic roughness is substantially different.

### 3.2 Calculation of Atmospheric Turbulence Friction Velocity

The program code in ADAM provides the user the flexibility of either inputting the value of the stability of the atmosphere or having the program calculate the stability based on the location of the place, time of day, and other local conditions. In the case the stability value is input, it is necessary to calculate the characteristics of atmospheric turbulence. This section gives the details of the calculation of wind friction velocity and Monin-Obukhov turbulence length scale.

#### 3.2.1 Assumptions

It is assumed in these calculations that

- a) the atmospheric stability value (SP) and the aerodynamic roughness  $z_0$  are given
- b) the mean wind speed  $U_w$  is specified at a height  $z_w$
- c)  $z_w \gg ez_0$

where "e" is the base of the natural logarithm.

The objective of the calculations is to determine the values of  $L$ , the Monin-Obukhov length and  $u_*$  the wind friction velocity.

#### 3.2.2 Analysis

Following Kunkel (1986), we write the equation for the atmospheric stability as

$$SP = A + B \log_{10} (100 z_0) \quad (3.21)$$

$$\text{where, } A = 3.5 + 21.67/L \quad (3.22a)$$

$$B = 0.48 \quad \text{for } \text{abs}(1/L) \geq 0.015 \quad (3.22b)$$

$$B = 43.63 (\text{abs}(1/L))^{1.08} \quad \text{for } \text{abs}(1/L) < 0.015 \quad (3.22c)$$

$$B = -B \quad \text{for } L < 0 \quad (3.23)$$

where SP is the given value of atmospheric stability,  $z_0$  the aerodynamic roughness, and L, the Monin-Obukhov atmospheric turbulence length scale. Given the value of SP and  $z_0$ , the value of L is determined by an iterative search procedure.

The wind friction velocity  $u_*$  is determined knowing the L value and wind velocity at a specified height. This procedure is indicated below

**Stable Atmosphere ( $L > 0$ )**

$$\frac{k U_* (z)}{u_*} = \ln (z/z_0) + 5.2 \alpha \quad (3.24a)$$

$$\alpha = \frac{z/L}{1} \quad \text{for } z < L \quad (3.24b)$$

$$\alpha = 1 \quad \text{for } z \geq L \quad (3.24c)$$

**Neutral Atmosphere [ $\text{abs}(L) \rightarrow \infty$ ]**

$$\frac{k U(z)}{U_*} = \ln (z/z_0) \quad (3.25)$$

**Unstable Atmosphere ( $L < 0$ )**

$$\left[ \frac{k U(z)}{u_*} \right] = 2 [\tan^{-1} x - \tan^{-1} x_0] + \ln \left( \frac{(x-1)(x_0+1)}{(x_0-1)(x+1)} \right) \quad (3.26a)$$

where

$$x = (1 - 15 z/L)^{0.25} \quad (3.26b)$$

$$x_0 = (1 - 15 z_0/L)^{0.25} \quad (3.26c)$$

The value of  $u_*$  is determined (by a process of iteration, if necessary) using one of the above velocity distributions appropriate for the stability value SP. These calculations have been coded into a subroutine called FRICTVEL.



### 3.3 Correlation For Molecular Diffusion Coefficient

In calculating the value of mass transfer coefficient to estimate the rate of evaporation from a pool of liquid on the ground, it is necessary to know the value of the molecular diffusion coefficient for the chemical vapor in air [see Equation 2.5.9 in the report by Raj and Morris (1987)]. The calculation procedure for determining the diffusion coefficient has been modified to take into account the more recent correlations.

The correlation used is the Fuller, et al., correlation (Reid, Prausnitz and Poling, 1987) and is given by

$$D_{AB} = \frac{1.43 \times 10^{-7} T^{1.75}}{P M_{AB}^{0.5} [A^{1/3} + B^{1/3}]^2} \quad (3.25)$$

where

$D_{AB}$  = Diffusion coefficient for Species A in Species B ( $m^2/s$ )

$T$  = Temperature (K)

$P$  = Pressure (atm)

$M_{AB}$  = Harmonic mean value of molecular weight of Species A and Species B =  $2/[1/M_A + 1/M_B]$

$A$  = Sum of atomic diffusion volumes of the atomic component of Species A

$B$  = Sum of atomic diffusion volumes of the atomic component of Species B

Table 3.1 shows atomic diffusion volumes for various elements. Also indicated in the table are the volume contraction for different types of molecules (aromatic ring, Heterocyclic ring, etc.).

### 3.4 Other Corrections To and Enhancements in ADAM

#### 3.4.1 Corrections

Several corrections were made to ADAM to bring the code to coincide with theoretical analysis. These include:

- i) correcting an error in the program code simulating the mixing of nitrogen tetroxide and air ("NOXTHRM"). The error in the determination of the equilibrium constant value in the subroutine EQUBCONS was corrected.
- ii) modifying an incorrect exponent value and the density calculation in the compressed gas release subroutine GASREL.

TABLE 3.1			
ATOMIC DIFFUSION VOLUMES			
Atomic and Structural Diffusion Volume Increments			
C	15.0	F	14.7
H	2.31	Cl	21.0
O	6.11	Br	21.9
N	4.54	I	29.8
Aromatic Ring	-18.3	S	22.9
Heterocyclic Ring	-18.3		
Diffusion Volumes of Simple Molecules			
He	2.67	CO	18.0
Ne	5.98	CO <sub>2</sub>	26.9
Ar	16.2	H <sub>2</sub> O	35.9
Kr	24.5	NH <sub>3</sub>	20.7
Xe	32.7	H <sub>2</sub> O	13.1
H <sub>2</sub>	6.12	SF <sub>6</sub>	71.3
O <sub>2</sub>	6.84	Cl <sub>2</sub>	38.4
N <sub>2</sub>	18.5	Br <sub>2</sub>	69.0
O <sub>2</sub>	16.3	SO <sub>2</sub>	41.8
Air	19.7		
SOURCE: Reid, Praunitz & Poling (1987)			

### 3.4.2 Enhancements

#### i) Leak From Pipes

ADAM was improved to give proper liquid release rates for a pipe leak situation when the pipe pressure was ambient but the hole was on the pipe wall wetted by the liquid. The release rate is conservatively estimated by assuming the hole to be at the lowest position on the pipe wall (i.e., largest hydrostatic head for liquid leak).

#### ii) Atmospheric Parameters

The atmospheric parameter calculation subroutine has been modified to take into account the possible differences in the value of the aerodynamic roughness at the meteorological tower site and at the place of vapor dispersion. The atmospheric stability and other

parameters are calculated on the basis of  $z_{0,MT}$ , the aerodynamic roughness at wind measuring site (or the meteorological tower). The Gaussian dispersion parameters  $\sigma_y$  and  $\sigma_z$  are calculated using the value  $z_0$ , the aerodynamic roughness at the dispersion location. Also, the correlations with which the values of  $\sigma_y$  and  $\sigma_z$  are calculated as function of downwind distance and atmospheric stability have been modified slightly to give a better fit to the Pasquill-Gifford curves.

### iii) Liquid Fraction Entrained in Vapor Cloud

The release of a compressed liquefied gas into the atmosphere results in the flash vaporization of a part of the released mass. A mass fraction  $f_v$  manifests as saturated vapor and the remainder as saturated liquid of mass fraction  $f_l$  ( $f_l + f_v = 1$ ). However, a part of this liquid mass can get entrained into the dispersing vapor cloud/plume. In fact, the evidence from field tests (the Burro series of pressurized ammonia releases, the Goldfish Series of hydrogen fluoride tests) seems to indicate that a large part of the liquid gets entrained as aerosol into the dispersing cloud.

In order to take into account different amounts of liquid entrainment into the initially formed vapor, a parameter  $\phi$  was introduced in the model in ADAM (see Section 2.6.2.2, Equation 2.6.5, p.2-41, of the report by Raj and Morris, 1987). This factor represents the (mass) fraction of the saturated liquid mass formed after flash which gets entrained into the dispersing vapor. The value of  $\phi$  can be in the range  $0 \leq \phi < 1$ .

In the original ADAM code, this parameter value was a user input. Unfortunately, this led to confusion. Hence, we have removed this as an input parameter and included that as a data item in the chemical property database. The default value is set to  $\phi = 1$  (i.e., all liquid is entrained into the vapor phase). We do realize that the value of  $\phi$  is not dependent solely on the chemical property but also on the conditions, shape, orientation, etc. of the hole and whether the jet impacts the ground or not. However, by including the value as a data item in the chemical property database, it provides the flexibility for an informed user to change the value if deemed necessary. Other users may not want to even bother with the parameter (it is transparent to them).

### 3.4.3 Panel/Menu Driven Inputs

A substantial improvement has been implemented to ADAM. This involves the complete revamping of the data input system. The previous system was based on inputting data through an editor routine. This was complex and sometimes confusing.

The revised data input system is based on the use of menu-driven panels. Also provided are "help" menus to define the various terms in the input. More details of these input panels, and other functions to run ADAM are indicated in Volume II of this report.

## CHAPTER 4

### COMPARISON OF EXPERIMENTAL DATA AND MODEL RESULTS FOR HYDROGEN FLUORIDE

In this chapter, we compare the data from the Goldfish series of HF release tests with the calculated results obtained by exercising the ADAM code simulating HF dispersion under the test conditions. First, we briefly describe the test conditions and other pertinent data. Then, the model results are compared with the test results. A discussion on the results is also given.

#### 4.1 Brief Description of Field Tests

A series of six field tests (called the Goldfish Series) involving the release of anhydrous hydrofluoric acid is reported by Blewitt, et al. (1987). The tests are also described in a recent report by Hanna, et al. (1989). Only three tests in the series were primarily HF vapor dispersion tests.

The tests consisted of releasing liquid anhydrous HF from a tank pressurized with nitrogen. The temperature of the liquid HF in the spill pipe was maintained close to 40 °C with an electric heater. The spill pipe was horizontal, at 1 m above ground and pointed in the downwind direction. Some of the data on the test facility and test conditions are given in Table 4.1. The HF release rate was measured by weighing the HF trailer continuously on a load cell and calculating the slope of the weight vs. time curve. The mean flow rate thus measured is indicated in Table 4.2.

It is reported by Blewitt, et al. (1987) that two types of HF concentration measuring instruments were used; only one type, the Integrated Filter Sampler (IFS), worked properly. Hence, only the concentration data from this type of instrument were used in our analysis. Temperature data were also measured at several locations downwind. No instruments were used to measure the aerosol content or the quality of HF in the plume (i.e., concentration of various oligomers). Also, the plume temperature data and concentration data were not measured at the same locations. More detailed information on the instrumentation, their location, accuracy of measurements can be obtained from the paper by Blewitt, et al. (1987), and in the report by Hanna, et al. (1989).

In the following section, we compare the experimentally measured parameter values with ADAM predictions.

#### 4.2 Release Rate and Flash

Several parameter values calculated using ADAM for the three test conditions are indicated in Table 4.2. This table gives the values for two sets of parameters, namely, the thermodynamic parameters

TABLE 4.1

## SUMMARY OF TEST CONDITIONS - GOLDFISH SERIES OF HF RELEASES

TEST #	RELEASE CONDITIONS					METEOROLOGICAL CONDITIONS				
	NOZZLE DIAMETER (cm)	NOZZLE UPSTREAM HF PRESSURE (Note 1) (psia)	NOZZLE UPSTREAM HF TEMPERATURE (deg C)	RELEASE DURATION (s)	AMBIENT PRESSURE (psia)	AMBIENT TEMPERATURE (Note 2) (deg C)	RELATIVE HUMIDITY (Note 3) (%)	MEAN WIND SPEED (Note 4) (m/s)	ATMOSPHERIC STABILITY	AERO ROUGHNESS (Note 5) (m)
1	4.15	113.09	40	125	15.13	37	4.9	5.6	0 (Neutral)	.0002
2	2.42	121.11	38	360	13.07	36	10.7	6.2	0	.0002
3	2.42	123.10	38	360	13.14	34	17.7	5.4	0	.0002

## \*\*\*NOTES:

1. The HF Nozzle upstream pressure data are from Hanna, et al. (1989). The data indicated by Blewitt, et al. (1987) are as follows: Test 1 = 111 psig (124.13 psia), Test 2 = 115 psig (128.07 psia) and Test 3 = 117 psig (130.14 psia). These are significantly different from the values, indicated by Hanna, et al.
2. Ambient temperature measured at 2.5 m above ground. Temps from Blewitt, et al. (1990), and Hanna, et al. (1989).
3. Relative humidity reported are the ambient values at an upstream of spill point location. In Test 3, the humidity near the release point was artificially increased by injecting hot water into a shallow, 250 m x 600 m, pond (upwind).
4. Measured at 2 m height.
5. From Blewitt, et al., (1990).

TABLE 4.2: TEST DATA and CALCULATED FLOW AND POST FLASH CONDITIONS OF JET

**** TEST DATA ****		----- CALCULATED EXIT CONDITIONS -----> <----- FLOW AND JET CONDITIONS AT EXIT ----->												
Conditions upstream of orifice		<----- Before Flash ----->					<----- After Flash ----->							
Test #	Abs Temp	Ambient	Exptl Mean	Satm Pr at	Sat Temp	Sat Liq Density	Eff Mol Wt	Sat Vap Density	Exit Stream Vel	HF Mass Flow Rate	HF Mass Flashing to Ph. flow	Initial Area of Two Ph. Jet		
Pr.	Temp	Abs Pr.	Rate	Upstream Temp	Pressure	at exit	of sat	at exit	(Note 4)	(kg/s)	(kg/s)	(m <sup>2</sup> )		
(Note 1)			(Note 2) 0				Exit	(Note 3)						
(N/m <sup>2</sup> )	(K)	(N/m <sup>2</sup> )	(kg/s)	(N/m <sup>2</sup> )	(K)	(kg/m <sup>3</sup> )	(kg/mol)	(kg/m <sup>3</sup> )	(m/s)	(kg/s)	(kg/m <sup>3</sup> )	(m <sup>2</sup> )		
1	7.792E5	313.2	0.9048E5	27.67	2.602E5	289.80	964.65	69.73	2.62	22.68	30.88	21.70	11.96	11.0 E-2
2	8.349E5	311.2	0.9008E5	10.46	1.878E5	289.70	964.87	69.76	2.61	23.57	19.76	19.90	12.97	3.4 E-2
3	8.421E5	311.2	0.9053E5	10.90	1.873E5	289.90	964.44	69.70	2.62	23.79	19.84	19.75	13.09	3.35 E-2

NOTES

- 1 Data from Hamra, et al., (1989). These are considerably different from those given by Blewitt, et al., (1967).
- 2 Tests 1 & 2 data taken from Hamra, et al. Value for test 3 measured from the graph of HF (railer wt vs time given by Blewitt, et al.
- 3 Calculated on the basis of the vapor being a perfect gas with indicated effective molecular weight.
- 4 Value of discharge coefficient (CD) assumed to be 0.6. Also, nominal orifice area used in flow calculations. Stream velocity indicated is the Bernoulli velocity \* CD.
- 5 Assumes that all liquid in the post flash stream is entrained into the jet.

and the flow parameters of the jet just after the exit from the orifice plate. There are only limited data from the field tests with which these calculated values can be compared.

Table 4.2 shows the HF temperature and pressure upstream of the orifice\*\*. The saturation pressures of HF corresponding to the temperatures of HF upstream of orifice are indicated in this table. The saturation pressure corresponding to the HF temperature upstream of the nozzle is lower than the pressure maintained in the tank with nitrogen. Hence, the HF liquid is in a compressed liquid state. It can be shown, however, that because of the relatively low enthalpy of liquid compression the specific enthalpy of the liquid HF upstream of the orifice is almost the same as the specific enthalpy of the saturated liquid corresponding to the upstream temperature. The details of this analysis are indicated in Appendix A.

When this compressed liquid is released to the atmosphere, a part of the liquid flashes to form vapor. The vapor and liquid formed are in the respective saturated states corresponding to the atmospheric pressure. The calculated mass fraction of the released HF which flashes to vapor is indicated in this table. Also shown are the temperature (saturation) of the vapor and liquid immediately downstream of the orifice.

The vapor formed after the flash will be a mixture of various polymers of HF. Therefore, the molecular weight of the vapor will be considerably different from that of the monomer. The effective molecular weight of the saturated vapor is calculated by the correlation (see Figure 2.2)

$$\mu_{\text{Sat Vap}}(T) = 156.67 - 0.3 T \quad (4.1)$$

where

$$\mu_{\text{Sat Vap}}(T) = \text{apparent molecular weight of the saturated vapor (kg/kmole)}$$

$$T = \text{saturation temperature (K)}$$

These apparent molecular weights of the vapor at a position immediately downstream of the orifice are indicated in Table 4.2 for the conditions of the tests. The density of vapor, calculated using these molecular weight values, ambient pressure, saturation temperature and the perfect gas assumption is also indicated in Table 4.2. Unfortunately, test data are not available to compare with these calculated values.

---

\*\* There is a discrepancy between the values for this parameter reported by Blewitt, et al, (1987) and by Hanna, et al. (1989). We have used the values published by Hanna, et al. (1989).

The second part of Table 4.2 contains the calculated flow rate values. The flow rates are calculated in ADAM using the Bernoulli equation and assuming a coefficient of discharge ( $C_d$ ) value of 0.6. This coefficient multiplies the Bernoulli exit velocity to give a reduced velocity. The mass flow rate is then determined by the product of orifice nominal area, reduced velocity and liquid (saturated) density at ambient pressure. These calculated values for the reduced velocity, liquid density and the mass flow rate are indicated in the table.

The flashing process results in the formation of a two-phase jet. Because of the reduction in the mean density (compared to the liquid density) of the flow consequent to the flashing process, the jet size expands very close to the exit section of the orifice. The calculated values of the mean density of the two-phase flow are indicated in the table. These values are determined based on the assumption that all of the liquid fraction (in the post flash stream) is entrained as aerosols into the jet. Also indicated in the table are the calculated cross section of the two-phase flow in the jet very close to the orifice.

#### Comparison of Source Condition Data with Calculated Results

No experimental data seemed to have been measured very close to the exit section of the orifice. Hence, the calculated results for jet velocity, quality of the two phase mixture, temperature, etc. at the exit section cannot be compared with test data. The calculated value for the initial diameter of the two phase jet can be compared to the jet diameter from photographs with some uncertainty on the photographic scales (due to perspective and mirage effects). The only source parameter that can be compared is the mass flow rate, since this can be inferred from the experimental data on the HF trailer weight vs. time.

The calculated mass flow rate values and the experimental values for tests 2 and 3 agree very closely; however, for test 1, ADAM predicts about 9% higher values. It is noted that there are discrepancies in the reported values for mass flow rates (test data) by different researchers. For example, for test 3, Hanna, et al. (1989) report a value of 10.27 kg/s. The value determined by us using the graph of weight vs. time for this test published by Blewitt, et al. (1987) is 10.9 kg/s. Blewitt, et al., gives the mass flow rate values in a table in units of gpm without indicating what values of liquid density were used in converting the raw data (kg/s) to gpm. Assuming the liquid density (for test 3, see Table 4.2) to be 964.44 kg/m<sup>3</sup>, we can convert the gpm data of Blewitt, et al. to kg/s; this calculation leads to 12.54 kg/s! However, the ADAM calculated value and the value measured off the graph for test 3 agree very closely. Therefore, we feel that the algorithm for source condition calculations in ADAM is quite accurate.

Comparison of other calculated source condition parameter values with test data are not possible because none of the other parameters were measured.



### 4.3 Dispersion Results

We consider the comparison of the results in two distinct flow/dispersion regimes. The first is the jet flow regime where the flow velocities in the plume are considerably higher than the velocity of the prevailing wind. The second regime combines heavy gas dispersion and passive dispersion.

#### 4.3.1 Jet Dispersion Regime

It is seen from Table 4.2 that the calculated jet velocities are about 23 m/s whereas the wind speeds are in the range 4.2 m/s to 5.6 m/s. Because of the relatively high speed with which the jet flows out of the orifice, air is entrained into the jet. In ADAM, the jet dilution is calculated. The calculations are terminated when the mean velocity in the jet is within 5% of the wind speed at the level of the top of the jet. The dispersion is then modeled using the heavy gas model until the density of the cloud is very close to that of air. At that time, the dispersion modeling is done using the Gaussian model.

In Figures 4.1a, 4.1b and 4.1c, the calculated values for variation of jet width, peak HF concentration<sup>2</sup>, mean velocity in the jet, and the centerline plume temperature are plotted as functions of downwind distance from the orifice. The Figure 4.1a results are for conditions of Goldfish Test #1. Similarly, Figure 4.1b and Figure 4.1c represent the plots for Test #2 and Test #3, respectively. An aerial photograph of the plume was available for Test #2. The data on plume width (obtained by measuring the visible cloud width) are plotted in Figure 4.1b. The concentration at which the plume becomes invisible is not known. This will depend on the relative humidity and (perhaps) on the optical properties of HF vapor. The calculated plume width plotted in Figure 4.1b is the equivalent "box" width in the jet region.

Data on plume temperature measured during the tests are also plotted on these figures.

#### Discussions on Jet Regime Results

The general trend for the variation of each of the parameters with distance for all three tests are similar. The temperature initially decreases from the saturation temperature corresponding to the ambient pressure up to about 15 m distance and then increases. The initial dip in the temperature is due to the

---

<sup>2</sup> Concentration is given in units of kg of total HF per unit volume (m<sup>3</sup>) of space. To convert this into molar or ppm units, a chemical molecular weight is needed. We use the molecular weight value corresponding to the monomer HF (20 kg/kmole). Hence, the concentration results expressed in ppm are monomer equivalent values.

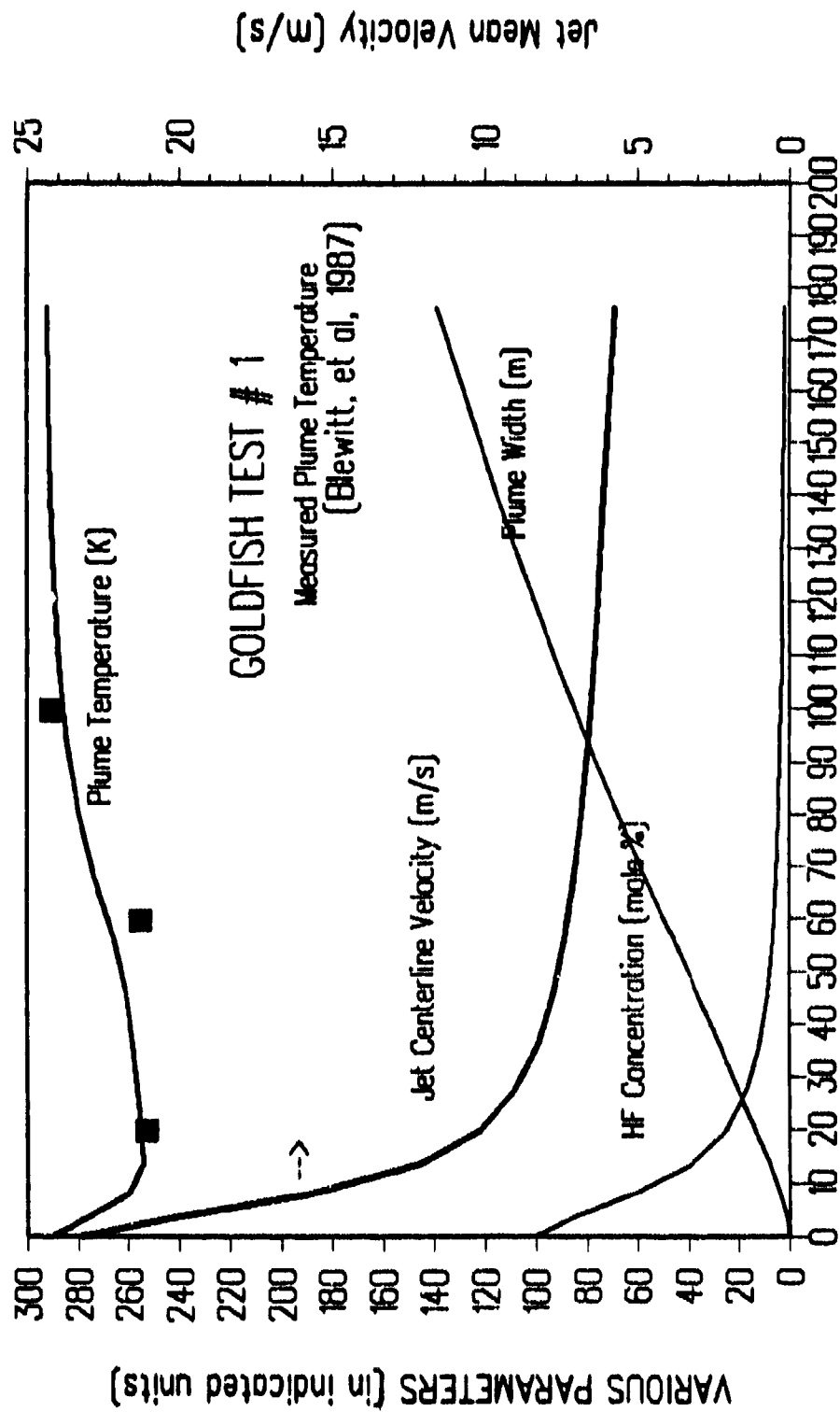


**FIGURE 4.1a: Variation of Jet Parameters vs Dist**

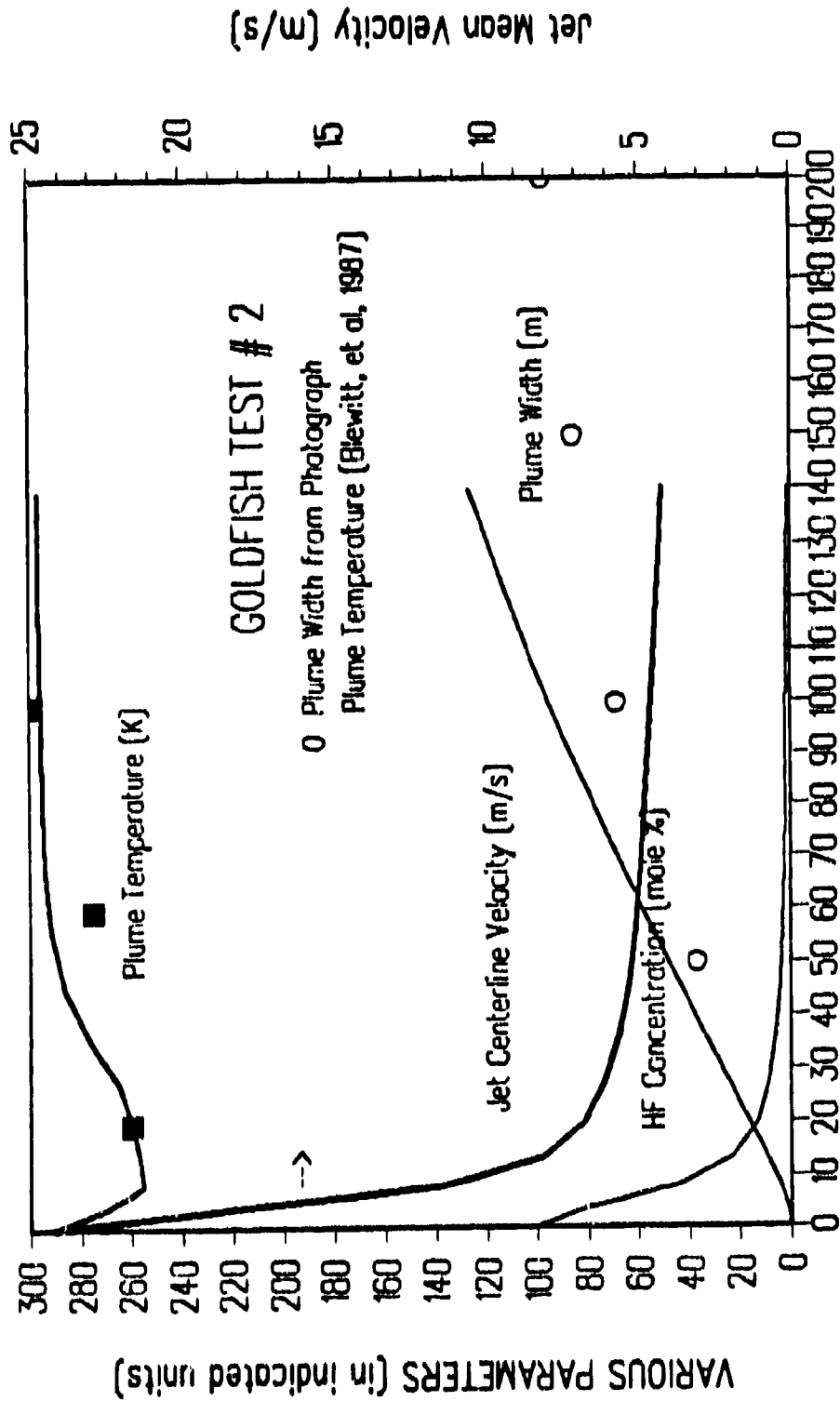


**FIGURE 4.1b: Variation of Jet Parameters vs Dist**

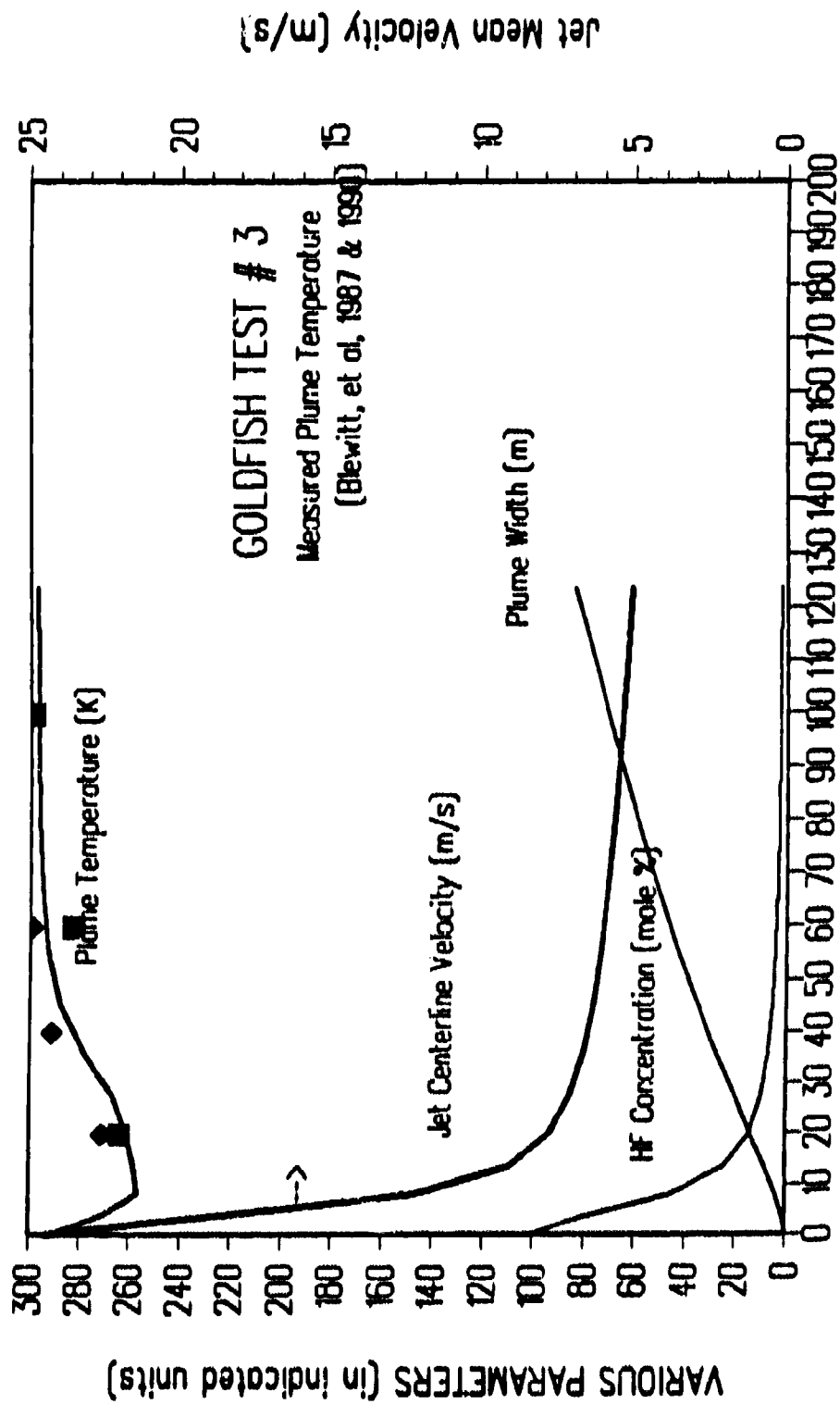


**FIGURE 4.1c: Variation of Jet Parameters vs Dist**

evaporation of liquid aerosols. At later stages, the exothermic reaction with moisture and the enthalpy of air together contribute to the gradual rise in plume temperature. The lowest temperatures recorded by instruments at different distances from the source are also plotted in the above figures. More detailed discussion on the temperature predictions are given in a later section.

The jet centerline velocity decreases - a requirement of conservation of momentum (with air mass entrained) and ground friction. We terminate the jet calculations when the mean velocity in the jet is within 5% of the wind speed at the height of the top of the plume. Based on this criterion, the "jet length" (i.e., the distance from the orifice within which the jet velocity is greater than wind speed at least by 5%) has been calculated for all three tests. It is seen that these jet regimes extend up to 176 m for Test #1, 140 m for Test #2, and 108 m for Test #3, respectively. These are indicated in Table 4.3.

It is noticed from the results presented in the above three figures that the HF concentration at the centerline varies rapidly reaching 1 to 2% level by the end of the jet regime. Hence, in the jet regime, a 2 order of magnitude reduction in concentration is effected. In the remainder of the dispersion regimes, another 2 to 3 orders of magnitude reduction in the concentration occurs.

The variation of the width of the plume with distance is also shown in the above three figures. It is seen from the ADAM results that the width seems to increase linearly with distance - a characteristic of axi-symmetric turbulent jets. This implies that the lateral expansion due to negative buoyancy effects is small, at least in the near field where jet velocity is considerably larger than the cross stream velocity induced by negative buoyancy. Only for one HF dispersion test (Test #2) was an aerial photograph of the plume available. A copy of this photograph is indicated as Plate 4.1. This picture was taken from a camera at 500 m above ground and 500 m upwind of the spill point. Hence, the picture suffers from the perspective distortion. We have determined the apparent horizontal (cross wind) and vertical (downwind) scale by noting the distance to the 300 m arc of masts and the separation distance between two instrument poles at 300 m (this separation distance is 15 m). Using this photographic data, we have measured the visible plume width at various downwind distances. These are plotted as data points in Figure 4.1b.

It is seen that the predicted width is larger than the measured width. A number of reasons can be put forth for this discrepancy. The first one is that the jet model over-dilutes the jet (perhaps due to the use of higher than actual entrainment coefficient). The second reason is that our determination of the scale of the photograph is not entirely correct since we have not considered the effect of perspective view on the change in the horizontal scale as one goes away from the camera. The third possible reason is that in the above comparison, we are comparing the width of an equivalent "box" type of jet with a real plume whose visible width

TABLE 4.3: SELECTED RESULTS FROM JET REGIME CALCULATIONS (1)

PARAMETERS	UNIT	GOLDFISH SERIES TEST #		
		1	2	3
JET LENGTH	m	176	140	108
LIQUID PERSISTENCE DISTANCE	m	250	177	441 (2)
HEAVY GAS TO PASSIVE DISPERSION TRANSITION DISTANCE	m	1596	1160	1028
MASS DILUTION RATIO (AIR/CHEMICAL) AT TRANSITION	.....	69.4	113.0	69.5

NOTES:

- 1) The value of aerodynamic roughness  $Z_0 = 0.0002$  m.
- 2) Relative humidity is assumed to be 17.7%.

GOLDFISH SERIES TEST #2  
HYDROGEN FLUORIDE

Scale

Downwind Scale 1 cm = 50 m  
Horizontal Scale 1 cm = 50 m



PLATE 4.1: Experimental Set up and Vapor Plume in an  
HF Release Test at DOE Test Facility

depends on both the aerosol content of the plume and the relative humidity in the atmosphere. However, a strong argument can be made for modifying the entrainment coefficient for two phase jets with its values substantially different from the ones for a single phase jet with the same initial momentum.

We are unable to compare other predicted results (HF concentration, jet velocity, aerosol content, etc.) with test data because none of these were measured within the jet region in the field experiments.

#### 4.3.2 Plume Temperature

The plume temperatures predicted by the thermodynamic model (discussed in Chapter 2) are indicated in Figure 4.2a and Figure 4.2b for the conditions of the three Goldfish dispersion tests. In Figure 4.2a, the relationship between cloud temperature and total HF concentration (monomer equivalent) over the entire range of 0 to 95% is presented. In figure 4.2b, the temperature variation over the HF concentration range of 0% to 5% is shown. It is seen that the plume temperature is above the (initial) saturation temperature of 290 K for HF concentration values below 3 to 4.5%, depending on the test conditions. Using those results and the ADAM calculated results for downwind plume centerline concentration at ground level with distance, we obtain the variation of temperature at ground level with distance. These calculated results are plotted in Figure 4.3a, b and c, and respectively for Tests #1, #2, and #3.

It is indicated by Blewitt, et al (1987) that plume temperatures were measured at 20m, 60m, 100m, 200m and 1000m from the spill point. The plume temperature data are provided (ibid) for the 20m, 60m, 100m, and 200m as function of time for all three tests. We have assumed that these data refer to the plume centerline at 1 meter height above ground (Blewitt, et al, do not specify this important information in their paper). The lowest measured temperature at each location is plotted as a function of the measuring location. These are indicated in Figure 4.3a, Figure 4.3b and Figure 4.3c. Table 4.4 also shows these "measured" lowest temperature data for all three experiments. Particularly noteworthy are the significant differences in the reported data for test # 3.

#### Discussions on the Temperature Results

In general, the temperatures measured in the three Goldfish tests and those predicted by ADAM are in reasonable agreement as can be seen from Figure 4.3a through Figure 4.3c. It should be noted that the temperatures predicted by the model are for a steady and uniform release; therefore, the plume temperature at specified downwind centerline location does not vary with time. The data published by Blewitt, et al., (1987) show the temperature at the location of the instruments to vary with time, significantly, even though the flow rate out of the pipe is constant over a significant period of the test. We speculate that this temporal variation in



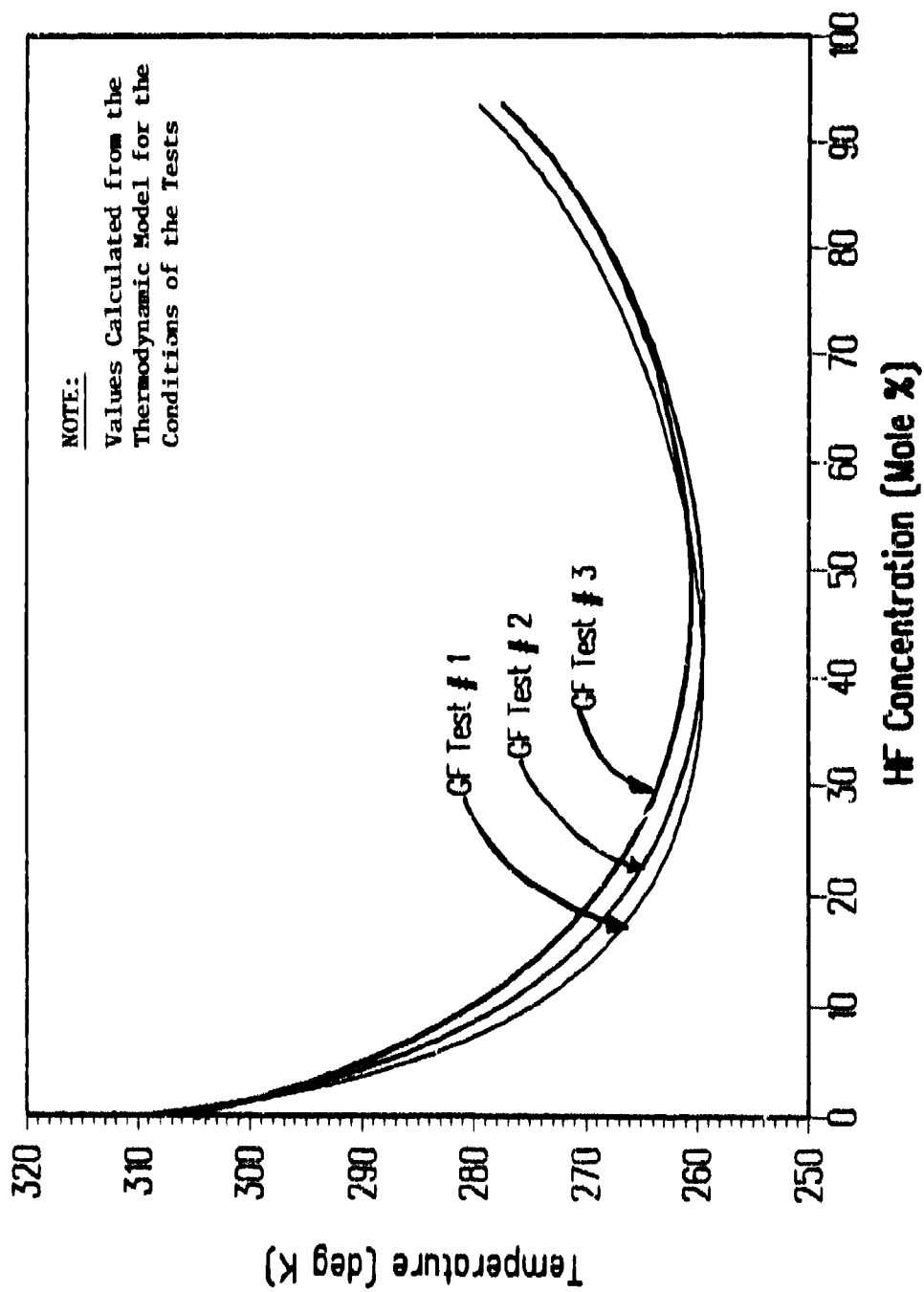


**FIGURE 4.2a: Temperature of HF-Air Mixture**

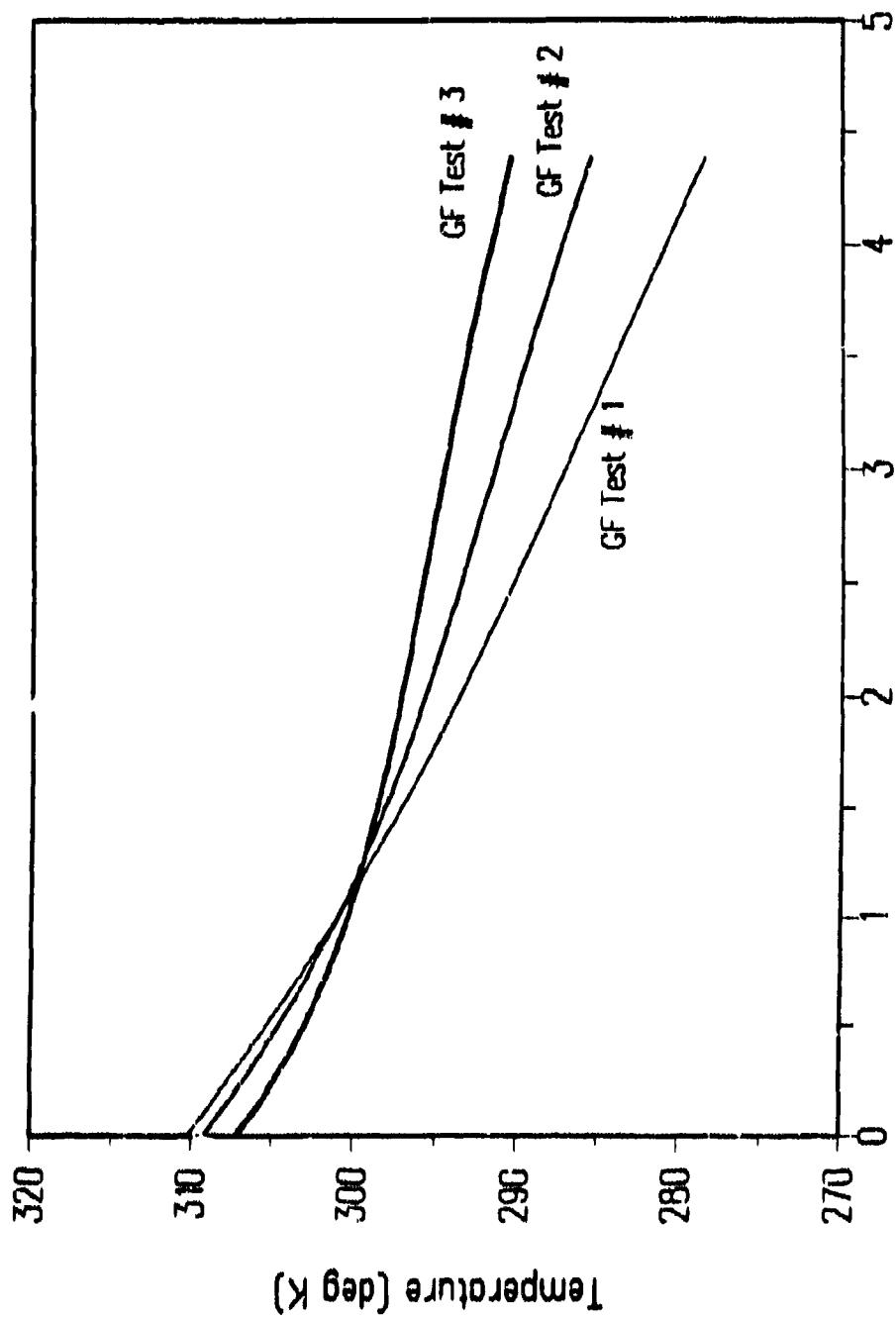
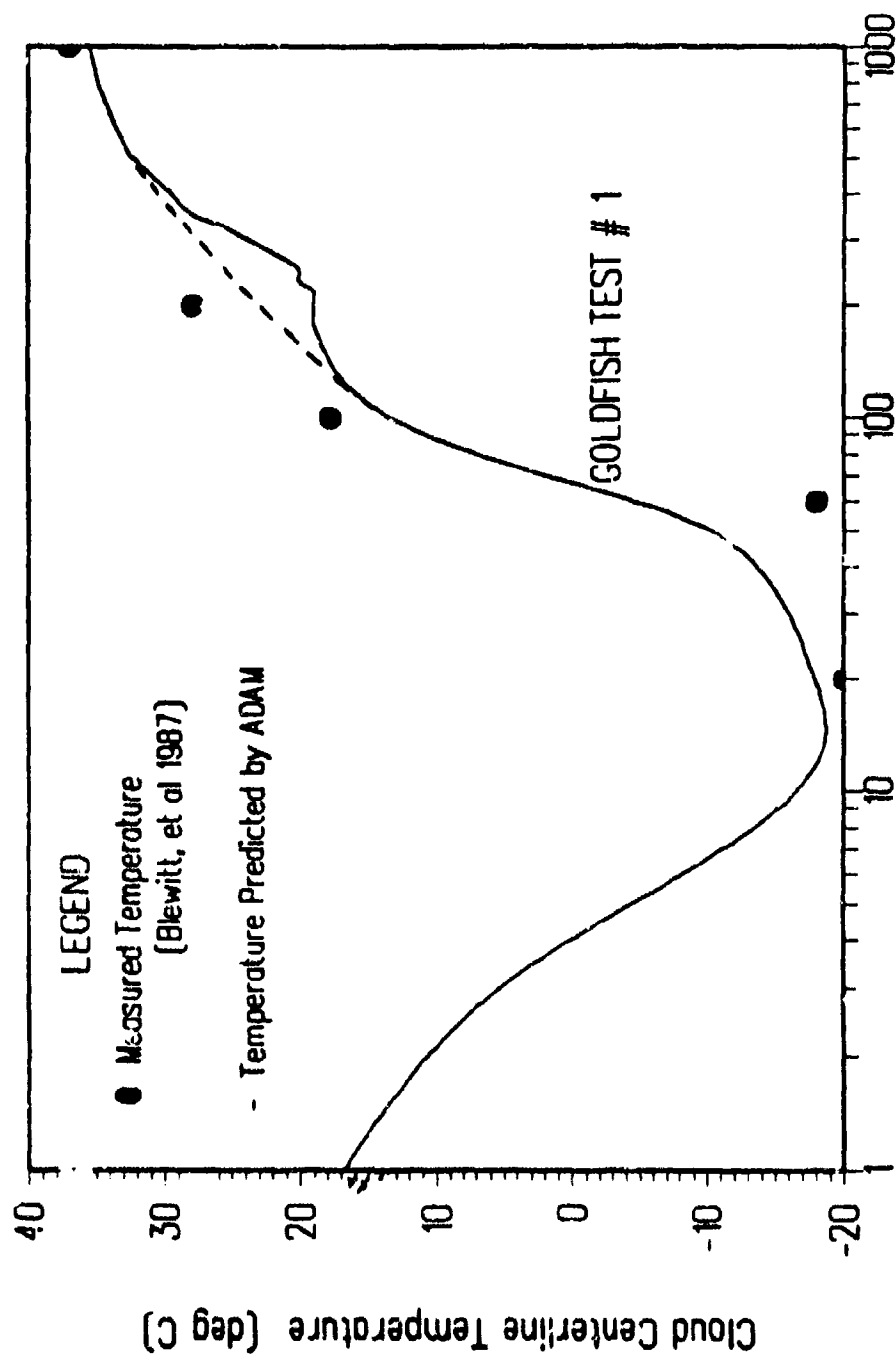


FIGURE 4.2b: Temperature of HF-Air Mixture



Distance from Source (meters)

FIGURE 4.3a: Measured & Predicted Temperature vs X

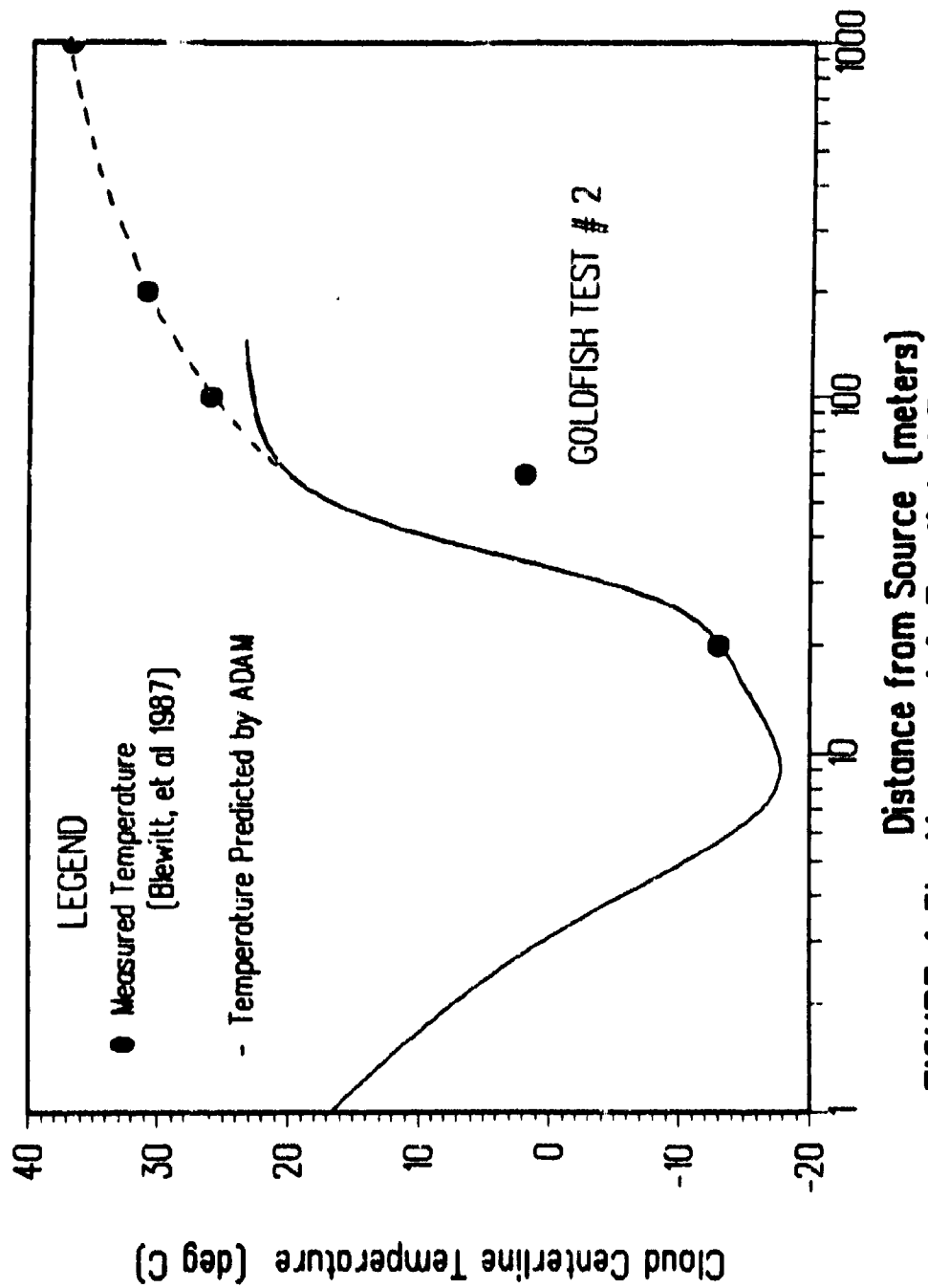
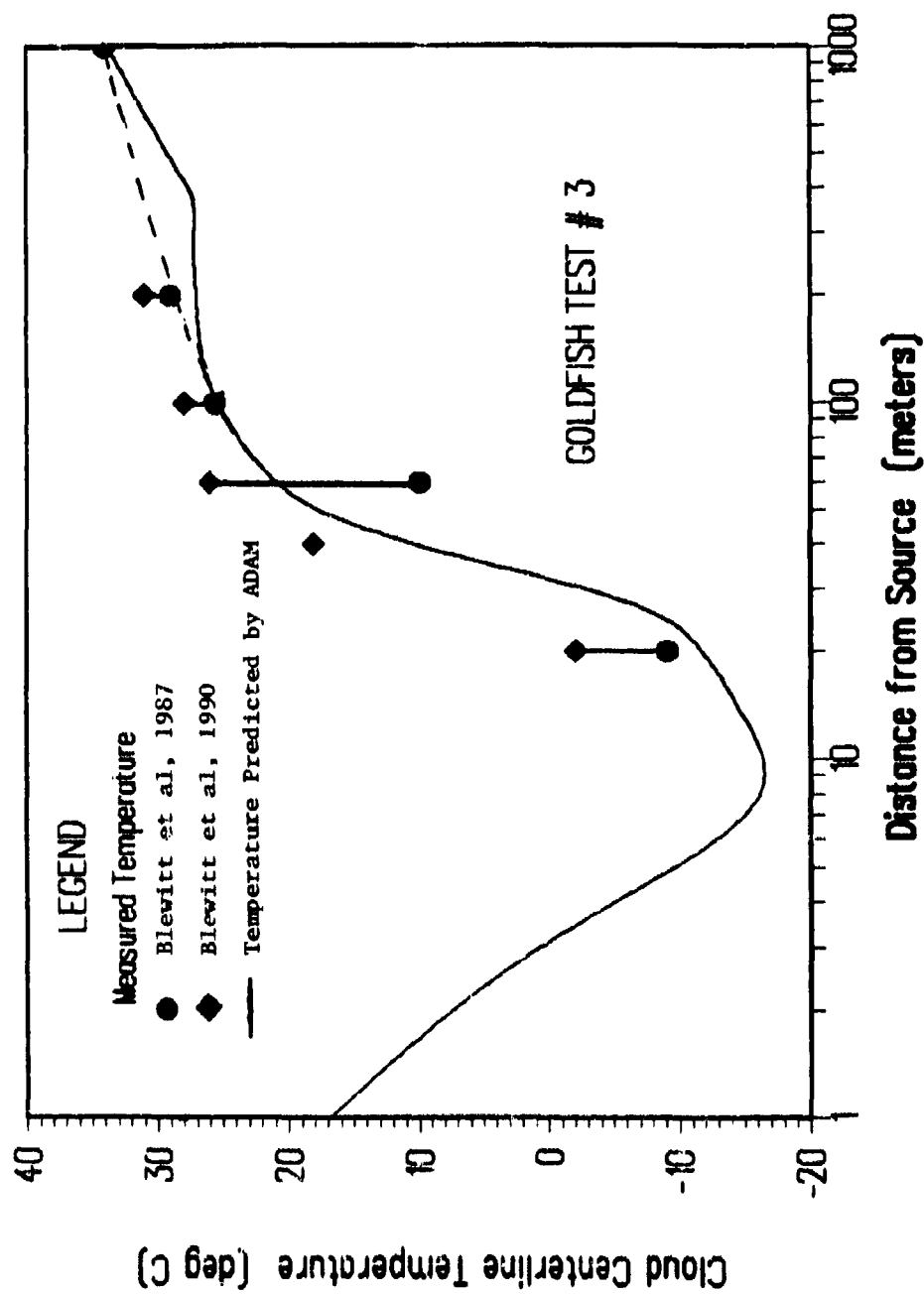


FIGURE 4.3b: Measured & Predicted Temperature vs X



**FIGURE 4.3c: Measured & Predicted Temperature vs X**

TABLE 4.4: GOLDFISH TEST DATA FOR PLUME TEMPERATURE

DISTANCE FROM SOURCE (m)	TEST #1	TEST #2 (Note 2)	TEST #3 (Note 2)	TEST #3 (Note 3)
20	253.0	260.0	264.0	271.0
40	N/A	N/A	N/A	291.0
60	255.0	275.0	283.0	299.0
100	290.8	299.0	298.6	301.0
200	301.0	304.0	302.0	304.0
1000	310.0	309.0	307.0	307.0

NOTES:

- 1) Ambient air temperature values are indicated in Table 4.1. These values are used in the above table.
- 2) These refer to the lowest measured temperature as read from the graphs published by Blewett, et al (1987). These graphs provide the values for temperature depression with respect to the ambient temperature.
- 3) Obtained from the data presented in Blewitt, et al (1990).

NA: Not Available

the experiments may have been caused by one or more of the following: i) meandering of the plume, ii) accumulation of HF liquid droplets on the thermocouple and their subsequent evaporation, or iii) an unknown instrument problem.

It can be seen from Figure 4.2a that the thermodynamic model based minimum temperature that can be attained in the cloud for the conditions of any of the three tests is 260 K. In Test #1, the measured minimum temperature is 253 K (see Figure 4.3a). It is doubtful that this minimum temperature measured is accurate because of the very noisy temperature data output from the recorders. The ADAM predicted temperature for Test #1 conditions slightly overpredicts the plume temperature for distances less than 100 m and underpredicts at distances greater than 100m when compared to the lowest temperatures measured at the different points. In the case of Test #2 and Test #3, the predicted temperature is very close to the measured values. In Figure 4.3c are shown the temperature data indicated by Blewitt, et al., in their two publications. The discrepancy in the measured temperature (reported) can be clearly seen. In view of the uncertainty in the measured values of the plume temperature and noting that in Figures 4.3a through 4.3c, we are comparing the minimum temperature measured at any point to the ADAM predicted temperature (which assumes a steady flow both in time and in direction) the agreement between the measured and predicted temperatures is very good.

The predicted temperature curves shown in Figure 4.3a through Figure 4.3c show some erratic behavior at about 300 m. This distance is close to the point at which all of the liquid in the aerosol form evaporates (see Table 4.3). The kinks in the curve may be a result of some difficulty in convergence in the thermodynamic program. The possible model temperature variation at distances beyond about 300 - 400 m is shown by dotted lines in Figures 4.3a to Figure 4.3c.

#### 4.3.3 Heavy Gas Dispersion Regime

##### Concentration Data and Predictions

We have obtained the measured HF concentration data principally from two references, namely, Blewitt, et al. (1987), and Blewitt, et al. (1990).

The concentration data in the Goldfish tests were measured at 300m, 1000m and 3000m distances (Blewitt, et al., 1987). Based on the information in the paper by Blewitt, et al. (1987), we infer that the concentrations reported represent average values over 66.6 seconds, 83.3 seconds or 100 seconds (no additional details are available as to which sensors were set to what averaging times). Blewitt, et al., have provided concentration contours for 300, 1000 and 3000m locations (in general) at two different times. Also provided in the referenced paper is a 3-D contour map of concentration as a function of crosswind position and time at a specified sensor elevation.

Table 4.5 shows the HF concentration data obtained from the above references. The numbers indicated in the table were measured off the figures published in the two papers. To the extent that accurate measurements cannot be made from small figures, we anticipate some errors (at best, a 15% error in reading off graphs). It can be clearly seen that the concentration values at specified locations vary quite significantly, not only between different figures in the same publication but also between the two referenced publications.

The ADAM predicted values for the variation of plume centerline, ground level concentrations with downwind distance are plotted in Figure 4.4a, Figure 4.4b, and Figure 4.4c for the conditions of Test #1, Test #2, and Test #3, respectively. Also plotted on the same figures are the respective measured values (indicated in Table 4.5). The predicted concentrations indicated are the "monomer equivalent" values. I.e., the cumulative concentration of all oligomers of HF (both vapor and liquid) are expressed as if they had a molecular weight of 20.

#### Discussions on the Concentration Results

There are no concentration data for distances less than 300 m. The jet plume region is within this distance. Hence, we are unable to compare the "near field" concentration predictions with test data.

The predicted concentration in Figure 4.4a is within a factor of 2 with the data presented by Blewitt, et al., (1990). However, in view of the significantly large data scatter, it can be concluded that the predicted curve is well within the acceptable accuracy.

In Figure 4.4b, the predicted concentration values are significantly lower than the experimental values. In fact, in this Test #2, the data scatter do not seem to be large. Unfortunately for this test, no data have been reported for the 3000 m instruments.

The predicted values for Test #3, shown in Figure 4.4c, seem to agree very closely with the data presented in the first paper by Blewitt, et al. (1987). Compared to the data indicated in the second paper (1990), the predicted values are lower in some locations by as much as a factor of 3. We are unable to explain such a large discrepancy.

The concentration predictions by ADAM are based on a concentration averaging time of 65 seconds. This value was chosen, based on the information indicated by Blewitt, et al. (1987) on the design of the HF samplers in the tests; the sampling time for the filter cassettes was 66.6s, or 83.3s or 100s. We also note that the ADAM code predictions are based on the assumption of a steady state plume (i.e., the source flow was steady). The data provided Blewitt, et al., are difficult to interpret. As an example, we consider the conditions of Test #3. The duration of the steady



TABLE 4.5: MEASURED DATA ON HF CONCENTRATIONS

TEST #1	DISTANCE (m)	HF CONCENTRATION (ppm)	REFERENCE # AND SUBREFERENCE
	300	3100	Figure 4.1 of Ref(A)
	300	21000	Figure 4.2 of Ref(A)
	300	20150	Figure 12 of Ref(B)
	300	17920	Figure 4.3 of Ref(A)
	1000	1500	Figure 4.6 of Ref(A)
	1000	2700	Figure 4.7 of Ref(A)
	1000	2300	Figure 4.8 of Ref(A)
	1000	3000	Figure 12 of Ref(B)
	3000	400	Figure 4.10 of Ref(A)
*****			
TEST #2	DISTANCE (m)	HF CONCENTRATION (ppm)	REFERENCE # AND SUBREFERENCE
	300	16300	Figure 13 of Ref(B)
	300	9300	Figure 4.11 of Ref(A)
	300	8300	Figure 4.12 of Ref(A)
	1000	1900	Figure 4.13 of Ref(A)
	1000	1950	Figure 13 of Ref(B)
*****			
TEST #3	DISTANCE (m)	HF CONCENTRATION (ppm)	REFERENCE # AND SUBREFERENCE
	300	6300	Figure 4.15 of Ref(A)
	300	7800	Figure 4.16 of Ref(A)
	300	18420	Figure 4.17 of Ref(A)
	300	15700	Figure 14 of Ref(B)
	1000	600	Figure 4.18 of Ref(A)
	1000	700	Figure 4.19 of Ref(A)
	1000	2323	Figure 4.20 of Ref(A)
	1000	2340	Figure 14 of Ref(A)
	3000	222	Figure 4.22 of Ref(A)
	3000	200	Figure 14 of Ref(B)

## NOTES:

- Ref(A) is the paper by Blewitt, et al., 1987.
- Ref(B) is the paper by Blewitt, et al., 1990.
- All concentration values refer to locations 1 m above the ground at plume centerline.

# GOLDFISH TEST # 1

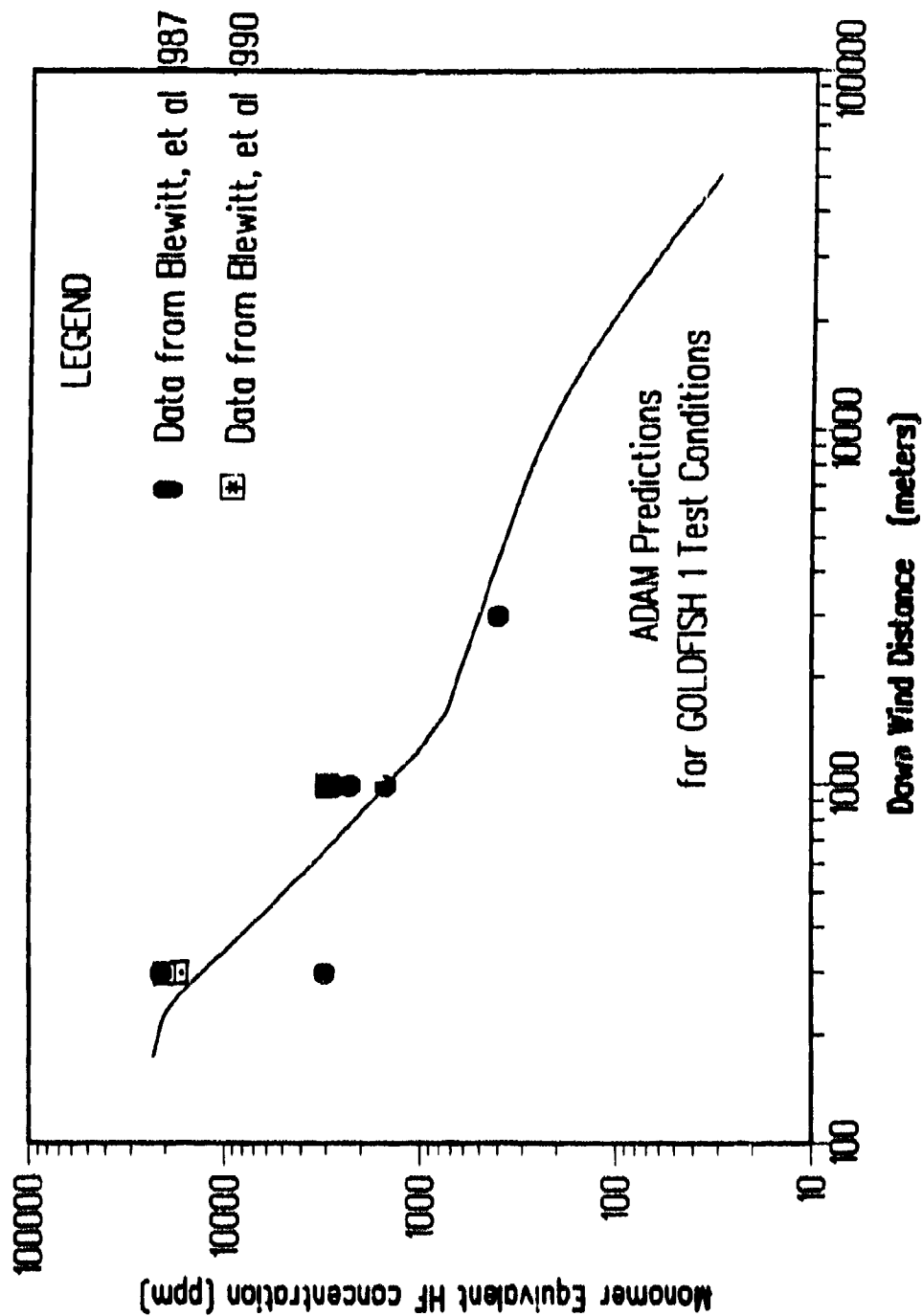


FIGURE 4.4a: Ground Level Concentration vs Distance

## GOLDFISH TEST # 2

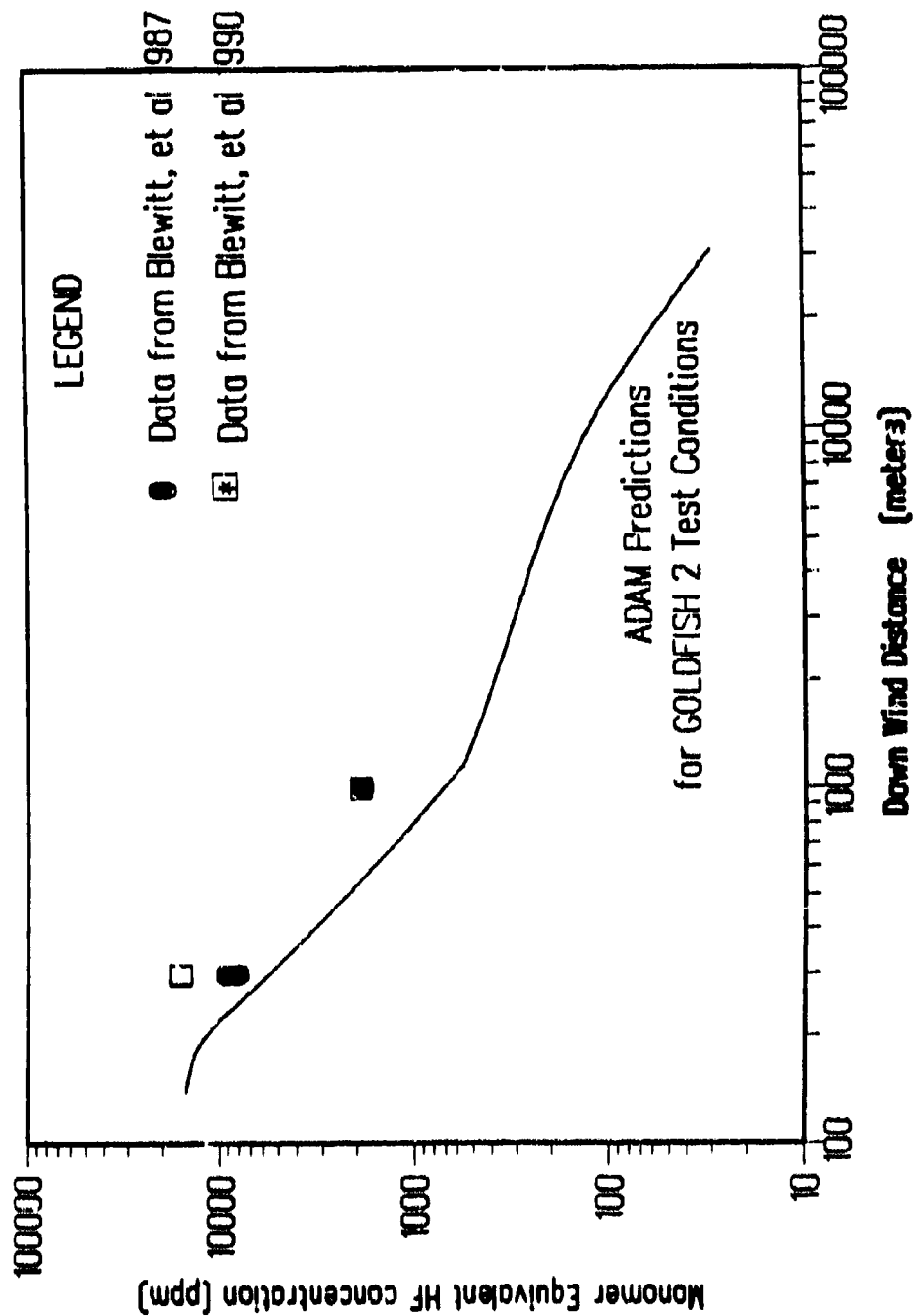


FIGURE 4.4b: Ground Level Concentration vs Distance

# GOLDFISH TEST # 3

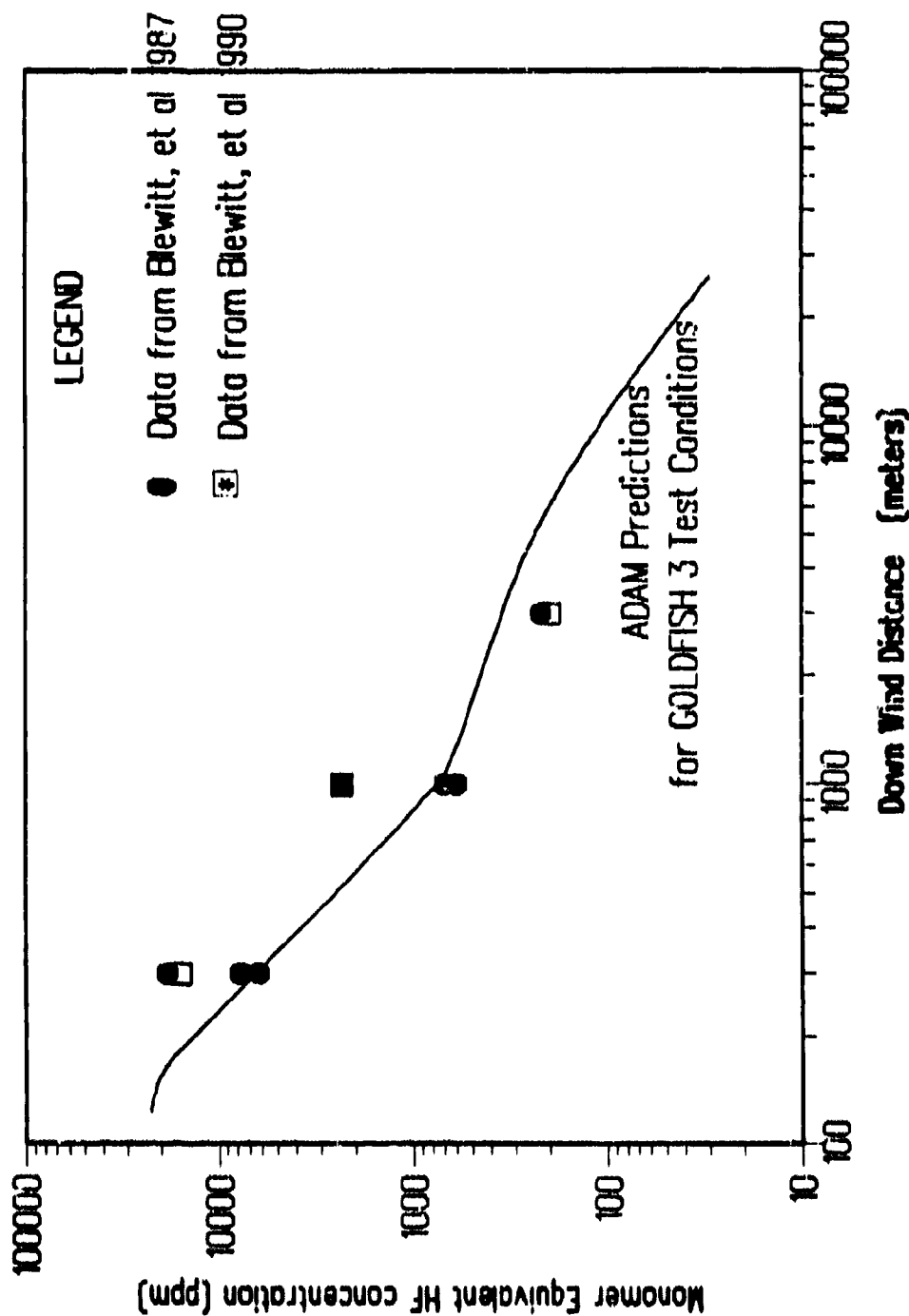


FIGURE 4.4c: Ground Level Concentration vs Distance

state release was about 380 seconds. Blewitt, et al. (1987) give two different concentration contours for 113s; in one the peak 1 m level concentration is 6300 ppm and for the other it is 7800 ppm. These data were obtained from the contour plots (Figure 4.15 and Figure 4.16) indicated by Blewitt, et al. (1987). What is not clear from these figures is the averaging time used for the plot of the concentration contours. Other questions are: Do the data presented refer to only one filter cassette? What was the variation of concentrations measured at the same location by different filter cassettes? What is the basis of the 3-D concentration contour figures presented by Blewitt, et al. (1987)? Finally, why are there discrepancies between concentration values published by the same author in two different publications for the identical test and measurement locations?

Also not certain is the algorithm by which the experimentally measured concentration values were converted to molar concentrations which are reported in the papers by Blewitt, et al. In the tests, integrated mass dose of total HF (vapor and liquid aerosols, if any) are collected for 66s, 88.3s or 100s on filter paper. The aspiration rate is given to be 3.5 liters per minute. Since no real time measurement of the temperature or molecular weight of the species were made at the positions where concentration measurements were made, it is our opinion that it is not possible to convert the dose data (actually obtained in the tests) to the ppm units reported. It is possible that a monomer equivalent is assumed (i.e., a molecular weight of 20 kg/kmole). Even in this case, the temperature of the cloud must be assumed in order to convert the raw data to the ppm values for the concentration. Blewitt, et al., have not indicated how this conversion to the reported units are made.

In view of the many uncertainties in the reported data, both in magnitude and the way in which the raw data may have been converted into the (reported) molar concentration values, we conclude that the ADAM predictions represent the test data reasonably well.

## CHAPTER 5

### FLUORINE

#### MODELS FOR AIR MIXING AND DISPERSION

##### 5.1 INTRODUCTION

Under normal ambient conditions, fluorine is a light yellow "permanent" gas with a critical temperature of 144 K. Due to its very reactive character, the chemical is shipped commercially in gaseous state in small steel cylinders (maximum 2.7 kg) at relatively low pressures. However, when larger quantities are to be shipped, the chemical is transported in a liquid state near its normal boiling point of 85 K. Accidents involving these tanks could lead to the release of large quantities of fluorine and the consequences of such an event provide the focus of the present discussion.

##### 5.1.1 Details of LF<sub>2</sub> Transport

Liquid fluorine (LF<sub>2</sub>) is transported in road tanker trailers which consist of three horizontal, concentric vessels. LF<sub>2</sub> is contained within the inner tank made of monel or stainless steel 304. An outer concentric tank made of stainless steel 304 contains liquid nitrogen and this tank is enclosed in a carbon steel cylinder. The annular space between the nitrogen tank and the carbon steel tank is filled with powdered insulation and evacuated. Figure 5.1 shows a cross-sectional view of the LF<sub>2</sub> and other tanks on the road tanker. Figure 5.2 shows the tank flow system in the fluorine trailer.

The inner product vessel has a capacity of 1.77 m<sup>3</sup> (468 gallons) with an ullage volume of about 1.5 m<sup>3</sup>. That is, the maximum product mass is 2260 kg (5000 lbs). This vessel has a service rating of 0.482 MPag (70 psig). Manual operation of the fluorine fill valves in the vapor phase is the only form of pressure relief device provided. In case of an emergency, a fifty-foot coil of copper tubing with the necessary fittings is available for the purpose of venting excess fluorine pressure. Changes in the temperature of the product are monitored with the use of fluorine product pressure gauge. Normal indication on this pressure gauge is 0. The high pressure alarm is set at 0.124 MPag (18 psig) which activates the warning lights and horn.

The temperature of the liquid fluorine is maintained by the middle vessel of liquid nitrogen (LN<sub>2</sub>) whose boiling point is 77.4 K (-360 °F). This temperature is about 8 K (14.5 °F) less than the boiling point of LF<sub>2</sub>. The annular space between the nitrogen tank and the outer carbon steel tank is filled with powdered insulation and evacuated to less than one millimeter of mercury, absolute pressure. The small heat leak from the atmosphere causes the LN<sub>2</sub>

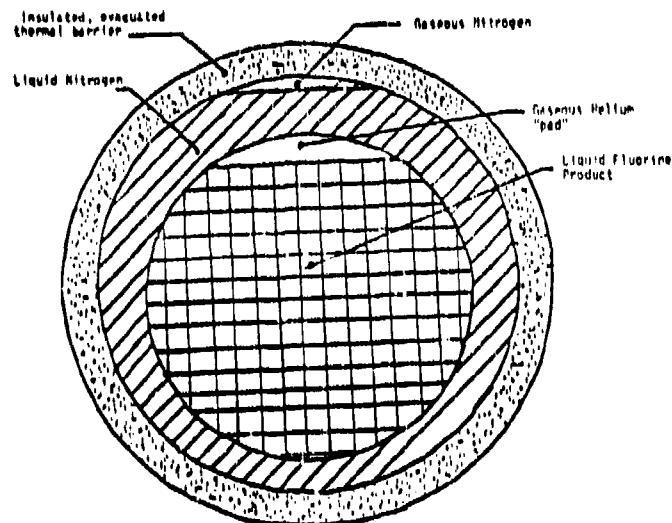


**FIGURE 5.1:** Cross-Sectional View of Fluorine (Road) Transport Trailer

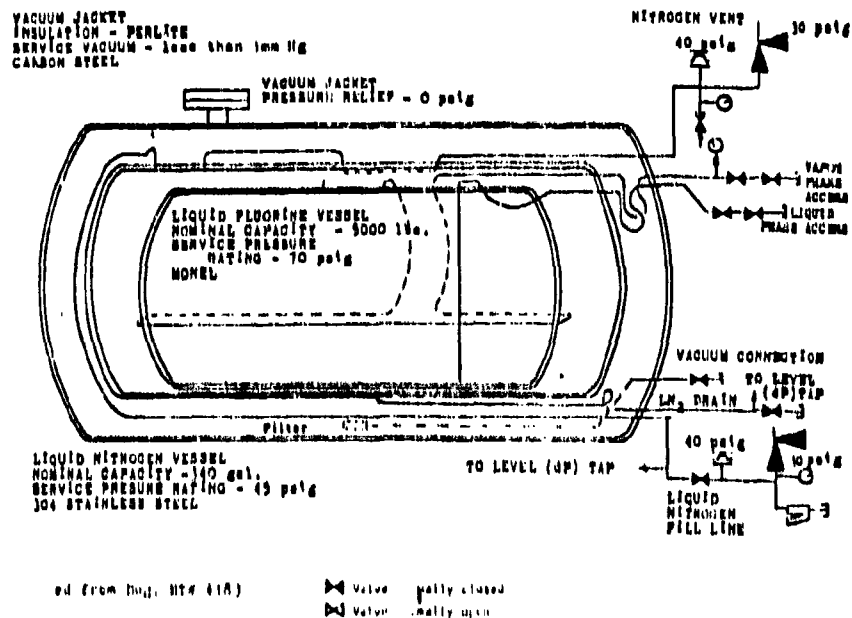


**FIGURE 5.2:** Liquid Fluorine (Road) Trailer - Tank System

to boil and the vaporized nitrogen is vented to the atmosphere thus maintaining the LN<sub>2</sub> at its boiling temperature.

The liquid nitrogen tank has a volume capacity of 1.287 m<sup>3</sup> (340 gallons). The boil-off rate is about 30.3 liters/day (8 gallons/day). The vessel has a service pressure rating of 0.31 MPag (45 psig) and is equipped with a spring loaded pressure relief valve set at 0.207 MPag (30 psig) and a pressure relief rupture disk designed for 0.276 MPag (40 psig) rupture.

Table 5.1 indicates the principal specifications and transport volumes of the fluorine road tanker.

## **5.2 Properties of Fluorine**

### **5.2.1 Physical Properties**

Fluorine is normally a gas at ambient temperature and pressure. Its critical temperature is 144 K. That is, in order to liquefy the element, it has to be cooled to temperatures below 144 K. Fluorine has a sharp, penetrating odor detectable by human beings at as low a concentration as 0.1 ppm. The principal thermodynamic properties of Fluorine of interest to this study are indicated in Table 5.2.

### **5.2.2 Chemical Properties**

Fluorine is a very reactive element and has the ability to combine with most organic and inorganic materials at or below room temperature. Reactions with organic materials are strongly exothermic. Organic and hydrogen containing compounds especially can burn or explode when exposed to fluorine. Elemental fluorine reacts directly with the noble gases xenon, radon, and krypton to form fluorides. Nitrogen and oxygen form fluorides but do not react directly with fluorine except in the presence of an electric charge.

Fluorine is the first member of the halogen family and has the lowest enthalpy of dissociation relative to the other halogens, which is in part responsible for its greater reactivity. Furthermore, the strength of the fluorine bond with other atoms is greater than that of the other halogens. The reactivity of fluorine compounds varies from extremely stable compounds (such as SF<sub>6</sub>, NF<sub>3</sub>, and fluorocarbons) to extremely reactive compounds such as the halogen fluorides. Volatile metal compounds such as WF<sub>6</sub>, MoF<sub>6</sub> are produced by the reaction of the metal with elemental fluorine.

Most reaction chemistry studies involving fluorine have been conducted at ambient temperatures and above, and the discussion below relates to findings in this temperature range. Leaks of very cold fluorine gas or liquid may show a different behavior, i.e.,



TABLE 5.1

## LIQUID FLUORINE TRANSPORT SPECIFICATIONS

## 1. Tank Specifications: Liquid Fluorine

Length		
Diameter		
Volume	1.770	m <sup>3</sup>
Tank Pressure Rating	590.000	kPa abs

## 2. Specifications of Liquid Fluorine (LF2)

Volume transported	1.500	m <sup>3</sup>
Mass of LF2 in tank	2260.000	kg
Liquid Temperature	77.400	K
Tank Pressure **	108.000	kPa (abs)

## 3. Tank Specifications: Liquid Nitrogen

Length		
Volume	1.287	m <sup>3</sup>
Tank Pressure Rating	310.000	kPa g

## 4. Specifications of Liquid Nitrogen (LN2)

Volume transported	1.287	m <sup>3</sup>
Mass of LN2 in tank	1018.000	kg
Liquid Temperature	77.400	K
Tank Pressure **	100.000	kPa (abs)

\*\* The ullage volume of the LF2 tank is filled with gaseous Helium which maintains an above ambient pressure in tank.

LF2 partial pressure at the liquid nitrogen boiling temperature (77.4 K) is 41.4 kPa (abs) or 0.41 atm abs.

TABLE 5.2

THERMODYNAMIC PROPERTIES OF  
FLUORINE and NITROGEN

Property	Fluorine	Nitrogen	Units
Molecular Weight	38.00	28.00	kg/kmol
Critical Temperature	144.30	126.20	K
Critical Pressure	5.52 E+06	3.39 E+06	N/m <sup>2</sup>
Boiling Point	84.45	77.40	K
Freezing Point	53.50	63.30	K
Liquid Density ( @ NBT )	1559.30	790.90	kg/m <sup>3</sup>
Sat Liq Enthalpy ( @ NBT )	0.00 ( @ NBT )	0.00 ( @ 273.16 K )	J/kg K
Sat Vap Enthalpy ( @ NBT )	1.73 E+05	NA	J/kg K

-----  
Equations for Temperature dependent parameters (all in SI units)

## FLUORINE:

Saturated Vap Pr  $p = p_{cr} * \exp\{[-6.18224 y + 1.18 y^{1.5} - 1.16555 y^3 - 1.50167 y^6]/(1-y)\}$   
with  $y = (1-T/T_c)$

Liq Heat Cap  $CL = 1087 + 1.79 T$

Heat of Vaporization  $XL = 1.73 E+05 ((1-y)/(1-y_r))^{0.38}$  with  $y_r = T_{ref}/T_c$   
 $T_{ref} = 84.45 K$

## NITROGEN:

Saturated Vap Pr  $p = p_{cr} * \exp\{[-6.09676 y + 1.1367 y^{1.5} - 1.04072 y^3 - 1.93306 y^6]/(1-y)\}$   
with  $y = (1-T/T_c)$

Liq Heat Cap  $CL = 2309 - 11.1 T + 0.1 T^2$

Heat of Vaporization  $XL = 1.99 E+05 ((1-y)/(1-y_r))^{0.38}$  with  $y_r = T_{ref}/T_c$   
 $T_{ref} = 77.4 K$

slower reactions, but it is possible that there could be local warming of pockets of fluorine so that it is only prudent to consider reactions occurring under ambient conditions.

a) Reactions with Water: There seems to be some controversy regarding the reactivity of fluorine with water or water vapor. Cady and Burger (1950) state that fluorine reacts with water to form oxygen fluoride and hydrogen fluoride.



Rudge (1962) considers  $OF_2$  to be unstable and to decompose to  $O_2$  and  $F_2$ . He also claims that  $H_2O_2$ , fluorine monoxide ( $F_2O$ ), and, in some cases, ozone are formed. Landau and Rosen (1951) state that "fluorine normally reacts vigorously with water in the form of either a vapor or a liquid to form hydrofluoric acid and oxygen. Nevertheless, inhibition has frequently been observed; that is, quantities of water vapor may accumulate in the presence of fluorine until the reaction is suddenly initiated with explosive violence." They also note that "When fluorine emerges into the wet atmosphere, e.g., through a leaking pipe flange, it reacts with condensed water and forms sparks and flashes that are readily visible at a considerable distance." The reaction



is very exothermic with an enthalpy of reaction of about 8 MJ/kg  $F_2$  (Stull and Prophet, 1971) and one kg of fluorine reacts with about 0.47 kg of water.

Thus, while there is some uncertainty concerning the rates of reaction between fluorine and water, most authors agree that reaction is possible. At low temperatures, rates of reaction should be small. Also, as air dilutes the fluorine, the reactivity decreases significantly as discussed below.

b) Reactions with Organic Materials: All investigators warn that fluorine in high concentrations will "burn" organic materials with the presence of flames. The enthalpies of reaction are high and much larger than comparable enthalpies of oxidation. For example, methane reacts (in theory) to form  $CF_4$  and HF. The enthalpy of this reaction is  $\sim -44$  MJ/kg  $CH_4$  whereas if  $CH_4$  reacts with  $O_2$  to form  $CO_2$  and water,  $\Delta H \sim -21$  MJ/kg  $CH_4$ .

The probability of ignition between fluorine and organic compounds appears to be a strong (but as yet unquantified) function of the fluorine concentration. In some crude but illuminating tests, Landau and Rosen (1951) placed organic materials various distances from a jet of fluorine issuing from an orifice on a fluorine gas tank at 4.5 bar. The orifice sizes were 3 and 9 mm in diameter. Cotton, wool, and wood surfaces were used. Ignition occurred when the distances were less than about 15 cm. In a very few tests

where the fluorine was diluted to 20 volume percent with nitrogen, no ignition took place even when the material (cotton cloth in most cases) was in very close proximity to the jet. Also, with 20% fluorine/80% nitrogen, there were no violent reactions with butyl rubber or neoprene gaskets, but the physical strength of the rubbers deteriorated rapidly.

One concludes that fluorine reacts violently with organic materials when pure and at ambient temperatures and above. The reactivity of fluorine decreases to lower levels when diluted to 10-20% or below. The effect of temperature is unknown, but it is reasonable to assume the reactivity diminishes as the temperature is lowered. Thus, in an accident, if air dilution can occur before the fluorine warms, there is a lower probability of ignition with organic materials (and water vapor) in the immediate vicinity of the spill.

c) Reactions with Metals and Other Materials: Due to the formation of a passive metal fluoride surface film, the reaction of fluorine with most common metals (iron, stainless steel, Monel, copper, aluminum) is relatively slow at room temperature and below but is vigorous at elevated temperatures. Landau and Rosen (1951) state that leaks of ambient temperature fluorine gas can burn iron piping should there be organic materials or water vapor in the vicinity of the leak to initiate the reaction. Experiments with clean copper, brass, and stainless steel tubing showed no reaction with pure fluorine gas flowing within the tubing. If, however, the tubing were contaminated by oil or grease, the copper tubing burned while the brass and stainless steel tubing were heated to a red heat. No reactions were observed in any of the tubing, even when oily, when the gas was 20% fluorine in nitrogen (Landau & Rosen, 1951).

Many inorganic compounds react with fluorine with the fluorine replacing oxygen in the material, but usually only at temperatures well above ambient. Rudge (1962) states that at room temperature, in the absence of hydrofluoric acid, "fluorine is without detectable effect on glass."

### 5.3 Release Scenarios

There are basically two fluorine release scenarios that need to be considered in modeling the dispersion hazard. These scenarios arise because of the nature of the chemical and the transport system used. These two scenarios are discussed below.

#### 5.3.1 Explosive Release of Fluorine and Flash Vaporization (SCENARIO A:)

Consider an accident or an operational malfunction in which the nitrogen coolant is drained out of the outer tank through a rupture hole and released into the atmosphere. It is assumed that the

inner LF2 tank is not damaged. In such an accident, the loss of the LN<sub>2</sub> cooling will result in the temperature of liquid fluorine to increase with a corresponding increase in the fluorine tank pressure. The fluorine tank has a service rating of 0.59 MPa (abs). At this pressure, the temperature of fluorine is only about 20 K higher than its normal boiling point of 85 K.

Continued heat leak beyond the point at which the tank pressure is 0.59 MPa may lead to the rupture of the tank and the consequent very rapid depressurization. In this scenario, the compressed, supersaturated fluorine liquid will flash instantly into vapor and liquid. The liquid may be entrained in the vapor cloud in the form of a fine mist at a temperature of 84.5 K. Some part of the liquid may spill on the ground, but it is assumed that the violence of the release may ensure that all of the liquid is entrained in the vapor cloud. This scenario is depicted schematically in Figure 5.3.

The violence of release will also entrain the ambient air into the vapor cloud. The density of this vapor cloud containing liquid F<sub>2</sub> aerosols will be higher than that of air; consequently the vapor cloud will disperse downwind as a heavy vapor cloud. During this dispersion, additional air will be entrained, liquid fluorine aerosols will evaporate, water vapor from the atmosphere will condense into the cloud and "react" with F<sub>2</sub> forming HF. All of these thermodynamic phenomena are discussed in section 5.4.

#### 5.3.2 Liquid Release and Boiling Pool Source of Vapor (SCENARIO B:)

In an accident, instead of just the nitrogen tank being punctured, both nitrogen and fluorine tanks are punctured, then two cryogenic liquid streams will issue out of the damaged section of the tank. Because both liquids will be at about the saturation temperature of nitrogen (i.e., 77 K), there will be no flash vaporization during release.

When the two liquids form a puddle on the ground, rapid vaporization is expected to occur because of heat leak from the relatively warm ground and from the ambient wind. Only vapors of nitrogen and fluorine will be generated. The vapor evolved will be carried downwind and dispersed. This scenario of release is shown in Figure 5.4.

In section 5.5, a source model is developed to analyze the distillation and evaporation from a pool containing two volatile liquids. More details of this model are indicated in Appendix B.

#### 5.3.3 Flashing of the Liquid Released

In Scenario A, the liquid fluorine is released from an elevated pressure and temperature (compared to the normal boiling temperature). This results in the flashing of the liquid forming

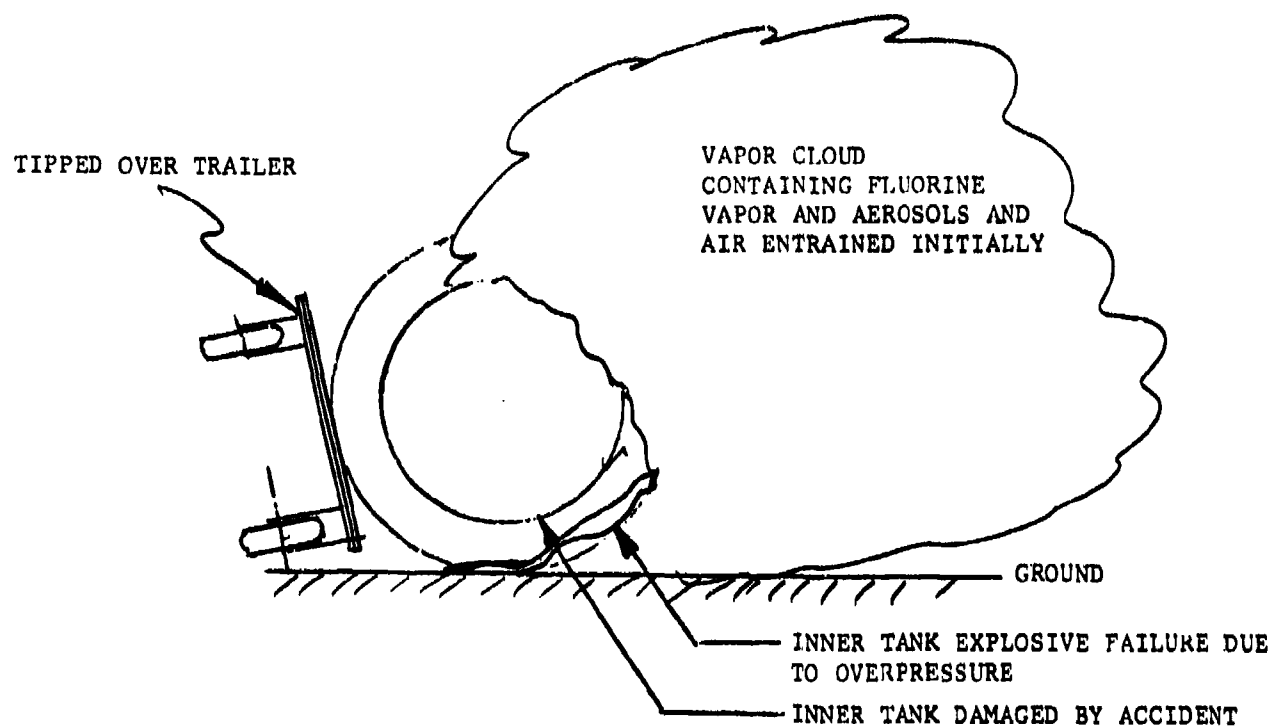


**FIGURE 5.3:** Schematic Representation of Scenario "A" Type Release of Fluorine

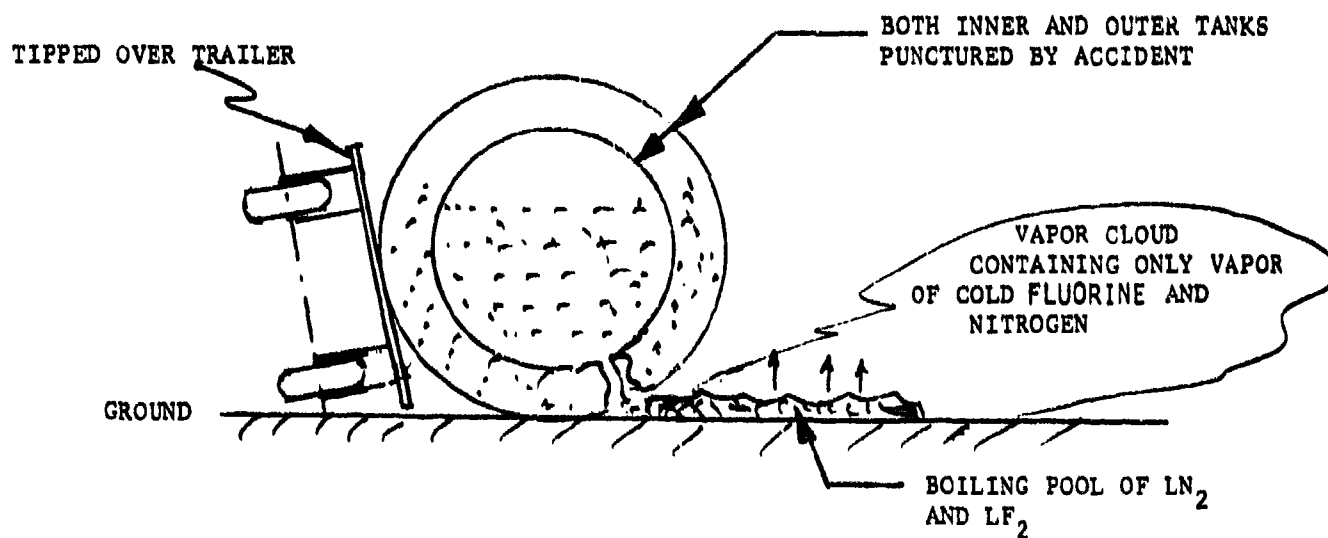


**FIGURE 5.4:** Schematic Representation of Scenario "B" Type Release of Fluorine

ambient pressure saturated vapor and saturated liquid. This phenomenon is discussed below and the fraction of liquid which flashes is calculated.

The phenomenon of flashing of a compressed liquid when released into ambient pressure has been discussed in an earlier companion report (see section 2.4 of report by Raj and Morris, 1987). We repeat here the formula for the mass fraction of vapor generated by the flashing process.

$$f_v = \frac{[h_L^{sat}(T_i) - h_L^{sat}(T_B)]}{\lambda(T_B)} \quad (5.3)$$

where,  $f_v$  represents the mass fraction of ambient pressure saturated vapor produced,  $h$ 's represent the saturated liquid enthalpies at the respective saturation temperatures indicated and  $\lambda$  represents the heat of liquid vaporization at ambient pressure or at the normal boiling temperature.

Table 5.3 shows the conditions of the  $LF_2$  at various temperatures and the values of the enthalpies at these temperatures. Also shown are the mass fractions of vapor flash for  $LF_2$  releases from various saturated conditions. These conditions correspond to the states that  $LF_2$  will be in during its heating from the loss of  $LN_2$  coolant. The density of the final mixture of vapor and liquid is also shown in this table. (In generating these mixture density values, it is assumed that all of the liquid in the post-flash stream is entrained into the vapor phase.) Figure 5.5 shows the mass fraction of vapor generated by the flashing of  $LF_2$  from different temperatures (or pressures). Also shown in the figure is the variation of the saturated vapor pressure of Fluorine with temperature.

It is seen that, if  $LF_2$  is released as a consequence of the tank failure at the rated pressure (590 kPa abs), then about 13.6 % of the mass of fluorine released will flash to vapor.

The density of the mixture of vapor and the post flash liquid entrained within the vapor cloud as fine aerosols is calculated as follows:

$$\rho_{mix} = \frac{1}{\left[ \frac{f_v}{\rho_v} + \frac{f_l}{\rho_l} \right]} \quad (5.4)$$

where,  $\rho_{mix}$  is the density of the mixture of vapor and entrained liquid aerosol,  $\rho_v$  and  $\rho_l$  are, respectively, the saturated vapor density and saturated liquid density at ambient pressure and  $f_v$  and  $f_l$  are respectively the mass fractions of vapor and liquid produced after the flashing.

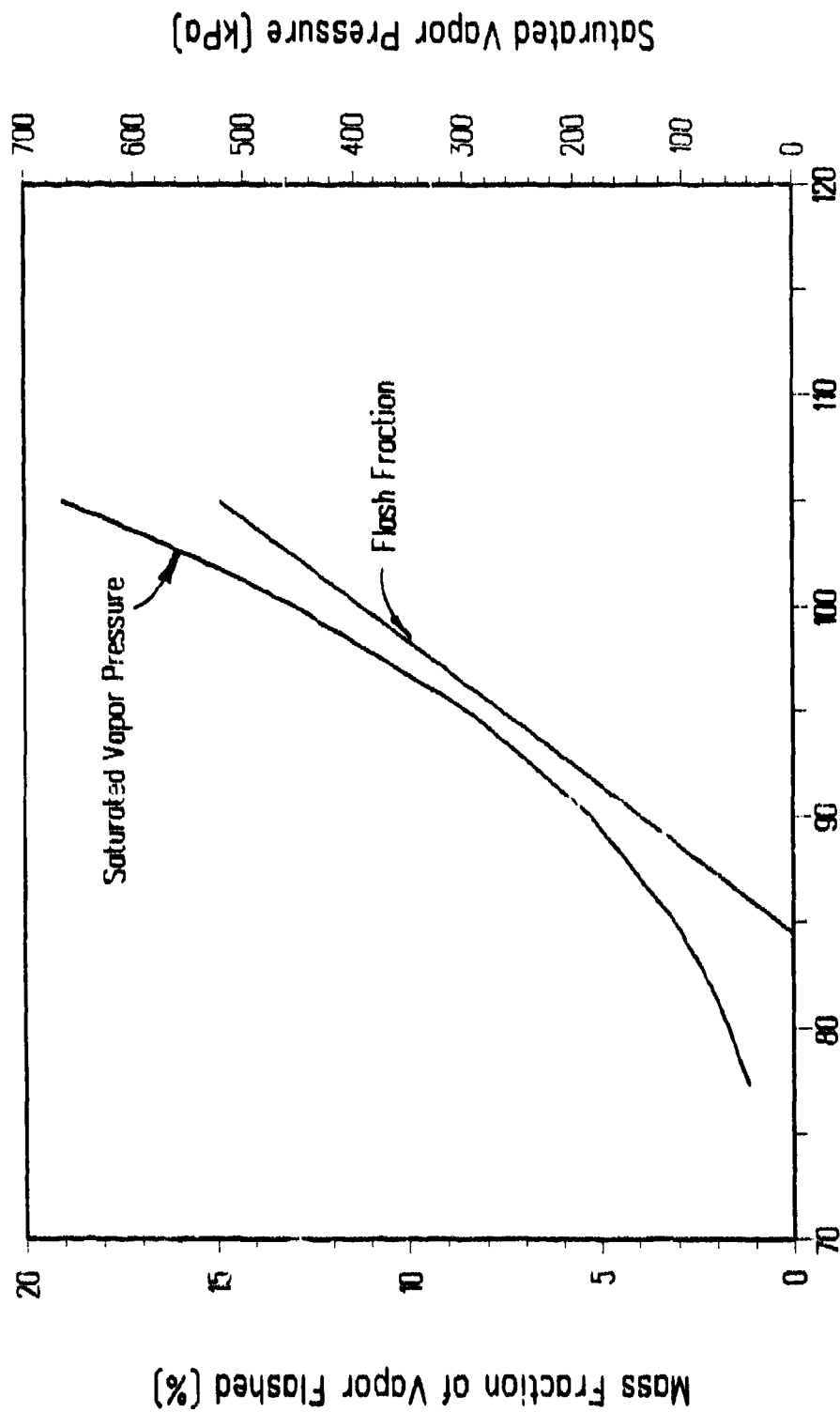
TABLE 5.3  
FLUORINE FLASH CALCULATIONS

<-----Saturated Fluorine----->				<---- Post Flash ----> conditions		REMARKS
Liquid Temp	Sat Pressure	Liquid Enthalpy	Latent Heat of boiling	Mass fraction of Vapor formed	Density of Final Vapor-liq Mixture	
		(note 1)				
(K)	(kPa abs)/(atm abs)	(J/kg K)	(kJ/kg)	(%)	(kg/m^3)	
77.4	41.4	0.41	-1018.1	180.5		Liq N2 saturation temperature
80.0	58.7	0.58	-655.8	177.8		
83.0	85.4	0.84	-222.6	174.6		
84.5	101.9	1.01	0.0	172.9	0.00	1559.3 <-- Normal Boiling Point
85.0	107.9	1.06	619.4	172.4	0.36	771.6
90.0	184.3	1.82	6837.5	166.7	3.95	127.8
95.0	296.4	2.92	13100.4	160.7	7.57	69.4
100.0	453.3	4.47	19408.0	154.3	11.22	47.5
101.0	490.9	4.85	20674.9	153.0	11.95	44.7
102.0	530.8	5.24	21943.6	151.6	12.69	42.2
103.0	573.0	5.66	23214.0	150.3	13.42	39.9
103.3	584.0	5.76	23531.9	149.9	13.61	39.4 <-- Pressure at which the tank is rated
104.0	617.7	6.10	24486.3	148.9	14.16	37.8
105.0	664.8	6.56	25760.4	147.4	14.90	36.1

Notes:

1. Liquid enthalpy reference temperature is the normal boiling point. That is at 84.5 K the saturated liquid enthalpy is equal to 0.
2. Liquid enthalpy is calculated by integrating the temperature dependent liquid specific heat (see Table 5.2) x dT from the reference temperature to the liquid temperature.
3. Heat of vaporization is obtained from the formula indicated in Table 5.2
4. The saturated vapor density at ambient pressure = 5.48 kg/m<sup>3</sup>





Fluorine Saturation Temperature (K)  
FRACTION FLASH VS FLUORINE TEMPERATURE IN TANK

FIGURE 5.5

The final mixture density of the vapor-aerosol mixture is shown plotted in Figure 5.6 as a function of the initial temperature of fluorine in the tank. This density is calculated on the basis that all of the post-flash liquid is entrained in the vapor cloud formed. It is seen that the combined density of the vapor cloud when fluorine is released from a pressure corresponding to the rated failure pressure of the tank (590 kPa abs) is  $39.4 \text{ kg/m}^3$ . This density is about 33 times the density of ambient air at 293 K.

#### 5.4 Thermodynamic Model for Fluorine Liquid Aerosol, Vapor and Humid Air Mixing

##### 5.4.1 Description of the Mixing Phenomenon

The final state of the fluorine-air-water vapor cloud depends upon the relative quantities of these components as well as upon any energy input from the ground, vegetation, etc. Also, the thermodynamic state of the cloud varies with time (or downwind distance) as air is continually entrained.

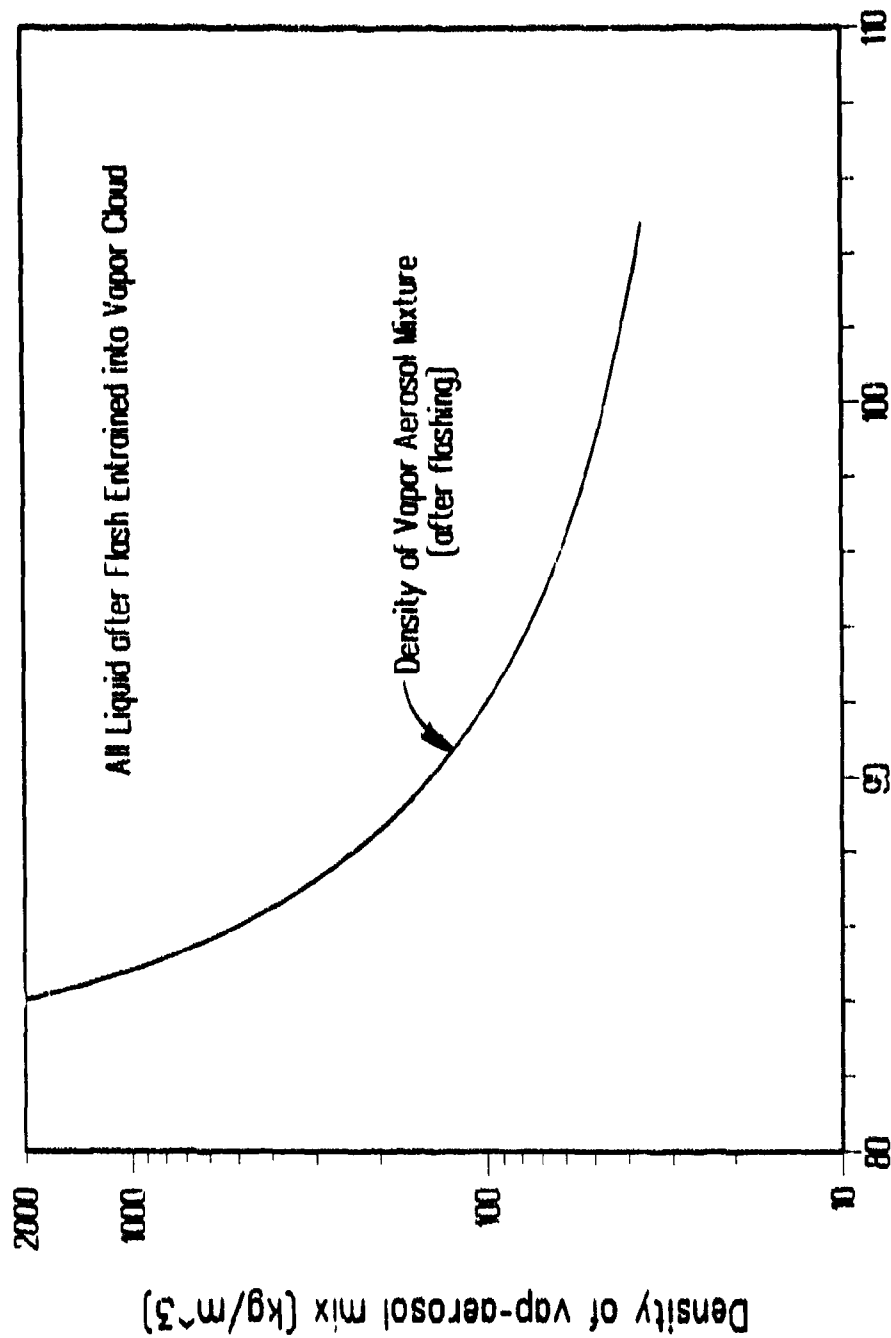
We consider the case where a specified quantity of fluorine is mixed with a definite amount of air with a given relative humidity - and with an energy input that is also specified. From an overall net enthalpy balance (since the mixing step is isobaric), one can determine the final state. In addition, equilibrium relationships are employed to ascertain if condensed phases (liquid fluorine, water ice, or water liquid) are present.

Before mixing with any air, the liquid (aerosol) and vapor fluorine are in equilibrium at the given ambient pressure. If this pressure were about one bar, the equilibrium fluorine temperature is  $\sim 85 \text{ K}$ .

When mixed with air, initially, the partial pressure of the fluorine decreases and, if liquid fluorine is present, evaporation occurs. Thus, while the warmer air tends to increase the temperature, as does the condensation (and freezing) of water, the fluorine evaporation step is the more important and the cloud temperature decreases. This trend continues with the admixture of additional air until the liquid fluorine has completely evaporated. The cloud temperature is then below the usual boiling temperature of fluorine (85 K) and essentially all water is in the form of ice.

Following this temperature drop caused by fluorine evaporation, mixing with more air results in a rise in temperature. As this continues, some water ice sublimates so as to maintain its equilibrium vapor pressure. When the mixture temperature reaches 273.2 K, the ice melts to liquid water. Above this temperature, only liquid and vapor water are present.

The scenario given above is true even if there is a significant energy input.



Fluorine Saturation Temperature (K)  
POST FLASH VAP-AEROSOL MIX DENSITY vs TANK TEMP

Figure 5.6

#### 5.4.2 Calculation Procedure

Thus in any calculational scheme, one must allow for various final "domains" depending upon the circumstances. We define the inlet conditions by specifying:

- o mass released, fraction flash, and temperature of the escaping fluorine.
- o amount of air mixed with the chemical, temperature, and relative humidity of the ambient air.
- o energy input from the ambient into the fluorine-air mixture.

We employ the information specified above, with appropriate equations representing the enthalpies of fluorine (vapor and liquid), water (vapor, liquid, and solid), air (vapor) as functions of temperature, to calculate the "initial stream enthalpy." This term is called  $H_i$  and has the dimensions of joules. No mixing has as yet occurred so the property values of pure fluorine are used.

We add to  $H_i$  the given energy input,  $Q$ , also in joules. The sum  $H_i + Q$  represents the total stream enthalpy at any time. Because of conservation of energy, the final enthalpy after mixing,  $H_f$ , is set equal to the initial stream enthalpy plus any external heat added  $Q$ .

When carrying out a calculation, one does not know at the start which condensed phases are present - and of those which are, the quantities of each. To overcome this difficulty, we first bracket the domains and compute  $H_f$  values at the extreme conditions. This technique readily allows one to determine the temperature range within which the final mixture temperature will occur. The final value can then be obtained quickly by an iterative procedure locating the final state which satisfies the equation  $H_f = H_i + Q$ , and the condensed phase equilibrium relationships (if condensed phases are found to exist).

We have identified five principal domains of the final mixture conditions, as shown below:

Domain	T(K)	Phases*
I	>273.2 to 373**	F <sub>2</sub> (gas); H <sub>2</sub> O(gas, liquid)
II	= 273.2	F <sub>2</sub> (gas); H <sub>2</sub> O(gas, liquid, and solid)
III	84.5 to 273.2	F <sub>2</sub> (gas); H <sub>2</sub> O(gas, solid)
IV	= 84.5	F <sub>2</sub> (gas, liquid); H <sub>2</sub> O(solid)
V	< 84.5	F <sub>2</sub> (gas, liquid); H <sub>2</sub> O(solid)

\* Air is always present as a gas

\*\* Chosen arbitrarily as the maximum possible temperature

Thus we begin with Domain I and calculate  $H_i$  at both extremes. If  $H_i + Q$  lies between these limits, we know the solution lies in Domain I. If  $H_i + Q < H_i$  at the lower temperature end of Domain I, then we repeat the procedure for Domain II, etc. In a few steps, we can locate the appropriate domain and then direct our attention to the computation of the final mixed state.

As noted earlier, if there are fluorine liquid aerosols in the release, the temperature of the cloud will drop upon mixing with air as the liquid fluorine evaporates. In developing and testing the model, one must make certain that the decrease in temperature does not cause a condensation of oxygen-enriched air. Pure air begins to condense at about 79 K. In the early phases of mixing, the partial pressure of air is below one bar so the condensation temperature is below 79 K. The following table indicates the condensation temperature of air as a function of the partial pressure of air.

Air Condensation Temperature (K)	Air Partial Pressure (bar)
78	0.91
75	0.64
70	0.32
65	0.15
64	0.12

Only by carrying out sets of example calculations can one determine if it is possible to condense air. If so, this step would need to be included in the enthalpy balance. Preliminary calculations do not suggest air condensation is a problem unless the fraction liquid fluorine is high.

Hence, the important step in determining the state of the final mixture (and hence, the mixture thermodynamic parameter values) is the evaluation of the final mixture enthalpy  $H_f$ . There are two approaches to performing this calculation. In the first method, the possible chemical reaction between fluorine and water vapor is neglected. In the second method, the complexity of fluorine - water vapor reaction is considered. This reaction is indicated in equation 5.1 and results in the formation of Hydrogen fluoride (HF) and oxygen ( $O_2$ ).

In considering the fluorine - water vapor reaction, all the water in the air is allowed to react with fluorine upon mixing with air. Here, the energy input is 8 MJ/kg of  $F_2$  reacting or 17 MJ/kg of water consumed. Then, one would have no further water, but the enthalpies of the HF and  $O_2$  products would have to be included. As an approximation, the masses of  $O_2$  and HF formed are added to the air present and not considered as individual species. For each

mole of water reacted, 2 moles of HF and one-half mole of  $O_2$  are produced - or per kg of water reacted, 0.89 kg  $O_2$  and 2.22 kg HF.

The rates of reaction of fluorine and water vapor are, however, expected to be negligible at the low temperatures prevailing in a liquid fluorine release. There are, in fact, no reaction kinetic data for fluorine and water vapor reaction at temperatures close to the saturation temperature of fluorine. When the temperature has risen to anywhere near ambient, the fraction fluorine in the vapor cloud is quite low so, again, reactions would not be important. Hence, the neglect of the heats of fluorine - water vapor reaction in determining the final thermodynamic state of the mixture would not in any way reduce the correctness of the calculations.

#### 5.4.3 Results from the Fluorine - Humid Air Mixing Model

The results obtained from the above model are indicated in Figure 5.7 and Figure 5.8. The variation of the final mixture density and the mixture temperature with the amount of air added are indicated in Figure 5.7. The temperature of air is set at 293 K and the relative humidity value is a variable. The mass of liquid present in the mixture in the form of aerosol is plotted in Figure 5.8 for various ambient relative humidities and dilution ratios. These plots are for a given initial composition of the saturated fluorine stream released. In the example shown, this is assumed to be the condition after flash occurring as a result of tank burst (the stream contains 13.61 % by mass of saturated vapor).

It is seen from Figure 5.7 that the mixture density is very high ( $35 \text{ kg/m}^3$ ) at low dilution ratios. This is because we have assumed that all of the liquid released after flash is entrained into the vapor cloud in the form of liquid aerosols. The density decreases continuously with increase in dilution. Also, the variation in the relative humidity of the ambient has very little effect on the final mixture density at any specified dilution.

The temperature variation is also shown in Figure 5.7. The temperature decreases, albeit very slightly (about 4 or 5 K) for dilution ratio below 0.6. This temperature decrease is due to the evaporation of the liquid  $F_2$  aerosols at the expense of the sensible heat of the system. The enthalpy provided by the mixing in air is insufficient to raise the temperature. The effect of partial pressure decrease (of  $F_2$ ) is dominating this early process. However, as more and more air is mixed, the liquid aerosols evaporate at a dilution ratio of about 0.6. Any additional air added increases the temperature. The effect of water is not noticeable in small dilutions. However, at larger dilutions, the heat of condensation of water provides the thermal energy to raise the temperature of the mixture (compared to the dry air case at the same dilution).

**FIGURE: 5.7**  
**F2-AIR MIXTURE THERMODYNAMIC CONDITIONS**

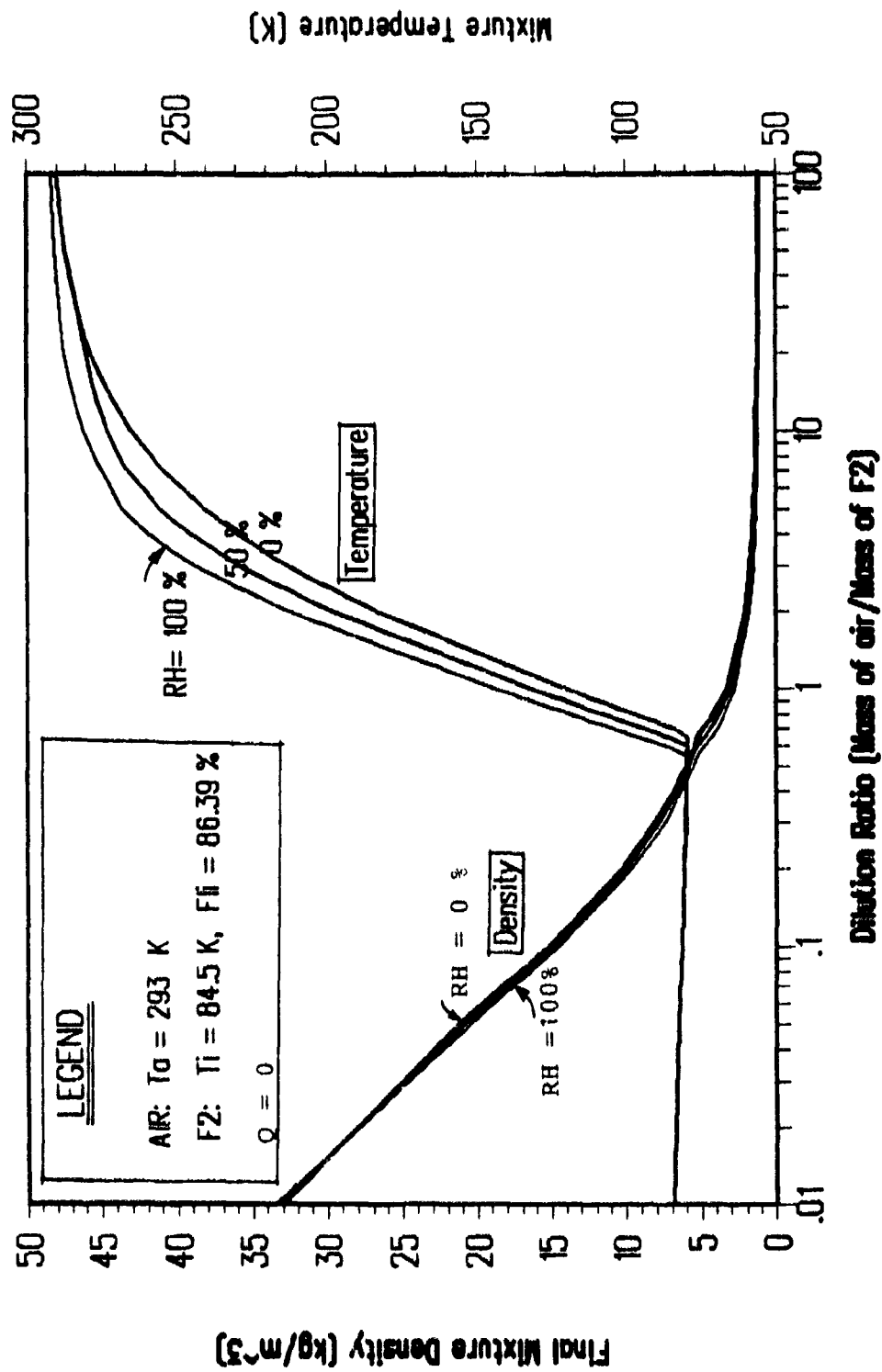
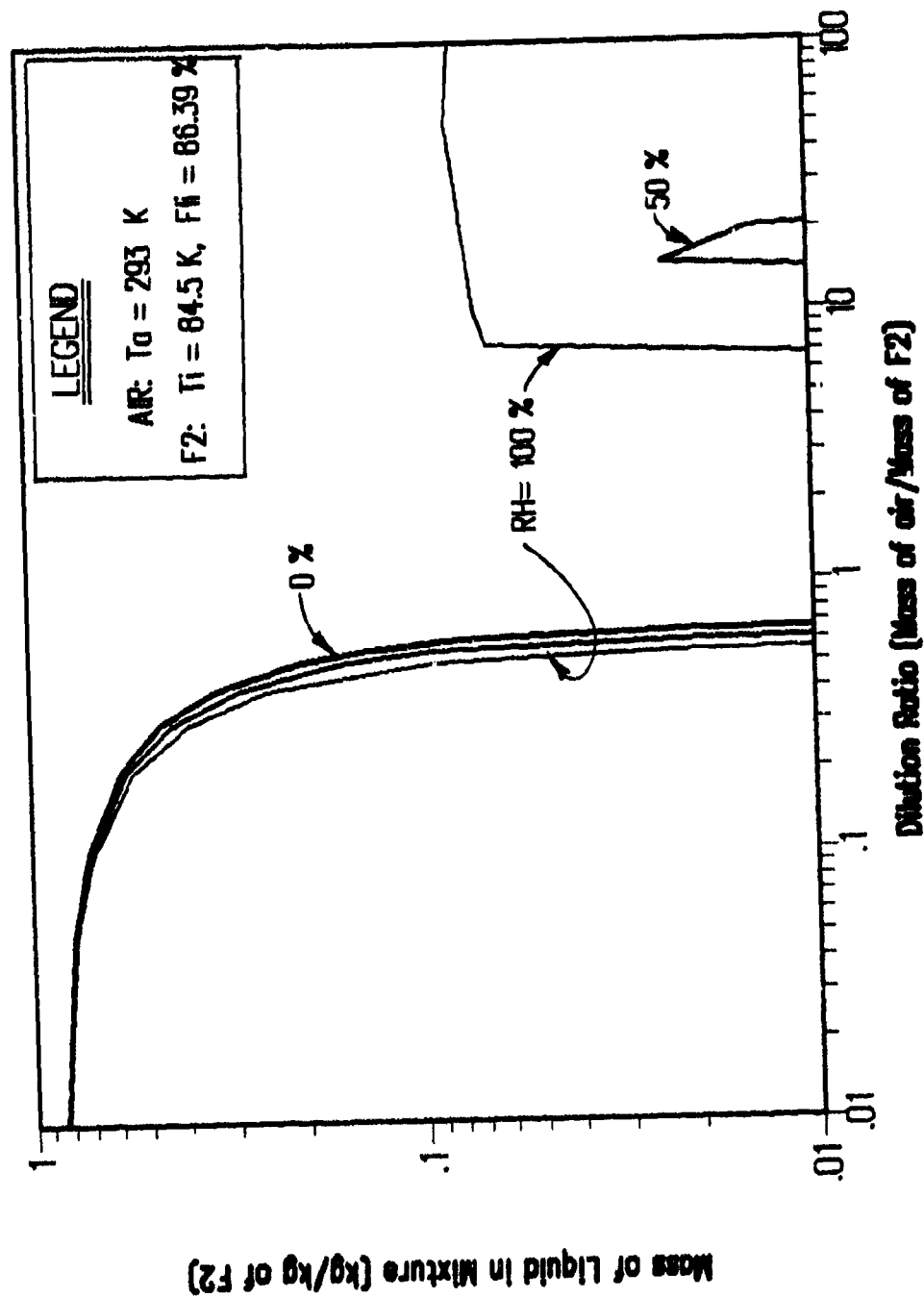


**FIGURE: 5.8**  
**F2-AIR MIXTURE THERMODYNAMIC CONDITIONS**





The variation of the liquid mass in the final mixture is illustrated in Figure 5.8. As can be seen, the initial 0.864 kg/kg of  $F_2$  liquid rapidly evaporates and the liquid is essentially completely vaporized by the time the dilution ratio is 0.6 or 0.7. However, the water at this stage is in the form of ice in the mixture. As the dilution increases beyond the above 0.6 or 0.7 value, there is no liquid in the system until the water ice melts to liquid water. This occurs at a dilution ratio of about 17 in the case of 100 % relative humidity air and at about 150 in the case of 50 % relative humidity. Note also the re-evaporation of the water liquid from the mixture as the dilution is greater than 200. This is because at a dilution of 200 the temperature of mixture is just above the wet bulb temperature in air at the 50% relative humidity. Table 5.4 gives the detailed numerical values for the various thermodynamic parameters of the final mixture of  $F_2$  and humid air for different dilution ratios and ambient relative humidities.

## 5.5 LN2 and LF2 Pool Boiling Model (SCENARIO B)

### 5.5.1 Source Rate Calculations

In section 5.3.2, we described the second type of release accident which can result in the formation of a liquid pool on the ground. The pool will contain both liquid nitrogen and liquid fluorine. These two liquids being very cold will rapidly boil on the ground surface, evaporate and form a vapor cloud consisting of cold fluorine and nitrogen vapors. The evolved vapor is carried downwind and mixed with ambient air. No liquid fluorine or liquid nitrogen aerosols are present in the source vapor. This boiling phenomenon is discussed in this section.

The detailed mathematical representation of the phenomenon of boiling and distillation of a pool containing two liquid components is discussed in Appendix B. When a release of both LN2 and LF2 occurs from the road transport as a result of an accident, initially a pool of liquid is formed on the ground. The extent of spread of this pool on the ground depends on the local topography, nature of the soil, slope in the ground and whether there are any containment depressions on the ground. In the model discussed in Appendix B, we assume that the pool spreads to an area corresponding to an initial depth of 1 cm.

This liquid pool evaporates due to the transfer of heat from the ground. The heat transfer from the ground to the liquids is modeled using the one dimensional heat transfer model (discussed in a previous report by Raj and Morris, 1987). Because the pool contains two liquids with differing boiling temperatures (77 K for  $N_2$  and 84.5 K for  $F_2$ ), the pool boiling process is similar to a process of distillation of a two component mixture. In the case of a LN2 - LF2 pool, nitrogen evaporates preferentially during the initial stages. Therefore, in the beginning the vapor evolved is

TABLE 5.4: RESULTS OF CALCULATIONS

## MIXTURE OF FLUORINE WITH DILUTED AIR

Initial Conditions  
Tair = 293 KF2 Mass = 1 kg  
F2 Liquid Fraction = 86.39 %  
F2 Temp = 84.5 K

Dilution Ratio	RELATIVE HUMIDITY OF AIR = 100 %					RELATIVE HUMIDITY OF AIR = 50 %					RELATIVE HUMIDITY OF AIR = 0 %				
	Tmix (K)	Phenix (kg/m <sup>3</sup> )	Mass of Liq (kg/kg)	Mass of Gas (kg/kg)	Total Moles	Tmix (K)	Phenix (kg/m <sup>3</sup> )	Mass of Liq (kg/kg)	Mass of Gas (kg/kg)	Total Moles	Tmix (K)	Phenix (kg/m <sup>3</sup> )	Mass of Liq (kg/kg)	Mass of Gas (kg/kg)	Total Moles
0.01	84.28	33.58	0.8477	0.1622	0.0223	0.0043	84.28	33.34	0.2866	0.1633	0.0223	0.0044	84.28	33.11	0.4555
0.05	82.67	28.52	0.7793	0.2210	0.0205	0.0075	82.61	28.87	0.7433	0.2663	0.0206	0.0074	82.55	21.21	0.7881
0.10	81.75	14.54	0.7013	0.2973	0.0185	0.0113	81.66	14.80	0.7694	0.3399	0.0187	0.0111	81.53	15.13	0.7301
0.20	80.95	9.63	0.5470	0.6502	0.0144	0.0183	80.76	9.94	0.5676	0.6291	0.0150	0.0132	80.58	10.24	0.5802
0.30	80.58	7.50	0.3339	0.9019	0.0104	0.0262	80.33	7.80	0.4322	0.8537	0.0114	0.0253	80.09	8.10	0.4563
0.40	80.33	6.35	0.2433	1.1451	0.0065	0.0315	80.09	6.59	0.2941	1.1031	0.0077	0.0323	79.84	6.82	0.3356
0.50	80.21	5.56	0.6938	1.4030	0.0024	0.0410	79.90	5.82	0.1614	1.3351	0.0042	0.0333	79.66	6.02	0.2355
0.55	80.15	5.28	0.0195	1.5228	0.0005	0.0456	79.84	5.53	0.0529	1.4533	0.0024	0.0428	79.59	5.71	0.1445
0.60	80.52	4.81	0.0000	1.5916	0.0000	0.0458	79.81	5.25	0.0126	1.5772	0.0005	0.0465	79.53	5.45	0.0315
0.65	95.87	4.31	0.0000	1.6439	0.0000	0.0435	95.15	4.79	0.0630	1.6355	0.0000	0.0487	94.06	5.24	0.0208
0.70	104.52	3.95	0.0000	1.6902	0.0000	0.0502	94.23	4.36	0.0530	1.6353	0.0000	0.0504	91.29	4.87	0.0303
0.75	112.24	3.66	0.0000	1.7395	0.0000	0.0519	101.95	4.01	0.0600	1.7483	0.0000	0.0507	121.05	3.30	0.0309
1.00	144.58	2.79	0.0000	1.9650	0.0000	0.0635	132.82	3.02	0.0520	1.9319	0.0000	0.0521	163.50	2.08	0.0050
2.00	212.93	1.81	0.0000	2.9720	0.0000	0.0947	193.60	1.93	0.0000	2.9863	0.0000	0.0952	212.93	1.76	0.0000
3.00	243.68	1.55	0.0000	3.9539	0.0000	0.1239	229.73	1.64	0.0000	3.9792	0.0000	0.1236	272.65	1.61	0.0000
4.00	259.60	1.44	0.0000	4.9434	0.0000	0.1633	245.45	1.51	0.0000	4.9735	0.0000	0.1541	272.65	1.52	0.0000
5.00	258.06	1.38	0.0000	5.9439	0.0000	0.1980	255.56	1.44	0.0000	5.9697	0.0000	0.1987	248.68	1.41	0.0000
7.50	276.33	1.32	0.0667	8.4333	0.0037	0.2848	257.69	1.36	0.0000	8.4672	0.0000	0.2556	256.48	1.36	0.0000
10.00	281.01	1.28	0.0711	10.9289	0.0040	0.3719	272.83	1.32	0.0000	10.9584	0.0000	0.3727	264.93	1.30	0.0000
15.00	285.59	1.25	0.0738	15.9282	0.0041	0.5855	277.69	1.28	0.0000	15.9764	0.0000	0.5471	271.79	1.28	0.0000
20.00	287.46	1.23	0.0762	20.9238	0.0042	0.7712	281.04	1.27	0.0000	20.9639	0.0000	0.7217	278.47	1.26	0.0000
25.00	288.63	1.23	0.0771	25.9229	0.0043	0.8953	281.60	1.25	0.0014	25.9855	0.0001	0.8554	281.21	1.25	0.0000
50.00	290.78	1.21	0.0827	50.9173	0.0046	1.7695	287.07	1.23	0.0000	51.0063	0.0008	1.7667	287.07	1.23	0.0000
100.00	291.95	1.20	0.0899	100.9261	0.0044	3.5173	290.00	1.21	0.0000	101.0630	0.0000	3.5071	290.00	1.22	0.0000

richer in nitrogen than in fluorine. However, at later stages the vapor consists essentially of pure fluorine.

The important parameters of interest to the dispersion process are the rate of generation of vapor and its quality (or concentration of F<sub>2</sub>). Also of interest is the total duration over which the cold liquids evaporate on the ground.

Detailed results from this vapor source rate model are presented in Appendix B. Figure 5.9 shows the variation with time of the concentration of fluorine and nitrogen in the vapor evolved. It is clearly seen that the vapor progressively becomes richer as time goes on. At first glance, this may seem to imply that the downwind dispersion distance for fluorine (for specified hazard concentration) will increase with time. However, the rate of evaporation decreases with time resulting in lesser mass rates of fluorine injection into the atmosphere. In Figure 5.10, the mass rate of evaporation of fluorine and nitrogen are indicated. As can be seen, the rates of evaporation of the two components are close and have the same trend with time.

One important result that is noticed from Figure 5.9 is that all nitrogen and fluorine are evaporated over a relatively short period of time, namely, about 14 seconds! This is due to the limited volume of liquids spilled (several hundred gallons) and the extremely high heat transfer rates from the ground.

#### 5.5.2 Consideration of Source Rate in Dispersion Model

It is anticipated that the above duration for pool evaporation (i.e., the duration over which the vapors are released) will be very small compared to the potential dispersion duration to dilute to concentrations below the F<sub>2</sub> hazard concentrations. Therefore, the dispersion calculations can be performed in one of two ways, namely, by assuming that:

1. all of the F<sub>2</sub> vapor is released instantaneously. In this case, an initial cloud of cold F<sub>2</sub> and N<sub>2</sub> vapors is assumed to be released. The dispersion is then modeled as an initially diluted puff.
2. F<sub>2</sub> vapor is released at a constant rate (corresponding to the mean rate) along with nitrogen vapor. The concentration of F<sub>2</sub> vapor in this steady stream of vapor is assumed to be at the mean value.

It is our contention that the former assumption makes more sense and provides a more conservative estimate of the extent of hazard posed by a F<sub>2</sub> release from a transport. Hence, in ADAM, we have coded the Scenario B discussed earlier (see section 5.5.1) as an instantaneous release of a F<sub>2</sub> - N<sub>2</sub> cloud. The rationale for this assumption is that any accident which is severe enough to puncture both the outer nitrogen tank and the inner fluorine tank will

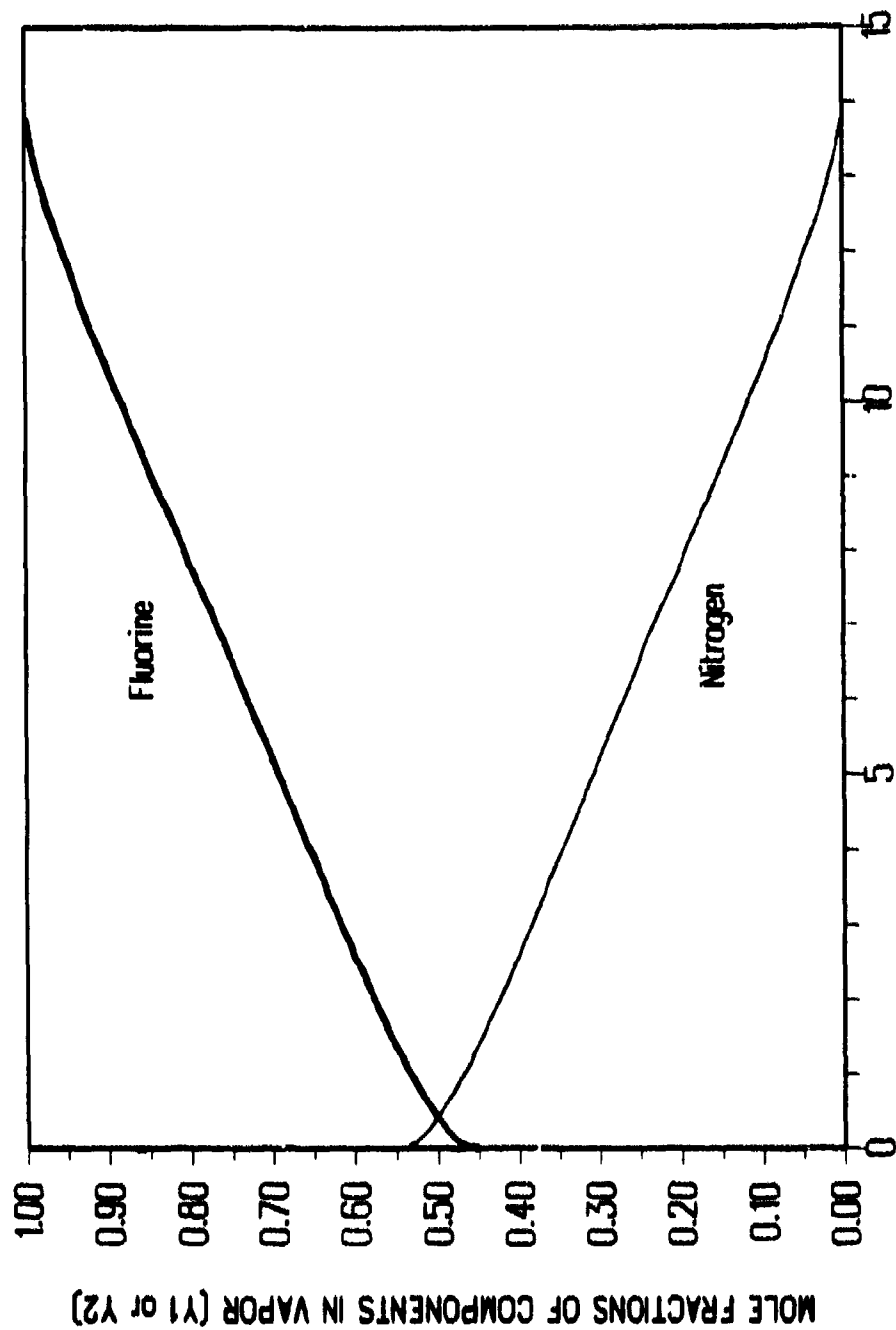


FIGURE: 5.9 Mole Fractions in Vapor vs Time

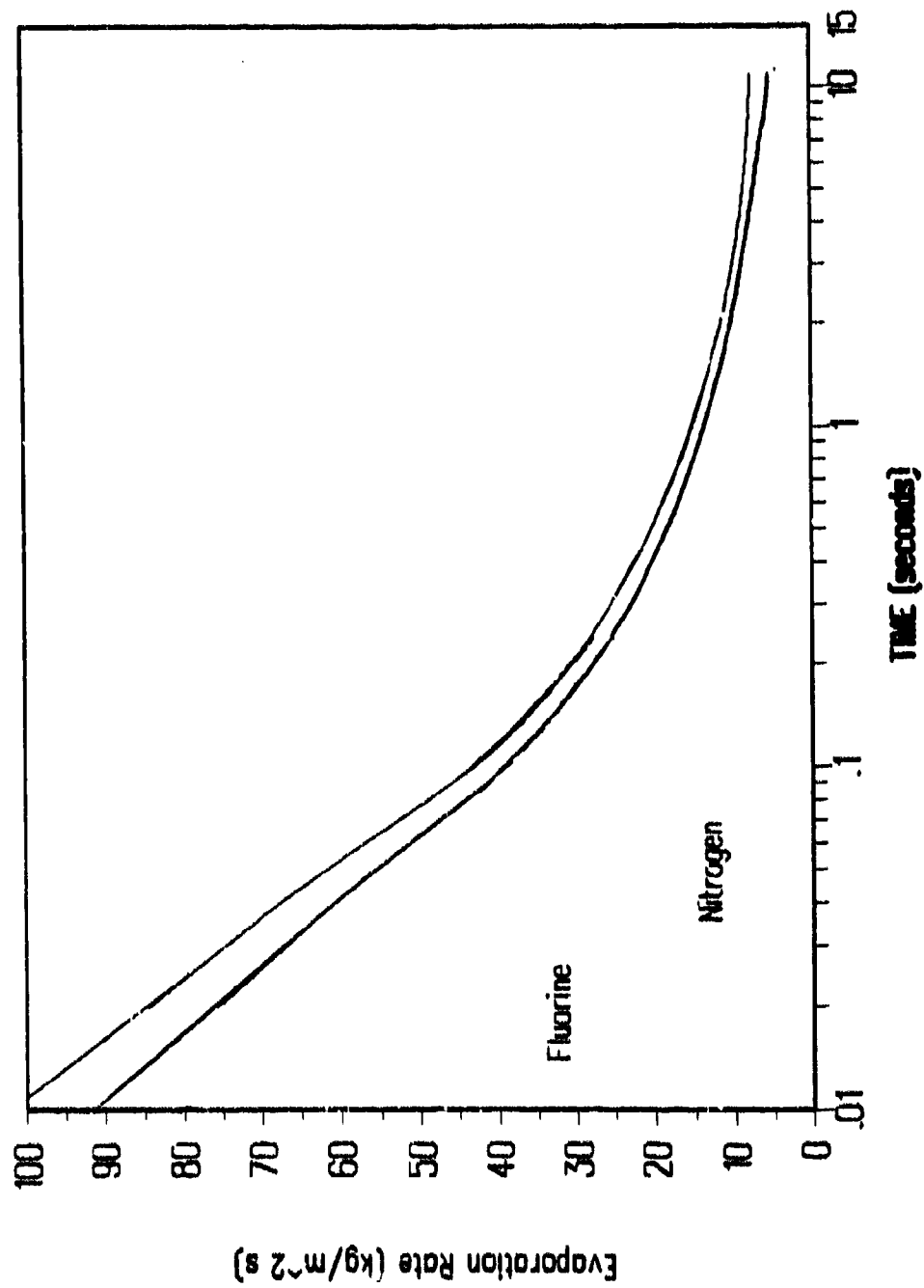


FIGURE: 5.10 Mass Evaporation Rate vs Time

both the outer nitrogen tank and the inner fluorine tank will create large holes in both tanks leading to a rapid draining of the tank contents. The evaporation of the liquids on the ground will be very rapid as has been shown in the previous section.

Therefore, the fluorine vapor source for the second scenario of release (Scenario B) is specified as a cylindrical vapor cloud consisting only of cold vapors of fluorine and nitrogen, completely mixed, and containing no liquid aerosols. This heavy gas cloud is then allowed to disperse in the prevailing atmospheric condition. The dispersion routines in ADAM are then utilized.

### 5.6 Discussion of Results from the Fluorine Dispersion Calculations

Calculations were performed for the case of fluorine release from a road transport vehicle carrying the chemical. The details of the volumes of liquid fluorine and liquid nitrogen carried were indicated in Table 5.1. These values are used in the dispersion calculations discussed in this section. Both scenario A type release and scenario B type of release have been considered.

In the case of scenario A type release (occurring as a result of nitrogen loss and inner fluorine tank failure due to overpressure), fluorine released flashes. It is calculated that 13.6% of the liquid flashes to vapor and the remaining 86.4% of the mass manifests itself as liquid. We have assumed that all of this liquid will be entrained into the vapor as aerosols. We also assume that a mass of air equal to 10 times the mass of air contained within a volume occupied by the vapor released from the explosive failure of the tank. Two atmospheric stability conditions, namely, D and F stabilities were used in the calculations.

Figure 5.11 shows the results for the case of fluorine release from the bursting of the tank due to overpressure under neutral stability (D stability) conditions with wind speed of 5 m/s. The contour plotted is the 1 ppm contour which is the short term exposure (toxic) concentration limit for fluorine. As can be seen that because of the very low hazard concentration for  $F_2$ , the hazard distance extends to significant distances, namely, about 21 km!

The dispersion of the same amount of fluorine released in a stable F type atmosphere is indicated in Figure 5.12. The maximum hazard in this case extends to an even longer distance of about 64 km!

Because of the low concentration to which the cloud has to be diluted, it is estimated that a substantial part of the dispersion takes place in the near neutral density dispersion regime. As a matter of fact, the hazard distance can be calculated with neutral density, point source release Gaussian model and come with substantially the same result.

SCENARIO A: TANK BURST STABILITY D (4.0)

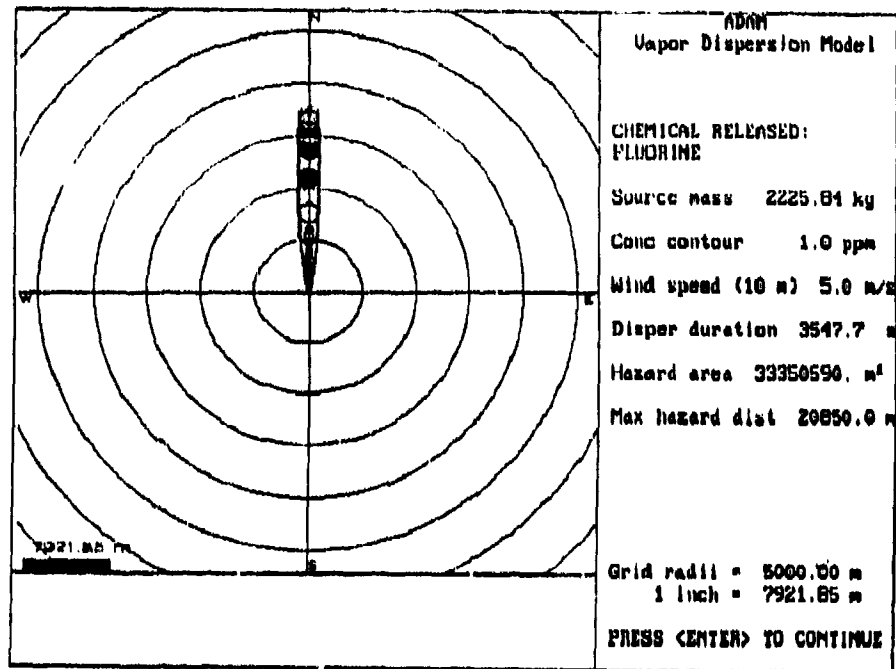


Figure 5.11: Dispersion under Neutral Stability Fluorine Cloud Released by a Transport Tank Burst

SCENARIO A: TANK BURST STABILITY F (5.5)

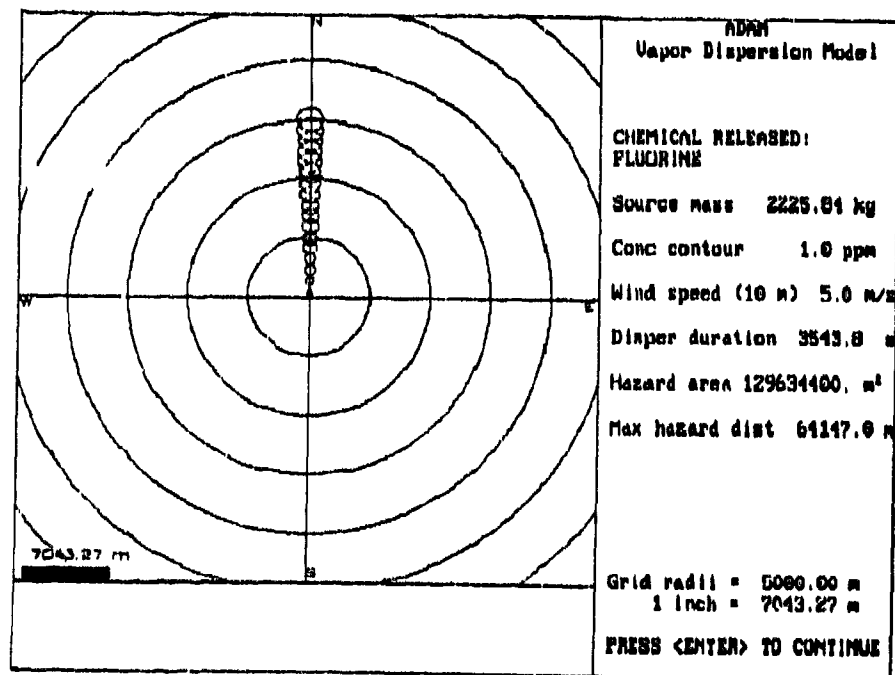


Figure 5.12: Dispersion under Stable Weather Conditions of a Fluorine Vapor Cloud Released by a Transport Tank Burst

The results for the case of release of fluorine and nitrogen liquids and the dispersion of the vapors thus produced are shown respectively, for D stability condition and F stability condition, in Figure 5.13 and Figure 5.14. Again, it is noticed that the distances are comparable to the previous numbers obtained in the case of tank burst. This is because of two reasons. The first is that the total mass of fluorine released is the same in both scenarios. Secondly, the dilution that is to be achieved to reach 1 ppm concentration is  $1:10^6$ . This is a very large dilution and the contribution from the initial dilution from the cold nitrogen vapors is relatively small.



SCENARIO B: TANK BREACH: STABILITY D (4.0)

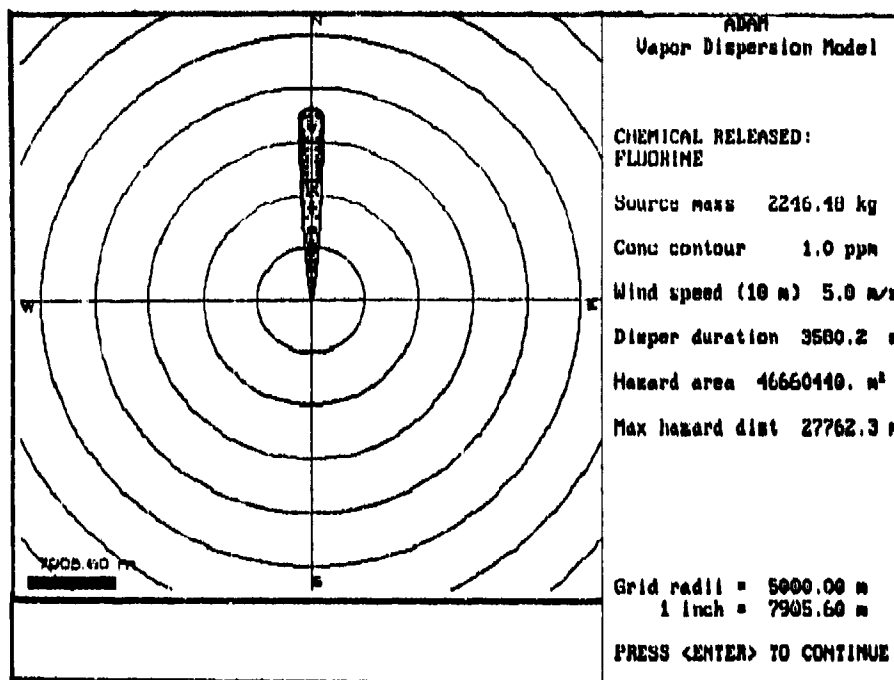


Figure 5.13: Dispersion under Neutral Stability Fluorine Cloud Released by a Transport Tank Breach

SCENARIO B: TANK BREACH: STABILITY F (5.5)

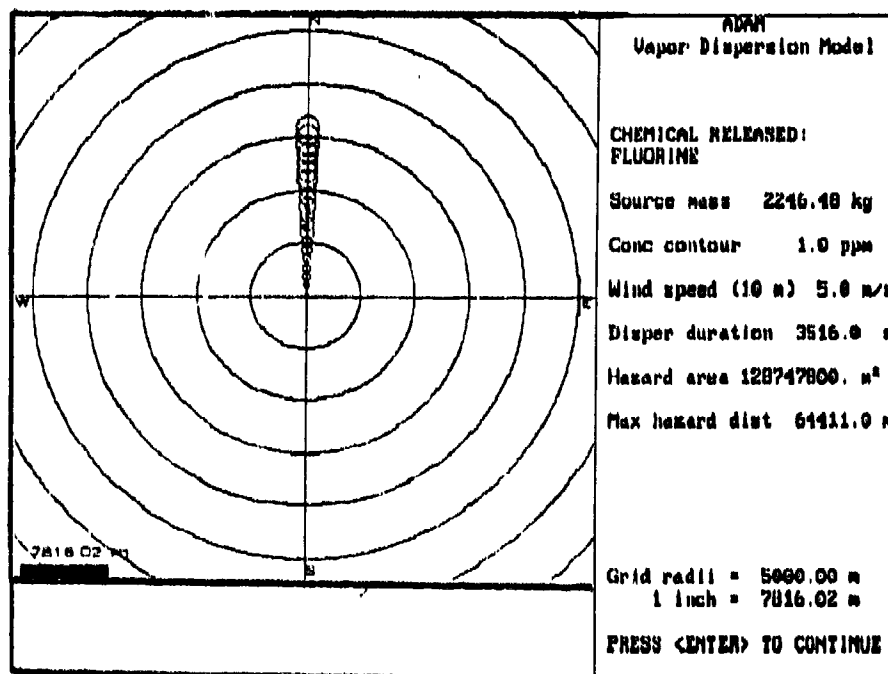


Figure 5.14: Dispersion under Stable Weather Conditions of a Fluorine Vapor Cloud Released by a Transport Tank Breach

## CHAPTER 6

### CONCLUSIONS

The scope of Air Force Dispersion Assessment Model (ADAM) has been expanded to include the simulation of accidental releases of two additional chemicals, namely, anhydrous hydrogen fluoride (HF) and fluorine. The analyses presented in this report include modeling both the release scenario ("source modeling") and dispersion of the chemical plume or cloud formed after release.

Inclusion of HF in the list of chemicals in ADAM required the evaluation of available HF-humid air reaction thermodynamic models, modifications and improvements. The dispersion algorithm for HF is the same as the one for other chemicals, namely a hybrid of a heavy gas (modified) box model and a modified finite size source Gaussian.

Release of fluorine from a transport vehicle was analyzed. Two different scenarios of fluorine release were identified. Detailed source models have been developed for the evaporation of a two component liquid pool (consisting of liquid nitrogen and liquid fluorine) and the flashing release of pressurized liquid fluorine. Also, a thermodynamic model was developed to calculate the effect of mixing of fluorine vapor (or vapor with aerosols) and humid air.

Based on the work accomplished in this project, we conclude the following:

#### Hydrogen Fluoride

1. The HF-humid air model is a modified Schotte model. It has been modified to expand its range of applicability and improve its accuracy. The model is robust and calculates the final HF-air mixture conditions for a variety of initial conditions of air and HF.
2. The source and dispersion calculations give results close to the values observed in one series of field tests with HF.
3. There are significant uncertainties in the field test data. Many questions regarding instrument calibration, conversion of raw field data to concentration values, discrepancies in reported values for the same data items in two publications remain unresolved.

4. The concentration values predicted by ADAM seem to be lower than observed values. Also at the transition regime (between heavy gas to passive dispersion), the concentration vs. distance curve seems to have a different trend than what one expects. This aspect needs a significantly more detailed model parameter analysis.
5. The HF model in ADAM predicts results that have accuracy acceptable for a rapid assessment of a potentially hazardous situation in an accident environment.

#### Fluorine

6. Two different fluorine release conditions can occur depending on the accident scenario. These are, (i) the simultaneous release of liquid nitrogen (from the jacket) and liquid fluorine at the saturation temperature of nitrogen and (ii) the flashing release of fluorine (only) due to inner tank rupture caused by elevated pressure.
7. Two component ( $LN_2$  and  $LF_2$ ) liquid pool evaporation model developed indicates that nitrogen evaporates preferentially. However, because of the very low boiling temperature of both nitrogen and fluorine, and the consequent high heat transfer rates from ground to the liquid pool, the evaporation of fluorine is very rapid (within a matter of tens of seconds).
8. In the flashing release of fluorine about 13.5% of the mass released flashes to vapor instantaneously. The cloud formed by the mixture of the liquid aerosol and the saturated fluorine vapor has very high density relative to that of air (32.8 to 1).
9. Mixing of cold fluorine vapor or a mixture of vapor and liquid aerosol with humid air results in five different final conditions of the mixture depending upon the amount of air mixed and the relative humidity of air. The final conditions refer to the presence of solids (water ice), liquid aerosols (water and fluorine) and all components in the vapor phase.
10. The results of the fluorine - air mixing model indicate that the final mixture density is relatively insensitive to the relative humidity of air but depends on the amount of air mixed (for specified initial conditions of fluorine).
11. The temperature of the mixture is relatively constant until about equal mass of air is mixed with fluorine. Beyond this dilution the mixture temperature rises and the rate of rise is dependent on the air relative humidity.

12. The dispersion distances calculated for the case of flashing fluorine release from a road transport for 1 ppm level of hazard are 21 km and 64 km, respectively for neutral and stable atmospheric conditions. These large distances arise due to the very low concentration levels to which fluorine has to be diluted.
13. Even in the case of liquid pool formation and evaporation the calculated hazard distances are comparable to the above. This is because the total mass of fluorine released is the same and the pool evaporates in relatively short time. Therefore, during most of the dispersion regime the cloud is dispersing as if it were released instantaneously.
14. Because of the very low hazard concentration of fluorine the extent of dilution to safety is of the order of  $10^6$ . By 100 to 1 dilution the fluorine air mixture has a density that is within 0.5 % of that of ambient air. That is, in the next  $10^4$  dilution the cloud disperses essentially as a neutral density vapor.

Hence, the overall effects of the higher than air density of the vapor-aerosol mixture affect the dispersion process only during the initial stages; they have very little effect on the final outcome of the dispersion model. Ordinary Gaussian models can be used therefore for evaluating the hazard distances for fluorine spills. However, if near field concentration values or cloud widths are needed a heavy gas model such as ADAM has to be used.

15. There are no experimental data on fluorine releases with which to compare the ADAM dispersion predictions.

**This page is left blank intentionally**

## APPENDIX A

### FLASHING OF ANHYDROUS HYDROGEN FLUORIDE RELEASED FROM A COMPRESSED LIQUID STATE

The normal boiling point of anhydrous hydrogen fluoride (HF) at atmospheric pressure is 20 °C. In the case of HF stored at ambient temperature but at an elevated pressure, the release of liquid results in the formation of vapor due to flash vaporization of the liquid released. The pressure inside the tank may be higher than the ambient pressure either due to the ambient temperature being higher than the saturation temperature (20 °C) corresponding to 1 atmospheric pressure or due to the pressurization of the tank by another inert gas (such as nitrogen).

In this appendix we discuss the calculation of the percent flash into vapor for HF releases from under higher than saturation pressure.

#### A.1: FLASH FRACTION

The mass fraction of released liquid HF which flash to vapor is given by,

$$f_v = [ h_{liq}(T_f) - h_{liq}(P_{atm}) ] / \lambda(P_{atm}) \quad (A.1)$$

where,

$h_{liq}(T_f)$  = Enthalpy of liquid at temperature of tank  $T_f$

$h_{liq}(P_{atm})$  = Enthalpy of saturated liquid at ambient pressure

$\lambda(P_{atm})$  = Latent heat of vaporization at ambient pressure

$T_f$  = Liquid storage temperature in the tank

The key to determining the flash fraction is to determine the liquid enthalpy at the tank temperature. In order to calculate this it is necessary to calculate the saturation pressure of HF corresponding to the tank storage temperature.

Let,

$P_f$  = Tank pressure

$P^{sat}(T_f)$  = Saturation pressure corresponding to  $T_f$

Depending on the relative magnitudes of the above two pressures there are three cases to consider in evaluating the liquid enthalpy.

Case 1:  $P_T \leq 1.01 * P^{sat}(T_T)$

That is the tank pressure is within 1 % of the saturation pressure corresponding to the tank temperature. In this case we can approximate the liquid enthalpy as follows:

$$h_{liq}(T_T) = h_{liq}(sat, T_T) = h_{liq}(P^{sat}(T_T)) \quad (A.2)$$

Case 2:  $P_T > P^{sat}(T_T)$

The liquid in the tank under this condition is in a compressed liquid state. Hence, the enthalpy is calculated by the formula

$$h_{liq}(T_T) = h_{liq}(sat, T_T) + (\delta h / \delta P)_T dP \quad (A.3)$$

where,

$$(\delta h / \delta P)_T = [ - 1 + \beta T ] / \rho_{liq} \quad (A.4)$$

$$\beta = - (1/\rho) ( \frac{\delta \rho}{\delta T_p} ) \quad (A.5)$$

= Coefficient of volumetric expansion of liquid with temperature under constant pressure.

The second term on the right hand side of equation A.3 (i.e., the integral) represents the contribution to the liquid enthalpy due to liquid compression over the saturation pressure. This term is represented by the symbol " $\Delta h$ ".

The calculation of  $\beta$  value for HF liquid is indicated in a section A.2.

Case 3:  $P_T < P^{sat}(T_T)$

This case implies that there is vacuum or that the liquid is not at saturated condition. That is, the liquid is superheated with respect to the tank pressure. This condition is not of interest to us.

## A.2: NUMERICAL VALUES

The values for the HF liquid enthalpies for non saturated conditions are not available in the literature. Also not available is the value for the coefficient of liquid expansion. Therefore, we use the indirect and approximate method to determine the values for the non saturated liquid enthalpy.

The following values are indicated in handbooks for coefficient of liquid expansion,  $\beta$ .

$$\beta(\text{hydrochloric acid}) = 0.49 \times 10^{-3} \text{ K}^{-1}, \text{ Ref: Handbook of Mech Engineering, p 4-9, Table 12.}$$

$$\beta(\text{organic liquids}) = 0.04314/(T_c - T)^{0.641} \text{ K}^{-1}, \text{ Ref: Chemical Engineers Handbook, p 3-227.}$$

We assume that the  $\beta$  for HF is close to that of hydrochloric acid and use that value given above.

$$\text{Density of HF liquid at 300 K } (\rho) = 940 \text{ kg/m}^3$$

Hence, using equation A.4 and the above values for  $\beta$  and  $\rho$  we can show that

$$(\partial h / \partial P)_T = -9 \times 10^{-4} \text{ (J/kg)/(N/m}^2\text{) at 300 K}$$

Also, we have the following thermodynamic values for the HF conditions at 313 K the tank temperature.

$$P^{\text{sat}}(313) = 2.02 \times 10^5 \text{ N/m}^2$$

$$h_{\text{liq}}(\text{sat}, 313) = 7.11 \times 10^4 \text{ J/kg, with the enthalpy base} = 0 \text{ at } 292.7 \text{ K}$$

$$P_T = 8.66 \times 10^5 \text{ N/m}^2 = \text{Tank pressure}$$

$$\lambda(P_{\text{atm}}) = 3.744 \times 10^5 \text{ J/kg}$$

Hence, we get for  $\Delta h$ , the contribution to liquid enthalpy due to liquid compression,

$$\Delta h = -598 \text{ J/kg}$$

It is noticed by comparing the saturated liquid enthalpy at the tank temperature and the value of  $\Delta h$  above that the latter forms a very small fraction of the liquid enthalpy. Hence, no great loss of



accuracy results if the saturated liquid enthalpy value is at the tank temperature is used for the actual liquid enthalpy.

### A.3: FLASH VALUES

The saturated liquid enthalpy value for anhydrous HF can be represented by the equation,

$$h_{liq}(sat,T) = 3500 (T - 292.7) \text{ J/kg} \quad (A.6)$$

where T is the temperature of the liquid in degrees Kelvin.

Using equation A.6 and equation A.1 we can show that the value of vapor mass fraction resulting from the flash is,

$$f_v (\text{in } \%) = 0.935 (T - 292.7) \quad (A.7)$$

The fraction that flashes to vapor for liquid release from 313 K is therefore calculated to be 19.12 %.

## APPENDIX B

### DISTILLATION OF A TWO COMPONENT SYSTEM

#### 1.0 INTRODUCTION

In this appendix, we consider the distillation of a pool of cryogenic liquid containing two volatile components, namely, fluorine and nitrogen. The pool of this cold liquid is on the ground and evaporating due to heat transfer from the ground.

The important objective of the calculations presented in this appendix is to determine the total time for evaporation of the pool. It is also desired to calculate the rate of evaporation of the liquids, the molar concentrations of the two components in the liquid pool and the vapor generated, as functions of time.

The details of the model formulation, equations, the computer code written in FORTRAN to solve the coupled differential equations and the results calculated are indicated in this appendix.

#### 2.0 THE EVAPORATION MODEL

The two component liquid mixture evaporating from a pool is assumed to be located on the ground. The energy for vaporization is assumed to come from the ground. The components are represented by subscripts 1 and 2. In our nomenclature, component 1 refers to Fluorine and component 2 refers to Nitrogen. (The definition of the symbols used in this model formulation are given at the end of this appendix.)

We now define the molar contents of the liquid pool as follows:

$$L_1 = X_1 L \quad (1a)$$

$$L_2 = X_2 L \quad (1b)$$

The heat from the ground evaporates both components of the liquid. For an incremental input of heat, the incremental change in the molar contents of the pool are given by,

$$dQ = - (h_1 dL_1 + h_2 dL_2) \quad (2)$$

Heat input to pool

The negative sign indicates that as heat is added to the pool the moles in the liquid decrease. The molar heats of vaporization are indicated by  $h_1$  and  $h_2$ .

Using Equations 1a and 1b, Equation 2 is reduced to:

$$dQ = - [ L ( h_1 dX_1 + h_2 dX_2 ) + ( h_1 X_1 + h_2 X_2 ) dL ] \quad (3)$$

We also note that

$$X_1 + X_2 = 1 \quad (4)$$

Hence, substituting Equation 4 in Equation 3, we get

$$dQ = - [ L ( h_1 - h_2 ) dX_1 + ( h_1 X_1 + h_2 ( 1 - X_1 ) ) dL ] \quad (5a)$$

$$\frac{dQ}{dt} = - \left[ L ( h_1 - h_2 ) \frac{dX_1}{dt} + ( h_1 X_1 + h_2 ( 1 - X_1 ) ) \frac{dL}{dt} \right] \quad (5b)$$

If a relationship is established between  $L$  and  $X_1$ , then, for specified heat input rate (LHS of Equation 5b), we can solve for the temporal variation of  $X_1$  (and hence,  $L$  and  $X_2$ ). The section below illustrates the development of the relationship between  $X_1$  and  $L$ .

### 3.0 RELATIONSHIP BETWEEN $X_1$ AND $L$

The evaporation of a liquid component results in the increase in the mole content of the vapor. Using a mass balance,

$$dL + dV = 0 \quad (6a)$$

$$d(X_1 L) + Y_1 dV = 0 \quad (6b)$$

where,  $Y_1$  represents the mole fraction of component 1 in the vapor generated and  $Y_1 dV$  is the total moles of component 1 generated in an infinitesimal time.

$$\frac{d(X_1 L)}{dL} = + Y_1 \quad (7a)$$

i.e.,

$$\frac{dX_1}{(y_1 - X_1)} = \frac{dL}{L} \quad (7b)$$

As  $Y_1$  and  $X_1$  are related by phase equilibria, Equation 7b can be integrated.

We now define

$$\beta = \frac{Y_1/X_1}{Y_2/X_2} \text{ -Relative Volatility of 1 wrt 2} \quad (8)$$

$$a = Y_1/X_1 \quad (9)$$

substituting Equation 9 in Equation 8 and noting the relationship in Equation 4, we obtain

$$a = \frac{\beta}{[\beta X_1 + (1 - X_1)]} \quad (10)$$

Equation 7b can be written (substituting Equation 9 and Equation 10)

$$\frac{dL}{L} = \frac{dX_1}{X_1 (a-1)} = \frac{dX_1}{X_1 \left[ \frac{\beta}{[\beta X_1 + (1 - X_1)]} - 1 \right]} \quad (11a)$$

i.e.,

$$\frac{dL}{L} = \frac{dX_1}{X_1} \frac{[\beta X_1 + (1 - X_1)]}{(\beta - 1)(1 - X_1)} = \frac{dX_1}{(\beta - 1)} \left[ \frac{1}{X_1} + \frac{\beta}{(1 - X_1)} \right] \quad (11b)$$

integrating the above equation, we get

$$\ln L = \frac{1}{(\beta-1)} [\ln X_1 - \beta \ln(1-X_1)] + \text{const} \quad (12a)$$

i.e.,

$$\ln\left(\frac{L}{L^1}\right) = \frac{1}{(\beta-1)} \left[ \ln\left(\frac{X_1}{X_1^1}\right) \left(\frac{1-X_1^1}{1-X_1}\right)^\beta \right] \quad (12b)$$

or

$$\frac{L}{L^1} = \left[ \left(\frac{X_1}{X_1^1}\right) \left(\frac{1-X_1^1}{1-X_1}\right)^\beta \right]^{\frac{1}{\beta-1}} \quad (12c)$$

where  $X_1^1$ , and  $L^1$  represent some known values (say, the initial values in the pool).

#### 4.0 MOLAR EVAPORATION RATE OF A COMPONENT OF INTEREST

##### 4.1 Heat Balance Equation

We repeat Equation 5 here for the sake of continuity.

$$\frac{dQ}{dt} = - \left[ L(h_1 - h_2) \frac{dX_1}{dt} + (h_1 X_1 + h_2 (1-X_1)) \frac{dL}{dt} \right] \quad (5b)$$

$$\frac{dQ}{dt} = - L h_1 \left[ \left[ 1 - \frac{h_2}{h_1} \right] \frac{dX_1}{dt} + \left\{ X_1 + \left( \frac{h_2}{h_1} \right) (1-X_1) \right\} \frac{dL}{dt} \right]$$

substituting for  $dL/L$  from Equation 11, we get

$$\frac{dQ}{dt} = -L^i \left( \frac{L}{L^i} \right) h_1 \frac{dX_1}{dt} \left[ \left( 1 - \frac{h_2}{h_1} \right) + \frac{(X_1 + \frac{h_2}{h_1} (1-X_1))}{(\beta-1)} \left\{ \frac{1}{X_1} + \frac{\beta}{(1-X_1)} \right\} \right] \quad (13)$$

We now define a function  $F$  as follows:

$$F = F(X_1) = \left( 1 - \frac{h_2}{h_1} \right) + \frac{1}{(\beta-1)} \left[ X_1 + \frac{h_2}{h_1} (1-X_1) \right] \left[ \frac{1}{X_1} + \frac{\beta}{(1-X_1)} \right] \quad (14)$$

Substituting Equations 12c and 14 in Equation 13 and rearranging, we get:

$$\frac{dX_1}{dt} = - \frac{q(t)}{h_1 L^i F(X_1) (L/L^i)} \quad \text{with } X_1 = X_1^i \text{ at } t = 0 \quad (15)$$

where,

$$q(t) = dQ/dt$$

Note that  $L/L^i$  is a function of  $X_1$  only.

The above equation can be solved by Runge Kutta method for specified  $q(t)$ .

#### 4.2 Mass Rate of Evaporation

The molar evaporation of specie 1 from the pool is given by:

$$N_1(t) = - \frac{dL_1}{dt} = - \frac{d(LX_1)}{dt} \quad (16a)$$

where,  $N_1(t)$  is the molar evaporation rate of component 1.

i.e.,

$$\dot{M}_1(t) = - \left[ X_1 \frac{dL}{dX_1} \frac{dX_1}{dt} + L \frac{dX_1}{dt} \right] \quad (16b)$$

Substituting for  $X_1/L$  and  $dL/dX_1$  from Equation 11 we get,

$$\dot{M}_1(t) = - L \frac{dX_1}{dt} \left[ \frac{\beta X_1 + (1-X_1)}{(\beta-1)(1-X_1)} + 1 \right] = - L \frac{dX_1}{dt} \frac{\beta}{(\beta-1)(1-X_1)} \quad (17a)$$

i.e.,

$$\dot{M}_1(t) = - L^{\frac{1}{\beta-1}} \left( \frac{L}{L^{\frac{1}{\beta-1}}} \right) \frac{\beta}{(\beta-1)(1-X_1)} \frac{dX_1}{dt} \quad (17b)$$

#### 4.3 Non-Dimensionalization of Equations

Let

$$t_{ch} = \text{characteristic time in the problem} \quad (18a)$$

$$\tau = t/t_{ch} = \text{non-dimensional time} \quad (18b)$$

We can determine the value for the characteristic time by imposing the following relation:

$$q(t_{ch}) t_{ch} = h_1 L^{\frac{1}{\beta-1}} \quad (19)$$

The above equation implies that  $t_{ch}$  is the total time for the evaporation of the entire pool if it contained only component 1 and received heat at a rate equal to that at time  $t_{ch}$ .

Let,

$$\bar{q}(t) = q(t)/q(t_{ch}) \quad (20)$$

Hence, Equation 15 reduces to:

$$\frac{dX_1}{d\tau} = - \frac{\bar{q}(t)}{F(X_1) (L/L^i)} \text{ with } X_1 = X_1^i \text{ at } \tau = 0 \quad (21)$$

Equation 17b is now written as:

$$\frac{M_1(t) t_{ch}}{L^i} = - \left( \frac{L}{L^i} \right) \frac{\beta}{(\beta-1)(1-X_1)} \frac{dX_1}{d\tau} \quad (22)$$

We can write an equation similar to equation 22 for the component 2 also. The mass rate of evaporation of component 2 is given by,

$$\frac{M_2 t_{ch}}{L^i} = - (L/L^i) \frac{1}{(1-\beta)(1-X_2)} \frac{dX_2}{d\tau} \quad (23)$$

where  $\beta$  is defined in equation 8. We also note that,

$$X_2 = 1 - X_1 \quad (24)$$

Therefore, equation 23 can be written as,

$$\frac{M_2 t_{ch}}{L^i} = - \frac{1}{(1-\beta)X_1} \frac{dX_1}{d\tau} \quad (25)$$



## 5.0 GROUND HEAT TRANSFER MODEL

The ground heat transfer rate is assumed to be given by the one dimensional model described in an earlier report (see Raj and Morris, 1987). This model assumes the following formulation for the heat transfer rate into the pool of liquid.

$$q''(t) = \frac{S \Delta T}{\sqrt{t}} \quad (25)$$

We also choose the following as the characteristic time for the problem:

$$t_{ch} = \left[ \frac{h_1 L^4}{2S \Delta T} \right]^2 \quad (26)$$

where,  $\Delta T$  is the temperature difference between the ground and the evaporating pool.

## 6.0 NUMERICAL EXAMPLE

### 6.1 Values of Parameters

We choose the following values for the various parameters. The volumes of the liquids spilled are equal to the volumes carried on a road transport. The depth of the pool is assumed to be 1 cm. The area of the pool is then calculated with the known volume of the liquids spilled.

Volume of Fluorine spilled =	1.771	m <sup>3</sup>
Volume of Nitrogen spilled =	1.287	m <sup>3</sup>
Assumed depth of pool =	0.01	m
Liquid pool temperature =	80.75	K (avg of boiling temp of F2 & N2)
Ground Temperature =	293.0	K
Ground heat transfer parameter =	1400.0	J/(m <sup>2</sup> s <sup>1/2</sup> )
Relative Volatility ( $\beta$ ) =	0.412	

The values of some of the calculated parameters for the initial conditions are as follows:

Area of the pool	=	305.8	m <sup>2</sup>
Initial molar contents			
of F2 = L <sub>1</sub> (i)	=	72.66	kmoles
of N2 = L <sub>2</sub> (i)	=	36.36	kmoles
Mole Fraction of F2	=	0.656	
in the liquid [X <sub>1</sub> (i)]			
Characteristic time (t <sub>ch</sub> )	=	15.51	s

## 6.2 Results

To solve the equations indicated in this appendix, a FORTRAN program was developed. Using this program, results were obtained.

The results are presented in the attached figures. Figure B-1 shows the variation of the molar fractions of Fluorine and Nitrogen in the liquid phase as a function of time. It is seen that the molar content of F2 increases and towards the end of the evaporation the liquid is rich in Fluorine. This is because nitrogen is much more volatile and therefore evaporates preferentially.

Figure B-2 shows the variation of the mole fractions of F2 and N2 in the vapor phase with time. Again due to the volatility of nitrogen, the concentration of nitrogen in vapor is high initially but decreases continuously with time.

Figure B-3 is a plot of the molar contents of the liquid pool with time. As expected, the total molar content decreases with time due to evaporation. The rate of decrease of nitrogen in the liquid pool is higher than that of fluorine. By about 0.87 nondimensional time units, almost all of the nitrogen has evaporated.

It is noticed that, at about 0.95 nondimensional time (dimensional time = 14.75 seconds), all of the liquid in the pool has evaporated. That is, the evaporation of the F2 - N2 pool is relatively rapid.

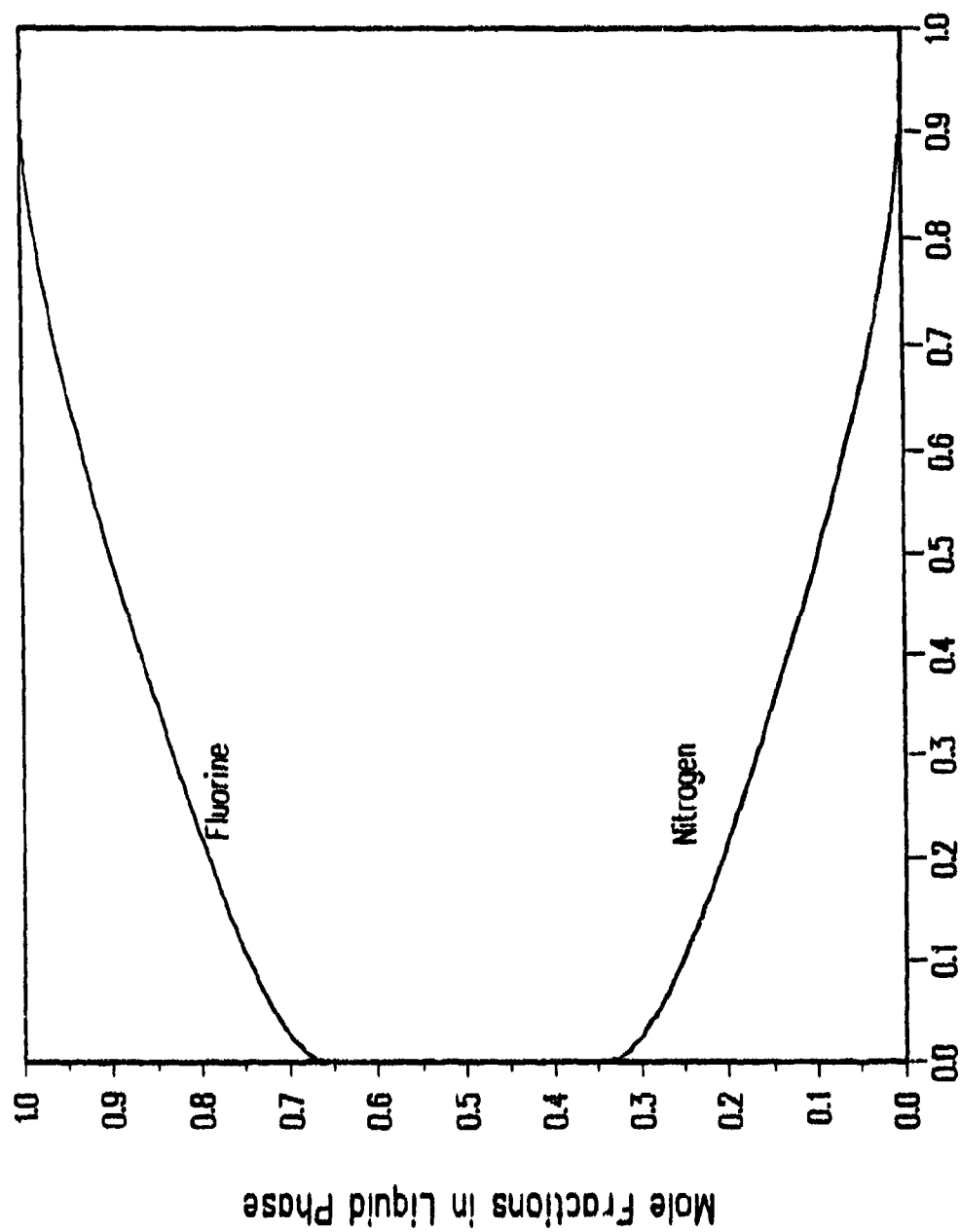


**Figure B.1: Liquid Mole fraction with Time**

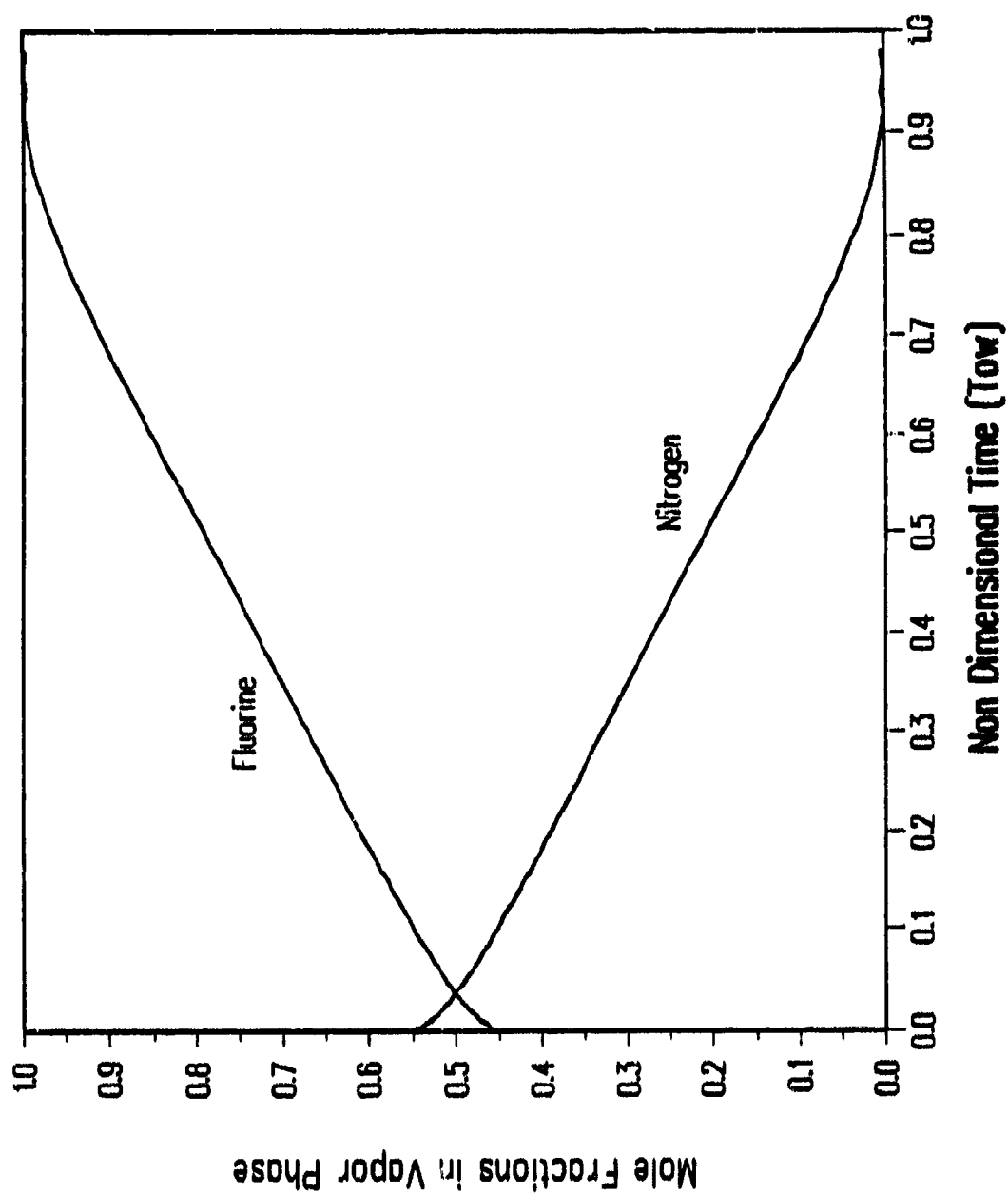


Figure B.2: Vapor Mole fraction with Time

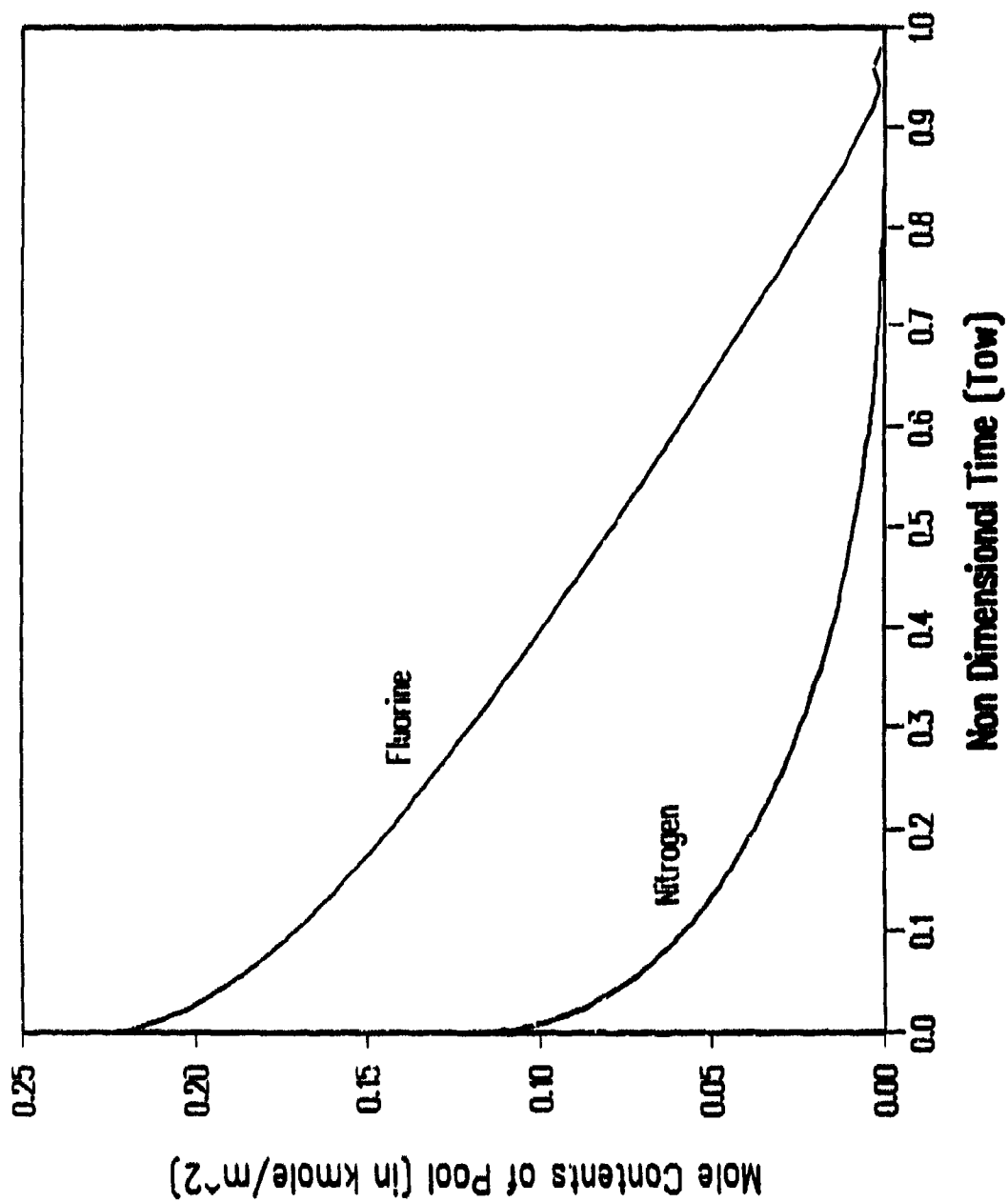


Figure B.3: Liquid Molar Content of Pool vs Time

**APPENDIX C**  
**THERMODYNAMIC PROPERTIES OF HYDROGEN FLUORIDE**

-1 0 3 0 HFXPROP.DAT  
 VERSION 2.11

```

-----
1 1 2 0 MOLECULAR WEIGHT (XMWT)
  REF: HACS
  20.006
2 1 2 0 CRITICAL POINT TEMPERATURE (TCRI) K
  REF: HACS
  461.00
3 1 2 0 CRITICAL POINT PRESSURE (PCRI) N/m2
  REF: HACS
  0.64800E+07
4 1 2 0 NORMAL BOILING POINT (XNBP) K
  REF: HACS
  292.70
5 1 2 0 NORMAL FREEZING POINT (XNFP) K
  REF: HACS
  190.00
6 8 2 0 VAPOR HEAT CAPACITY (CPV) PARAMETERS J/kg K
  REF: HACS
  1.45300E+03  3.30500E-02  -1.0160E-04  1.25200E-07  600.00
  250.00      0.00000E+00  0.00000E+00
7 8 2 0 LIQ HEAT CAPACITY (CPL) PARAMETERS J/kg K
  REF: HACS; Upper temp set to TCRI 11/20/89 (was 293.00)
  3500.0      0.00000E+00  0.00000E+00  0.00000E+00  461.00
  265.00      3500.0      270.00
8 7 2 0 LIQUID DENSITY (RHOL) PARAMETERS kg/m3
  REF: HACS
  1.85300E+03  -3.9710      3.12500E-03  300.00      210.00
  0.00000E+00  0.00000E+00
10 8 2 0 VAPOR PRESSURE (PSAT) PARAMETERS N/m2
  REF: HACS
  -9.74369      4.68496      -2.98358      9.65825      0.0000
  461.00      273.16      1.00000
11 2 2 0 ENTHALPY OF SAT LIQUID (HLIQS) PARAMETERS J/kg
  REF:
  0.00000E+00  292.7
12 2 2 0 ENTHALPY OF SAT VAPOR (HVAPS) PARAMETERS J/kg
  REF:
  3.74400E+05  292.7
  
```

13 6 2 0 ENTHALPY OF VAPORIZATION (XLAMDA) J/kg  
 REF:HACS :XLAMDA value from Allied Chem Co publication on HF properties.  
 461.00 292.70 3.74400E+05 0.38000 461.00  
 181.00

14 6 2 0 SOLUBILITY (SOL) PARAMETERS kg/100 kg  
 REF: HACS  
 0.00000E+00 0.00000E+00 0.00000E+00 0.00000E+00 0.00000E+0  
 0.00000E+00

15 1 2 0 ENTHALPY OF FUSION (DHF) J/kg  
 REF: HACS  
 2.29000E+05

16 1 2 0 ENTHALPY OF COMBUSTION (DHC) J/kg  
 REF: HACS  
 0.00000E+00

17 1 2 0 ENTHALPY OF DECOMPOSITION (DHDC) J/kg  
 REF: HACS  
 0.00000E+00

18 1 2 0 ENTHALPY OF SOLUTION (DHS) J/kg  
 REF: HACS  
 -0.30756E+07

19 1 2 0 ENTHALPY OF REACTION WITH WATER (DHWR) J/kg  
 REF: HACS  
 -0.30756E+07

20 1 2 0 ENTHALPY OF POLYMERIZATION (DHPY) J/kg  
 REF: HACS  
 0.00000E+00

21 1 2 0 AEROSOL ENTRAINMENT FRACTION (XPHI)  
 REF:  
 1.0

101 7 2 0 LIQ THERMAL COND (XKL) PARAMETERS W/m K  
 REF: HACS  
 0.710 -8.6220E-04 -6.4400E-07 438.0 190.0  
 0.00000E+00 0.00000E+00

102 8 2 0 VAP THERMAL COND (XKV) PARAMETERS W/m K  
 REF:  
 3.85700E-03 5.27600E-05 2.26100E-08 0.00000E+00 1000.0  
 175.000 0.00000E+00 0.00000E+00

103 8 2 0 LIQ VISCOSITY (XMUL) PARAMETERS N s/m2  
 REF: HACS  
 -1.4040E+01 1.87900E+03 2.97500E-02 -3.0600E-05 453.00  
 193.00 0.00000E+00 0.00000E+00

104 7 2 0 VAP VISCOSITY (XMUV) PARAMETERS N s/m<sup>2</sup>  
 REF: Allied Chemical Corp; "Hydrofluoric Acid", 1978  
 -1.0000E-06 4.5000E-08 0.00000E+00 373.000E+00 233.000E+0  
 1.2000E-05 288.700E+00  
 105 8 2 0 SURFACE TENSION (STEN) N/m  
 REF: Allied Chemical Corp; "Hydrofluoric Acid", 1978  
 8.6000E-03 461.0 273.15 1.555 297.2  
 270.0 0.00000E+00 0.00000E+00  
 106 2 2 0 INTERFACIAL SURFACE TENSION (XITEN) N/m  
 REF: HACS  
 0.00000E+00 0.00000E+00  
 201 1 2 0 LOWER FLAMABILITY LIMIT (XLOFLM) %  
 REF: HACS  
 0.00000E+00  
 202 1 2 0 UPPER FLAMABILITY LIMIT (UPFLM) %  
 REF: HACS  
 0.00000E+00  
 203 1 2 0 BURN RATE (BRAT) m/s  
 REF: HACS  
 0.00000E+00  
 204 1 2 0 ADIABATIC FLAME TEMPERATURE (ADFT) K  
 REF: HACS  
 0.00000E+00  
 205 1 2 0 MOLAR RATIO REACTANTS/PRODUCTS (MRAT)  
 REF: HACS  
 0.00000E+00  
 206 1 2 0 AIR FUEL RATIO (AFRT)  
 REF: HACS  
 0.00000E+00  
 207 1 2 0 FLAME TEMPERATURE (FLTM) K  
 REF: HACS  
 0.00000E+00  
 211 1 2 0 LIMITING VALUE OF MOLECULAR FN CONC (XMFRC)  
 REF: HACS  
 0.00000E+00  
 212 0 2 0 GREY BODY FIRE EMISSIVE POWER (kW/m<sup>2</sup>)  
 REF:  
 213 0 2 0 EMISSIVITY (fraction)  
 REF:  
 214 0 2 0 EFFECTIVE FIRE TEMPERATURE (K)  
 REF:  
 301 1 2 0 TOXIC INHALATION LIMIT/TLV (TOX1) ppm  
 REF: HACS  
 3.0000



302 1 2 0 SHORT TERM INHALATION LIMIT (TOX2) ppm  
 REF: HACS  
 3.0000

303 1 2 0 SHORT TERM INHALATION TIME LIMIT (TOX3) s  
 REF: HACS  
 900.00

304 1 2 0 LOWER TOXICITY INGESTION LIMIT (TOX4) kg/kg  
 REF: HACS  
 0.80000E-04

305 1 2 0 UPPER TOXICITY INGESTION LIMIT (TOX5) kg/kg  
 REF: HACS  
 0.00000E+00

306 0 2 1 LATE TOXICITY LEVEL (TOX6)  
 REF: HACS

800 1 2 1 NAME OF CHEM (CNAM)  
 REF: COMPUTERIZED DATA IN CHRIS\_ALL.DAT  
 HYDROGEN FLUORIDE

801 1 2 1 SHIPPING STATE CODE  
 REF: HACS

L

802 1 2 1 HAZARD CLASS (HACL)  
 REF: COMPUTERIZED DATA IN CHRIS\_ALL.DAT  
 Corrosive

803 1 2 1 HAZARD CLASS NUMBER (HACN)  
 REF: COMPUTERIZED DATA IN CHRIS\_ALL.DAT

8

804 1 2 1 DOT. NUMBER (DOTN)  
 REF: COMPUTERIZED DATA IN CHRIS\_ALL.DAT

1052

805 1 2 1 PATH CODE (PATC)  
 REF: COMPUTERIZED DATA IN CHRIS\_ALL.DAT

A-C-K-M-N-O

806 0 2 1 ENVIRONMENT BEHAVIOR CODE  
 REF:

APPENDIX C (contd)  
THERMODYNAMIC PROPERTIES OF FLUORINE

-1 0 3 0 FXXPROP.DAT  
 VERSION 2.11

```

-----
1 1 2 0 MOLECULAR WEIGHT (XMWT)
  REF: HACS
  37.997
2 1 2 0 CRITICAL POINT TEMPERATURE (TCRI) K
  REF: HACS
  144.30
3 1 2 0 CRITICAL POINT PRESSURE (PCRI) N/m2
  REF: HACS
  0.55200E+07
4 1 2 0 NORMAL BOILING POINT (XNBP) K
  REF: HACS
  84.45
5 1 2 0 NORMAL FREEZING POINT (XNFP) K
  REF: HACS
  53.500
6 8 2 0 VAPOR HEAT CAPACITY (CPV) PARAMETERS J/kg K
  REF: HACS
  611.00      0.96240      -9.50900E-04      3.16900E-07      1000.0
  84.45      0.00000E+00      0.00000E+00
7 8 2 0 LIQ HEAT CAPACITY (CPL) PARAMETERS J/kg K
  REF: HACS
  1087.0      1.79      0.00000E+00      0.00000E+00      110.0
  55.0      1238.26      84.5
8 7 2 0 LIQUID DENSITY (RHOL) PARAMETERS kg/m3
  REF: HACS
  1559.3      -0.73000      0.00000E+00      173.16      84.450
  1500.0      84.450
10 8 2 0 VAPOR PRESSURE (PSAT) PARAMETERS N/m2
  REF: HACS
  -6.18224      1.18062      -1.16555      -1.50167      0.00000E+0
  144.30      64.000      1.0
11 2 2 0 ENTHALPY OF SAT LIQUID (HLIQS) PARAMETERS J/kg
  REF:
  0.00000E+00      84.45
12 2 2 0 ENTHALPY OF SAT VAPOR (HVAPS) PARAMETERS J/kg
  REF:
  0.17300E+06      84.45
  
```

13 6 2 0 ENTHALPY OF VAPORIZATION (XLAMDA) J/kg  
 REF: HACS  
 144.30 84.450 0.17300E+06 0.38000 144.30  
 54.000

14 6 2 0 SOLUBILITY (SOL) PARAMETERS kg/100 kg  
 REF: HACS  
 0.00000E+00 0.00000E+00 0.00000E+00 0.00000E+00 0.00000E+00  
 0.00000E+00

15 1 2 0 ENTHALPY OF FUSION (DHF) J/kg  
 REF: HACS  
 4.10000E+04

16 1 2 0 ENTHALPY OF COMBUSTION (DHC) J/kg  
 REF: HACS  
 0.00000E+00

17 1 2 0 ENTHALPY OF DECOMPOSITION (DHDC) J/kg  
 REF: HACS  
 0.00000E+00

18 1 2 0 ENTHALPY OF SOLUTION (DHS) J/kg  
 REF: HACS  
 0.00000E+00

19 1 2 0 ENTHALPY OF REACTION WITH WATER (DHW) J/kg  
 REF: HACS  
 0.00000E+00

20 1 2 0 ENTHALPY OF POLYMERIZATION (DHPY) J/kg  
 REF: HACS  
 0.00000E+00

21 1 2 0 AEROSOL ENTRAINMENT FRACTION (PHI)  
 REF:  
 1.0

101 7 2 0 LIQ THERMAL COND (XKL) PARAMETERS W/m K  
 REF: HACS  
 0.2565 -6.7950E-04 -4.9580E-06 133.0 54.0  
 0.00000E+00 0.00000E+00

102 8 2 0 VAP THERMAL COND (XKV) PARAMETERS W/m K  
 REF:  
 7.81200E-04 8.28700E-05 5.19300E-08 0.00000E+00 600.0  
 145.0 0.00000E+00 0.00000E+00

103 8 2 0 LIQ VISCOSITY (XMUL) PARAMETERS N s/m<sup>2</sup>  
 REF: HACS  
 -3.6290 1.97200E+02 -9.3780E-04 -6.2750E-06 88.0  
 54.0 0.00000E+00 0.00000E+00

104 7 2 0 VAP VISCOSITY (XMUV) PARAMETERS N s/m2  
 REF:  
 2.09000E-04 0.00000E+00 0.00000E+00 1000.0 0.0  
 0.00000E+00 0.00000E+00

105 8 2 0 SURFACE TENSION (STEN) N/m  
 REF: HACS  
 0.01460E+00 144.300E+00 81.0000E+00 1.00000E+00 100.000E+0  
 55.0000E+00 0.00000E+00 0.00000E+00

106 2 2 0 INTERFACIAL SURFACE TENSION (XITEN) N/m  
 REF: HACS  
 0.00000E+00 0.00000E+00

201 1 2 0 LOWER FLAMABILITY LIMIT (XLOFLM) %  
 REF: HACS  
 0.00000E+00

202 1 2 0 UPPER FLAMABILITY LIMIT (UPFLM) %  
 REF: HACS  
 0.00000E+00

203 1 2 0 BURN RATE (BRAT) m/s  
 REF: HACS  
 0.00000E+00

204 1 2 0 ADIABATIC FLAME TEMPERATURE (ADFT) K  
 REF: HACS  
 0.00000E+00

205 1 2 0 MOLAR RATIO REACTANTS/PRODUCTS (MRAT)  
 REF: HACS  
 0.00000E+00

206 1 2 0 AIR FUEL RATIO (AFRT)  
 REF: HACS  
 0.00000E+00

207 1 2 0 FLAME TEMPERATURE (FLTM) K  
 REF: HACS  
 0.00000E+00

211 1 2 0 LIMITING VALUE OF MOLECULAR FN CONC (XMFRC)  
 REF: HACS  
 0.00000E+00

301 1 2 0 TOXIC INHALATION LIMIT/TLV (TOX1) ppm  
 REF: HACS  
 1.0000

302 1 2 0 SHORT TERM INHALATION LIMIT (TOX2) ppm  
 REF: HACS  
 0.50000

303 1 2 0 SHORT TERM INHALATION TIME LIMIT (TOX3) s  
 REF: HACS  
 300.00

304 1 2 0 LOWER TOXICITY INGESTION LIMIT (TOX4) kg/kg

REF: HACS

0.00000E+00

305 1 2 0 UPPER TOXICITY INGESTION LIMIT (TOX5) kg/kg

REF: HACS

0.00000E+00

306 0 2 1 LATE TOXICITY LEVEL (TOX6)

REF: HACS

800 1 2 1 NAME OF CHEM (CNAM)

REF: COMPUTERIZED DATA IN CHRIS\_ALL.DAT

FLUORINE

801 0 2 1 SHIPPING STATE CODE

REF: HACS

802 1 2 1 HAZARD CLASS (HACL)

REF: COMPUTERIZED DATA IN CHRIS\_ALL.DAT

Nonflammable gas

803 1 2 1 HAZARD CLASS NUMBER (HACN)

REF: COMPUTERIZED DATA IN CHRIS\_ALL.DAT

2

804 1 2 1 DOT. NUMBER (DOTN)

REF: COMPUTERIZED DATA IN CHRIS\_ALL.DAT

1045

805 1 2 1 PATH CODE (PATC)

REF: COMPUTERIZED DATA IN CHRIS\_ALL.DAT

A-C

806 0 2 1 ENVIRONMENT BEHAVIOR CODE

REF:

APPENDIX C (contd)  
THERMODYNAMIC PROPERTIES OF NITROGEN

-1 0 3 0 N2.DAT NITROGEN ACIJ  
 VERSION 2.11

```

-----
1 1 2 0 MOLECULAR WEIGHT (XMWT)
  REF: HACS
  28.013
2 1 2 0 CRITICAL POINT TEMPERATURE (TCRI) K
  REF: HACS
  126.20
3 1 2 0 CRITICAL POINT PRESSURE (PCRI) N/m2
  REF: HACS
  33.9E+05
4 1 2 0 NORMAL BOILING POINT (XNBP) K
  REF: HACS
  77.40
5 1 2 0 NORMAL FREEZING POINT (XNFP) K
  REF: HACS
  63.30
6 8 2 0 VAPOR HEAT CAPACITY (CPV) PARAMETERS J/kg K
  REF: REID
  1112.00 -0.8440 9.5670E-04 -4.1690E-07 600.00
  298.00 1.0420E+03 298.00
7 8 2 0 LIQ HEAT CAPACITY (CPL) PARAMETERS J/kg K
  REF: YAWS,C.L., "PHYSICAL PROPERTIES", MCGRAW-HILL, NY, P.220.
  2309.00 -11.100 0.100 0.0000E+00 90.00
  70.00 2.0490E+03 77.4
8 7 2 0 LIQUID DENSITY (RHOL) PARAMETERS kg/m3
  REF: HACS (THI from CEH p.3-167 (was 293))
  790.9 4.7700 -0.05818 120.00 70.00
  812.0 126.2
10 8 2 0 VAPOR PRESSURE (PSAT) PARAMETERS N/m2
  REF: REID, P.658, NO.22
  -6.09676 1.13670 -1.04072 -1.93306 0.0000E+00
  126.20 63.0 1.0
11 2 2 0 ENTHALPY OF SATURATED LIQUID (HLIQS) J/kg
  REF: BASIS
  .00000 273.16
12 2 2 0 ENTHALPY OF SATURATED VAPOR (HVAPS) J/kg
  REF: HACS
  0.0000E+00 0.0000E+00
  
```

13 6 2 0 ENTHALPY OF VAPORIZATION (XLAMDA) J/kg  
 REF: HACS  
 126.20 77.40 1.9900E+05 .38000 110.0  
 75.00

14 6 3 0 SOLUBILITY (SOL) PARAMETERS kg/100 kg  
 REF: SCONCE,J.S., "CHLORINE", KREIGER PUBLISHING, HUNTINGTON, NY, 1972.P.33.  
 REF: FLDS 1-4 HACS FLDS 5,6  
 5.3927 -.01569 323.16 282.77 .65000  
 298.16

15 1 2 0 ENTHALPY OF FUSION (DHF) J/kg  
 REF:  
 .90330E+05

16 1 2 0 ENTHALPY OF COMBUSTION (DHC) J/kg  
 REF: HACS  
 .00000

17 1 2 0 ENTHALPY OF DECOMPOSITION (DHDC) J/kg  
 REF: HACS  
 .00000

18 1 2 0 ENTHALPY OF SOLUTION (DHS) J/kg  
 REF: HACS  
 .00000

19 1 2 0 ENTHALPY OF REACTION WITH WATER (DHWR) J/kg  
 REF: HACS  
 .00000

20 1 2 0 ENTHALPY OF POLYMERIZATION (DHPY) J/kg  
 REF: HACS  
 .00000

21 1 2 0 AEROSOL ENTRAINMENT FRACTION (PHI)  
 REF:  
 1.0

101 7 2 0 LIQ THERMAL COND (XKL) PARAMETERS W/m K  
 REF: YAWS, P.224.  
 2.629E-01 -1.5450E-03 -9.450E-07 121.0 64.00  
 1.1500E-01 91.0

102 8 2 0 VAP THERMAL COND (XKV) PARAMETERS W/m K  
 REF: YAWS, P.208.  
 3.919E-04 9.8160E-05 -5.0670E-08 0.0000E+00 1470.00  
 115.0 2.5100E-02 298.0

103 8 2 0 LIQ VISCOSITY (XMUL) PARAMETERS N s/m2  
 REF: YAWS, P.212.  
 -2.795E+01 8.660E+02 2.7630E-01 -1.0840E-03 78.00  
 68.00 1.8000E-04 73.0

104 7 2 0 VAP VISCOSITY (XMUV) PARAMETERS N s/m<sup>2</sup>  
 REF: YAWS, P.210.  
 4.2150E-06 0.0000E+00 4.5000E-08 373.0 173.00  
 1.2000E-05 173.00

105 8 2 0 SURFACE TENSION (STEN) N/m  
 REF: YAWS, P.218.(PARS 1-6) HACS(PARS 7,8)  
 8.750E-03 126.2 77.80 1.235 100.00  
 78.00 0.0000E+00 0.0000E+00

106 2 2 0 INTERFACIAL SURFACE TENSION (XITEN) N/m  
 REF: HACS  
 .00000 .00000

201 1 2 0 LOWER FLAMABILITY LIMIT (XLFLM) %  
 REF: HACS  
 .00000

202 1 2 0 UPPER FLAMABILITY LIMIT (UPFLM) %  
 REF: HACS  
 .00000

203 1 2 0 BURN RATE (BRAT) m/s  
 REF: HACS  
 .00000

204 1 2 0 ADIABATIC FLAME TEMPERATURE (ADFT) K  
 REF: HACS  
 .00000

205 1 2 0 MOLAR RATIO REACTANTS/PRODUCTS (MRAT)  
 REF: HACS  
 .00000

206 1 2 0 AIR FUEL RATIO (AFRT)  
 REF: HACS  
 .00000

207 1 2 0 FLAME TEMPERATURE (FLTM) K  
 REF: HACS  
 .00000

301 1 2 0 TOXIC INHALATION LIMIT/TLV (TOX1) ppm  
 REF: HACS  
 1.0000

302 1 2 0 SHORT TERM INHALATION LIMIT (TOX2) ppm  
 REF: HACS  
 3.0000

303 1 2 0 SHORT TERM INHALATION TIME LIMIT (TOX3) s  
 REF: HACS  
 300.00

304 1 2 0 LOWER TOXICITY INGESTION LIMIT (TOX4) kg/kg  
 REF: HACS  
 .00000



305 1 2 0 UPPER TOXICITY INGESTION LIMIT (TOX5) kg/kg  
REF: HACS  
.00000  
306 0 2 1 LATE TOXICITY LEVEL (TOX6)  
REF: HACS  
701 1 2 0 LIMITING VALUE OF MOLECULAR FN CONC (XMERC)  
REF: HACS  
.00000  
800 1 2 1 NAME OF CHEM (CNAM)  
REF: COMPUTERIZED DATA IN CHRIS\_ALL.DAT  
NITROGEN  
801 1 2 1 SHIPPING STATE CODE  
REF: HACS  
L  
802 1 2 1 HAZARD CLASS (HACL)  
REF: COMPUTERIZED DATA IN CHRIS\_ALL.DAT  
Nonflammable gas; Poison  
803 1 2 1 HAZARD CLASS NUMBER (HACN)  
REF: COMPUTERIZED DATA IN CHRIS\_ALL.DAT  
2 and 6  
804 1 2 1 DOT. NUMBER (DOTN)  
REF: COMPUTERIZED DATA IN CHRIS\_ALL.DAT  
1017  
805 1 2 1 PATH CODE (PATC)  
REF: COMPUTERIZED DATA IN CHRIS\_ALL.DAT  
A-C-I-J  
806 1 2 1 ENVIRONMENT BEHAVIOR (ENVB)  
REF:  
VW

## REFERENCES

- o Allied, "Hydrofluoric Acid," Publication by Allied Chemical Corp., Industrial Chemicals Division, Solvay, NY 13209, December 1978.
- o Armitage, J.W., P. Gray, and P.G. Wright, J. Chem. Soc. (1963), p. 1796.
- o Blewitt, D.N., K. McFarlane, A. Prothero, J.S. Puhock, F.J. Rees, P.T. Roberts, and H.W.M. Witlox, "Development of HFSYSTEM Programs for Hydrogen Fluoride Dispersion Assessment", AIChE Health and Safety Symposium, 1990.
- o Blewitt, D.N., J.F. Yohn, R.P. Koopman, and T.C. Brown (1987), "Conduct of Anhydrous Hydrofluoric Acid Spill Experiments", Intl. Conf. on Vapor Cloud Modeling, Cambridge, MA, November 1987.
- o Brosheer, J.C., F.A. Lanfesty, and K.L. Elmore, Ind. Eng. Chem. **39**, 423 (1947).
- o Cady, G.H. and L.L. Burger, "Physical Properties of Fluorine", Chapter 9 in Fluorine Chemistry, ed. J.H. Simons, Academic Press Inc., New York, 1950.
- o Chem. Ind. Assn. (1978), "Guide to Safe Practice in the Use and Handling of Hydrogen Fluoride", Chemical Industries Safety and Health Council; Chemical Industries Association, Ltd., London SE1-7TU, England.
- o Clough, P.N., D.R. Grist, and C.J. Wheatley, "Thermodynamics of Mixing and Final State of a Mixture Formed by the Dilution of Anhydrous Hydrogen Fluoride with Moist Air," SRD/HSE/R-396, United Kingdom Atomic Energy Authority, Culcheth, Great Britain, January, 1987a.
- o Clough, P.N., D.R. Grist, and C.J. Wheatley, "The Mixing of Anhydrous Hydrogen Fluoride with Moist Air," Paper presented at the International Conference on Vapor Cloud Modeling, November 2-4, 1987b, Cambridge, MA.
- o Franck, E.U. and W.Z. Spalthoff, Z. Elektrochem. **51**, 348 (1957).
- o Hanna, S., D. Stirmitis, and J. Chang (1989), "Results of Hazardous Material Response Model. Evaluations Using Desert Tortoise and Goldfish Databases", Draft Report by Sigma, Inc. to American Petroleum Institute, Washington, DC, October 1989 - UNPUBLISHED.

# REFERENCES (Continued)

- o Jarry, R.L. and W. Davis, J. Phys. Chem. **57**, 600 (1953).
- o Johnson, G.K., P.N. Smith, and W.N. Hubbard, J. Chem. Thermodyn. **5**, 793 (1973).
- o Kozhevnikov, O.A., V.A. Volkov, and L.S. Kozhevnikova, Izv. Vyssh. Uchebn. Zaved., Khim. Khim. Tekhnol. **25**, 1471 (1982).
- o Landau, R. and R. Rosen, "Industrial Handling of Fluorine", Chapter 7 in Preparation, Properties, and Technology of Fluorine and Organic Fluoro Compounds, C. Slessor, ed., McGraw-Hill Book Co., New York, 1951.
- o Maclean, J.N. et al., J. Inorg. Nucl. Chem. **24**, 1549 (1962).
- o Munter, F.A., O.T. Aeppli, and R.A. Kossatz, Ind. Eng. Chem. **39**, 427 (1947).
- o Munter, P.A., O.T. Aeppli, and R.A. Kossatz, Ind. Eng. Chem. **41**, 1504 (1949).
- o Reid, R.C., J.M. Prausnitz, and B.E. Poling, "The Properties of Liquids and Gases," McGraw-Hill Book Co., New York City, NY, Fourth Edition, 1987.
- o Rudge, A.J., "The Manufacture and Use of Fluorine and Its Compounds", Oxford University Press, London, 1962.
- o Rushmere, J.D., "The Molecular Association of Hydrogen Fluoride. A Short Review of the Published Literature," UKAEA Report SCS-TN-31, 1954.
- o Schotte, W., Ind. Eng. Chem. Process Des. Dev. **19**, 432 (1980).
- o Schotte, W., Ind. Eng. Chem. Res. **26**, 300 (1987).
- o Schotte, W., Personal Communication, 1988.
- o Sheft, I., A.J. Perkins, and H.H. Hyman, J. Inorg. Nucl. Chem. **35**, 3677 (1973).
- o Stull, D.R. and H. Prophet, "JANEF Thermochemical Tables", NSRDS-NBS 37, National Bureau of Standards, 1971.
- o Thomas, R.K., Proc. Roy. Soc. (London), Ser. A, **A344**, 579 (1975).
- o Thorvaldson, T. and E.C. Bailey, Can. J. Res. **24B**, 51 (1946).
- o Tyner, M., Chem. Eng. Prog. **45** (1), 49 (1949).

#### REFERENCES (Continued)

- o Vanderzee, C.E. and W.W. Rodenburg, J. Chem. Thermodyn. 2, 461 (1970); ibid. 3, 267 (1971).
- o Vieweg, R., Chem. Technologie. 15, 734 (1963).
- o Wheatley, C.J., "A Theory of Heterogeneous Equilibrium Between Vapour and Liquid Phases of Binary Systems and Formulae for the Partial Pressures of HF and H<sub>2</sub>O Vapor," SRD R 357, 1985.
- o Yabroff, R.M., J.C. Smith, and E.H. Lightcap, J. Chem. Eng. Data 9, 178 (1964).

**This Page is left Blank Intentionally**